Ya. E. Yudovich, M. P. Ketris, N. V. Rybina

THE APATITE-DECEIVER AS AN UNIQUE INDICATOR PARENT ROCKS AND ORES, AS WELL AS PETRO-, LITHO- AND ORE GENESIS

Melbourne, 2022

Ya. E. Yudovich, M. P. Ketris, N. V. Rybina

THE APATITE-DECEIVER AS AN UNIQUE INDICATOR PARENT ROCKS AND ORES, AS WELL AS PETRO-, LITHO- AND ORE GENESIS

Melbourne, 2022

Information about the authors

Yudovich Yakov Elievich, Chief Researcher of the Komi Scientific Center's Institute of Geology, the Ural Branch of the Russian Academy of Sciences; Doctor of Geological and Mineralogical Sciences, Academician of the Russian Academy of Natural Sciences and the New York Academy of Sciences, laureate of the A. P. Vinogradov Prize of the Russian Academy of Sciences (2011)

Ketris Marina Petrovna, Senior Researcher at the Institute of Geology of the Komi Scientific Center of the Ural Branch of the Russian Academy of Sciences; winner of the A. P. Vinogradov Prize of the Russian Academy of Sciences (2011).

Rybina Natalia Valerievna, Senior Laboratory Assistant at the Institute of Geology of the Komi Scientific Center of the Ural Branch of the Russian Academy of Sciences

CONTENTS

THE APATITE-DECEIVER AS AN UNIQUE INDICATOR PARENT ROCKS AND ORES, AS WELL AS PETRO-, LITHO- AND ORE GENESIS

Institute of Geology of Komi SC UB RAS, Syktyvkar
EYuYa@Yandex.ru

An extensive review describes the unique properties of apatite, which, due to the peculiarities of its structure, allows for diverse isomorphic substitutions both in its cationic part (Mn, Sr, Ba, REE, U, etc.) and in the anionic part (CO_2, SO_3, SiO_2, OH, F, Cl, etc.). Since these substitutions occur under well-defined conditions in both endogenous thermal and exogenous low-temperature processes, the composition of apatite turns out to be an indicator of these processes.

At the same time, the conditions of formation of most igneous and metamorphic rocks can be judged by the composition of accessory apatite, and the genesis of phosphorus ores, both endogenous (Khibiny, Kiruna type, etc.) and exogenous (phosphorites), is judged by the composition of ore-forming apatite.

The review is based on the recent "Irish" review 2020, covering 147 literary sources and compiled by 4 co-authors from Dublin and one from Stockholm [130]. Since the compilers of the "Irish" review practically did not use literature in Russian, it became necessary to seriously supplement it with the data given in the domestic literature, as well with a number of foreign works that are not covered by the "Irish" review.

The resulting text should make it much easier for the geologist reader to use apatite in practice as a remarkable mineral-an indicator of various geological processes.

Keywords: *apatite, carbonate-apatite (francolite), halogens, sulfate, trace elements, REE, manganese, strontium, neodymium, uranium*

01. THE UNIQUENESS OF THE APATITE STRUCTURE

As the authors of the "Irish" review [130] note, the surprisingly wide (ubiquitous) distribution of accessory apatite is explained by the inability of the main rock-forming minerals to retain a significant amount of phosphorus in their crystal lattice.

Apatite as a rock-forming mineral is present only in some cumulative and rare types of igneous rocks – some pegmatites, nelsonites and carbonatites, as well as in hypergenic phosphorites (the world's largest source of phosphorus for fertilizers).

The simplest apatite formula is usually given in the form $Ca_5(PO_4)_3(F, Cl, OH)$, but is often written with twice the number of formula units as $Ca_{10}(PO_4)_6(OH, F, Cl)_2$ in order to display the two structural positions of Ca.

The unit cell of apatite can be simplified to the formula $A_5(XO_4)_3Z$ and, as a rule, has a hexagonal structure.

In position A, Ca^{2+} is placed in two structural nodes with coordination 9 and 7: Ca1 and Ca2 (for more details, see below).

In the X-position with quadruple coordination there is P^{5+}, and in the monovalent Z-position there are halogens (Cl or F, with trace amounts of Br and I), OH-group or vacancy.

The replacement elements in position A may include significant amounts of Sr^{2+}, Mn^{2+}, Pb^{2+}, U^{4+} and Th^{4+}.

In the X position, P^{5+} can be replaced by small highly charged cations, such as S^{6+}, As^{5+}, V^{5+} and Si^{4+}. Three-charge lanthanides + yttrium – $REYs^{3+}$(REY = REE + Y) enter apatite by conjugate substitution of either calcium or calcium + phosphate:

$$2\ Ca^{2+} \leftarrow REE^{3+} + Na^+$$
$$Ca^{2+} + PO_4^{3-} \leftarrow REE^{3+} + SiO_4^{4+}$$
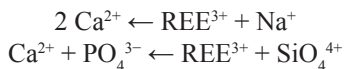
REE + Y and Sr accumulate strongly in magmatic apatites, so that in magmatic systems apatite can control a significant part of the entire budget of REE and Sr. Therefore, apatite can be a useful indicator in studies of magmatic petrogenesis.

According to Wikipedia, the first scientific description of apatite in 1788 was made by A. G. Werner, who proposed the name of this mineral. The term comes from the Greek πατάω – "deceive". This is due to the fact that apatite occurs in nature in different types and looks similar to the minerals beryl, diopside or tourmaline. The main diagnostic feature of apatite is the prismatic appearance of crystals; apatite differs from beryl similar to it in significantly lower hardness.

According to the Irish review [130] and Wikipedia, there are three types of apatites – finite members of isomorphic series:

– **hydroxyapatite** (these are all "bioapatite") – $Ca_{10}(PO_4)_6(OH)_2$;

– **fluorapatite** (the most common phosphate, these are most of the high-temperature magmatic apatites) – $Ca_{10}(PO_4)_6(F)_2$;

– **chlorapatite** (these are some of magmatic and hydrothermal apatites) – $Ca_{10}(PO_4)_6(Cl)_2$.

Since only the final members of the isomorphic series are indicated here, among these "types of apatites" there is no such widespread and particularly important variety of apatite as low-temperature *fluorine-carbonate-apatite (francolite)* – the main component of almost all exogenous phosphoric ores (phosphorites). Its general formula is given [52] in the form

$$Ca_{10-a-b}\,Na_aMg_b[PO_4]_{6-x}\,(CO_3)_{x-y-z}\,(CO_3F)_y(SO_4)_zF_2$$

The reader will find a more detailed description of francolite below, in section 6.

The peculiarities of the structure of hexagonal apatite make possible an unusually large number of isomorphic substitutions, despite the fact that these substitutions are quite naturally associated with certain varieties of apatite [52].

With the cationic substitution of Ca^{2+}, fluorapatite, chlorapatite, francolite, and even (oddly enough) hydroxyapatite are formed. In particular, when $Ca^{2+} \leftarrow Na^+, K^+, Ag^+$ is substituted, fluorapatite is obtained, and when $Ca^{2+} \leftarrow U^{4+}$ is substituted, chlorapatite is obtained.

When replacing $Ca^{2+} \leftarrow Sr^{2+}, Mn^{2+}, Mg^{2+}, Zn^{2+}, Cd^{2+}, Ba^{2+}$ – francolite is formed, and when Ca^{2+} is substituted $\leftarrow Sc^{3+}, Y^{3+}, REE^{3+}, Zn^{2+}, Cd^{2+}, Br^{3+}$ is hydroxyapatite.

During anionic substitution of $PO_4^{3+} \leftarrow CO_3^{2-}, SO_4^{2-}. Cr_2O_4^{2-}$, dallite $Ca_{10}(OH)_2[PO_4, CO_3]_6$ is formed, and when replacing $PO_4^{3-} \leftarrow AsO_4^{3-}, VO_4^{3-}, CO_3F^{3-}, CO_3OH^{3-}$ – wilkeite $Ca_{10}(O,OH,F)_2[SiO_4, PO_4 SO_4]_6$.

In additional complication in the processes of cation substitution in apatite make two types of Ca atoms in its structure, referred to as CA1 and Ca2 – Fig. 1.

As can be seen from the figure, where the projection of the unit cell of the apatite structure along the C axis is given, in the position Ca1, the calcium atom is in 9-coordination, in the center of a regular trigonal prism (CaO_9), surrounded by oxygen anions

In the position of Ca2 calcium atom is 7-coordinate, in the wrong polyhedron (CaO_{6A}), 6 vertices are occupied by oxygen anions, and the seventh – anions F^-, Cl^-, or OH^- (icon **A** in the figure).

The significantly different structural position of the Ca atoms causes different mechanisms of substitution of Ca with trivalent ions, in the most typical case – ions of rare earth elements REE^{3+}, as can be seen in equations (1) and (2):

$$2REE^{3+} + vacancy = 3Ca^{2+} \tag{1}$$

$$REE^{3+} + O^{2-} = Ca^{2+} + A^- \tag{2}$$
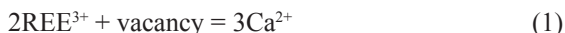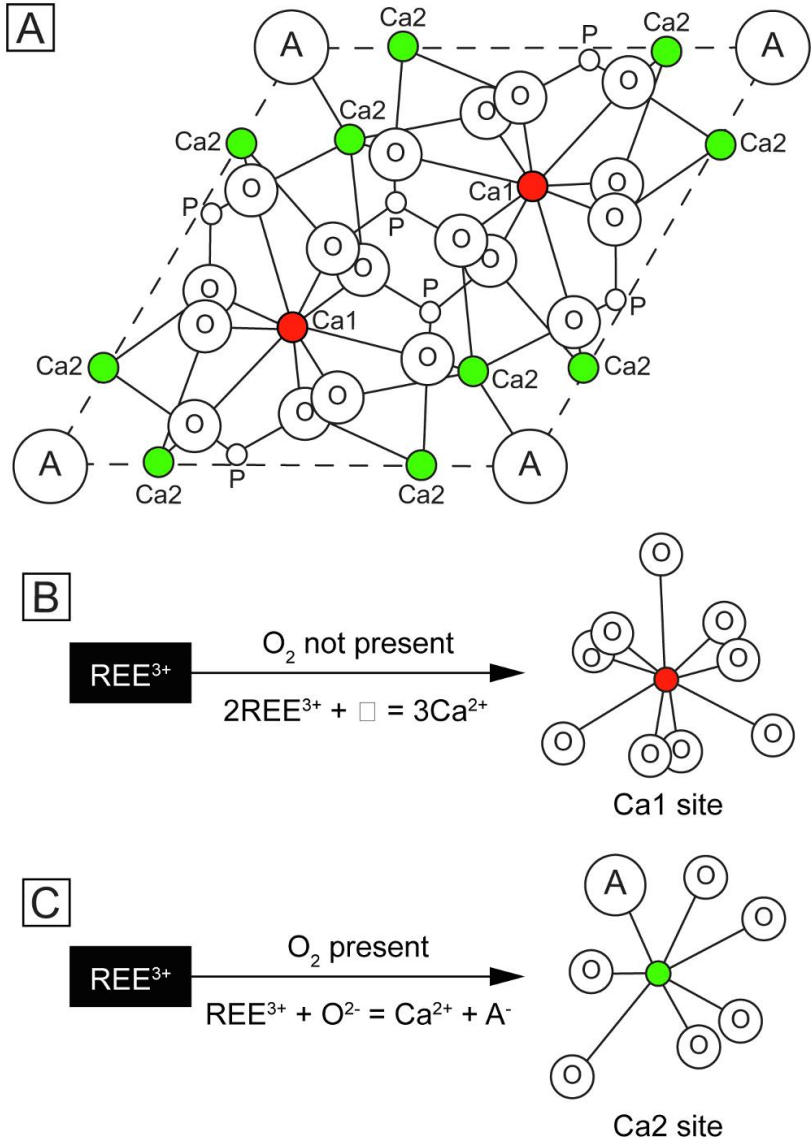
Figure 1. Scheme of occurrence of rare earth element cations (REE^{3+})
in the structure of apatite, depending on the structural position of calcium
atoms in the unit cell. Taken from an article by Amanda Garcia [104]

The first substitution reaction occurs in an oxygen-free reducing medium, while the second one occurs in an oxidizing medium. ***Thus, the presence or absence of vacancies adjacent to the Ca atoms in the structure of apatite containing admixtures of rare-earth elements (as can be judged by Raman Raman scattering spectra) allows us to judge the redox situation of apatite formation.***

Amanda Garcia [104] conducted special experiments to establish the possibility of using the rare earth element samarium as an oxygen paleo-barometer, which is of particular importance for Ediacaran and Lower Cambrian phosphorites that arose during the critical epoch of the evolution of the Earth's atmosphere. She mixed hydroxyapatite powder with 2.5 wt.% Sm_2O_3 and with 10 wt. % $SmCl_3$ solution and heated the mixture at 900 °C for 5 hours, after which the Raman spectra were studied. The extreme oxygen concentrations were 0% (argon atmosphere or vacuum) and 20.9%, with intermediate values of 0.2, 1.2 and 10% gaseous O_2.

As a result, she was shown that a change in oxygen concentration from 0 to 20.9% led to a shift in the bands in the Raman spectra of Sm^{3+} Raman scattering from 605 to 607 nm and from 652 to 654 nm. The spectral resolution of the T64000 device used by her was only 0.03 nm, which is significantly less than the observed shift in the position of the bands (which, thus, significantly exceeds analytical error.

02. "IRISH" REVIEW

As a "trigger" for the following presentation, a recent review-2020, covering 147 literary sources, served for us. The review was compiled by four co-authors from Dublin and one from Stockholm, and for simplicity we called it "Irish" [130].

Since the compilers of the Irish review practically did not use literature in Russian, it became necessary to seriously supplement it with the data given in the domestic literature, mainly in publications of the first two decades of the 21st century.

In addition, as the name shows (***The trace element composition of apatite and its application to detrital provenance studies***), the authors' main attention was focused on high-temperature *endogenous detrital apatite* from terrigenous sedimentary rocks, the composition of which allows us to fairly confidently judge the provenances, as well as apatite from endogenous ores, for example, such as apatite-magnetite "Kiruna type". At the same time, much less attention in the Irish review is paid to *low-temperature hypergenic apatitis*, which the authors call "autigenic". This is primarily fluor-carbonate-apatite (francolite) of phosphorites, as well as biogenic apatite, that is, hydroxyapatite is a component of animal teeth and bones. Therefore, in this part of the Irish review we have significantly supplemented with modern data.

1. ANIONIC MINERAL-FORMING COMPONENTS OF APATITE

1.1. Hydroxyl

Crystallization of Ca phosphate from very weakly supersaturated solutions occurs by the so-called "classical" mechanism, when ionic monomers are slowly deposited on the active growth surface. If the solution is supersaturated, then the "classical" growth mechanism gives way to the "non-classical" one, when whole ion clusters quickly settle on the active surface. In particular, the height of the steps on the surface of active growth (0.8 nm) exceeds the width of the molecular unit of 0.24 nm for the phosphate ion PO_4^{3-}, and the kinetic coefficient of attachment of the growth unit to the steps (i.e., the kinetic coefficient of the step) under physiological conditions (pH 7.4) is 100 times less than for similar ionic minerals.

This can be seen as the reason that in natural conditions biogenic **hydroxyapatite $Ca_{10}(PO_4)_6(OH)_2$** is not formed immediately, but is preceded by biophosphate-1 – or **octacalcium phosphate $Ca_8(HPO_4)_2(PO_4)_4 \cdot 5H_2O$**, or **brushite $CaHPO_4 \cdot 2H_2O$**, and with particularly strong supersaturation – **amorphous Ca-phosphate $Ca_xH_y(PO_4)_z nHO$** (n = 3–4.5). Hydroxyapatite turns out to be biophosphate-2, it is formed only by the substrate of biophosphate-1, most often – octacalcium phosphate.

Studying urolites, Syktyvkar mineralogist Valentina Katkova proved that phosphate spherulites and spherocrystals of monomineral composition in urolites are ***pseudomorphoses of carbonate hydroxyapatite by octacalcium phosphate***. In agreement with foreign predecessors [88; 133], she admits that the transformation process was the result of hydrolysis with loss of three water molecules by octocalcium phosphate at elevated pH:

$$5Ca_8H_2(PO_4)_6\ 5H_2O \Rightarrow 4\ Ca_{10}H_2(PO_4)_6\ (OH)_2 + 6\ H_3PO_4$$
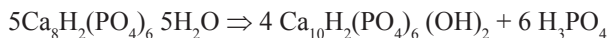
At the same time, it is noted [29, p. 12]:

"in phosphate urolites, as a rule, the main mineral components are struvite, carbonate-containing hydroxylapatite and newberyite."

It has recently been shown that based on the study of the morphology of crystals of the so-called nanohydroxyapatite (NGAP), it is possible to judge which polysaccharides were present in the environment at the origin of NGAP crystals. The fact is that natural polysaccharides play an important role in the formation of NGAP crystals in biological systems. Chinese researchers [101] synthesized NGAP crystals in the presence of four polysaccharides: pectin, carrageenan, chitosan and amylose, designated as PeHa, CaHa, CsHa and AmHa, respectively. The shape of the obtained crystals is needle-shaped/rod-shaped in all cases, and their size increases in the order of PeHa $\Rightarrow$ CaHa $\Rightarrow$ CsHa $\Rightarrow$ AmHa.

The presence of polysaccharides induces heterogeneous nucleation of NGAP and further modulates crystal growth. However, a high concentration of polysaccharides and a short reaction time are unfavorable for the growth of NGAP crystals, especially for polysaccharides with carboxyl groups. As a result, the results obtained can give an idea of the effect of polysaccharides with various chemical functional groups ($-COOH$, $-OSO_3H$, $-NH_2$, $-OH$) on the formation of NGAP crystals.

One of the natural ways of bioapatite formation (which allows for the "repair" of damaged bones) is to obtain it by metasomatic phosphatization of porous calcium carbonate structurally compatible with phosphate. It has long been known that hydroxyapatite can be obtained by treating corals with a phosphate solution, and recently a successful experiment was conducted on phosphatization of the lamellar [region] of the cuttlefish bone (Sepia officinalis). The main thing in this experiment is to first obtain an intermediate compound - amorphous carbonate. As a result, an **amorphous calcium hydrophosphate dihydrate, $CaHPO_4\ 2H_2O$**, was obtained in a short time (up to several hours) [96].

Not so long ago, it was experimentally shown that in urolithiasis (nephrolithiasis), the formation of calcium oxalate monohydrate of **whewellite $CaC_2O_4\ H_2O$** is closely related to the earlier formation of hydroxyapatite. Model experiments were

carried out that showed the full reality of the substitution of carbonate hydroxy-apatite with wevellite [125].

The fact is that the so-called Randall plaques, known to urologists for a long time, forming lighter organo-mineral spots directly in the renal tissue, in their mineral part consist just of carbonate hydroxyapatite $Ca_5(PO_4)_3OH$. Under the influence of a pathogenic decrease in the pH of urine up to pH = 4.5, Randall plaques partially dissolve, releasing Ca^{2+} into the liquid phase, and thereby induce the deposition of whewellite on them. Indeed, doctors have long known that many oxalate stones "sit" directly on Randall's plaques.

Sometimes **nitrogen admixture** is found in samples of obviously biogenic hy-droxyapatite according to EPR spectra, which, generally speaking, should not be here. As N. O. Dudchenko experimentally showed [22], nitrogen-containing radi-cals (NO_4^{2-}) are formed in samples during heat treatment of biogenic hydroxyapa-tite under conditions of lack of oxygen. During the heat treatment of the mineral in conditions of excess oxygen, such radicals are not formed. At the same time, the maximum intensity of the EPR spectrum of nitrogen-containing radicals or their maximum amount is observed during annealing in the temperature range of 800-850° C. The Ukrainian author came to the conclusion that this nitrogen-containing center is included in the structure of biogenic hydroxyapatite due to the isomor-phic substitution of phosphorus with nitrogen (P←N). Thus, the admixture of ni-trogen in natural biogenic apatite indicates that it has undergone thermal effects

Moreover, natural heating of obviously biogenic apatites can form such rare minerals as **berlinite Al[PO_4]** and **hydroxyl-ellestadite $Ca_5[(Si, P, S)O_4]_3(OH, F, Cl)$**, found in the Romanian Cyclovina cave. Since they were formed from cave guano, and it is impossible to imagine any external heating of guano, the authors of this amazing find suggested that high temperatures somehow arose in the guano itself [116]. Some materials on the topic were given in our 2011 book [80, p. 284]. The references made there to the literature are replaced here with angle brack-ets – <...>. In particular, it was reported that phosphate nodules in the Kuonam formation of the Cambrian on the Molodo River differ greatly in composition from the host (practically carbonless) black siliceous-clay mudstones. According to Siberian geologists, this indicates the biochemical (bacterial) nature of phos-phate <...>.

The source of phosphorus in phosphorites among cyanobacterial mats on Polynesian atolls is clearly biogenic <...>. Among the fused cluster-like clusters of juvenile pelicypods in Naragansett Bay (*Merceparia merceparia*) and Boca Kiega Bay in Florida (*Agropecten irradians*), microconcretions, up to 250 mi-crons in size, of amorphous Ca-phosphate (sometimes with an admixture of Al-phosphates) with a concentric-zonal structure are described. Most likely, these formations are biogenic – coprolites <...>.

1.2. Halogens

As it was shown during the study of the Magnitogorsk ore-magmatic complex of the Southern Urals, the ratio of halogens in apatite is an excellent indicator of the fluid regime in petro- and ore genesis [10]. The fact is that there are two trends of magmatic differentiation: (1) tholeiitic – the evolution of the melt towards the accumulation of iron and the formation of ferruginous gabbroids, with which the titanium-magnetite ores of the Kuibass massif are associated, and (2) calcareous-alkaline – the evolution of the melt towards an increase in its silicity and alkalinity, which reflects the change in the ferruginous magmatites of the subvolcanic and hypabyssal facies of the gabbro-granite Magnitogorsk intrusion, which is associated with skarn-magnetite mineralization. According to experimental data, the occurrence of tholeiitic and calcareous-alkaline trends in the differentiation of melts is due to the liquation orthopyroxene barrier, the overcoming of which depends on the degree of saturation of the melt with water. These trends are well documented by the content of chlorine and fluorine in apatites. As can be seen on the "chlorine - fluorine" graph compiled by the authors [10, Fig. 2, p. 31], clear fields are distinguished here by the magnitude of the Cl/F ratio:

a) in rocks of gabbro-granite intrusion Cl/F = 0.0-0.35;

(b) in oreless gabbro Cl/F = 0.35-0.90;

(c) in ore-bearing (titanium-magnetite) gabbro Cl/F = 0.90-3.40.

As it moves upward from "dry" reduced magmas to more aqueous and oxidized ones, the fluid becomes more chlorinated. Thus, the quantitative content of chlorine and fluorine in apatites of rocks and ores is a qualitative characteristic of the fluid regime during their formation.

Researchers of three North Chilean iron-phosphorus deposits (Kiruna type) of Cretaceous age in the Andes also indicate that the ratio of halogens in apatites is an important indicator of the fluid regime during their formation [118]. Despite the inconsistency of the proposed models, the authors are inclined to a new flotation model in which microliths of magmatic magnetite crystallize from a silicate melt, and then rise, carried away by bubbles of liquids dissolved in magma. As these suspensions of magmatic magnetite rise, they merge, and the magnetite content increases due to the deposition of hydrothermal magnetite in the form of rims on the primary magnetite and filling the intermediate space up to the level of neutral buoyancy, which reflects a continuous process – from magmatic to hydrothermal.

In 8 stratified trap intrusions of the Siberian Platform, the geochemistry of chlorine and fluorine in accessory apatites, as well as in rock-forming micas and amphiboles was studied according to over 1000 analyses [54]. In the overwhelming mass of apatites F > Cl. The maximum halogen contents have chlorapatite (Cl = 6.97 wt.%) and fluorapatite (F = 6.04 wt.%). The total ferruginous content (f = Fe/(Fe + Mg), at.%) of femic minerals varies: in micas from 2 to 98 at.%, in

amphiboles from 22 to 95 at.%. The graphs of the dependence of Cl - f and F - f in minerals show an increase in the content of Cl with an increase in f, and an increase in F with a decrease in f. ***Thus, chlorine exhibits pronounced ferrophilicity, and fluorine exhibits magnesiophilicity.***

In rock-forming minerals, the richest halogens are: fluorophlogopite (F = 7.06 wt.%, f = 7 at.%), chlorannite (Cl = 6.30 wt.%, f = 89 at.%), chlorferrigastingsite (Cl = 5.22 wt.%, f = 90 at.%). It is assumed that the crystallization of halogen-containing minerals occurred under conditions of increased fluid pressure of halo-carbon fluids at the levels of MW-, IW- and QIF buffers. An indicator of the reducing conditions of the magmatic process are the finds in the rocks of graphite and native metals/

Of particular interest is the thorough study of phosphate minerals from the Ural, Ozernoye and Chelyabinsk chondrites carried out in 2014, samples of which are on display at the Ural Geological Museum at the Ural State Mining University (Yekaterinburg) [24]. In all cases, chlorapatite and merrillite were found in the chondrites. **Merrilite $Ca_9Na(Fe, Mg)[PO_4]_7$** is an anhydrous terminal element of a series of 14 solid solutions, and the hydrolyzed terminal element is **whitlockite $Ca_9 (Fe, Mg) [HPO_4][PO_4]_6$.** However, contrary to earlier (less thorough) studies, vitlokit was not found in the studied chondrite samples,

The study of other meteorites has shown that merrillite is the predominant primary Ca-phosphate mineral in Martian meteorites and, consequently, on Mars. The mineral is the main phase in the study of differences in geological processes between Earth and Mars. It is assumed [82] that merrilite even has astrobiological significance – it could serve as a source of phosphorus for life on Mars!

As for the Ural meteorites, the content of Cl in 4 grains of chlorapatite from the Ural chondrite was 4.28-4.70%, in the grain of apatite "Lake" Cl = 4.09%, and in 4 grains of chlorapatite from the Chelyabinsk chondrite Cl = 3.04–4.07%. At the same time, two varieties of chlorapatite have been identified in the Chelyabinsk chondrite – extremely chlorinated and with a high content of the hydroxyl group.

Unfortunately, as our geologists note [24], the study of samples of the Ozernoye meteorite turned out to be associated with a very unsightly history. This meteorite was found in 1983 by a shepherd N. L. Hismatullin 4 km north of the Ozerny site of the Trans-Ural state farm of the Almenevsky district of the Kurgan region (about 100 km southwest of Kurgan). In 1985, the same person discovered a second piece of identical chondrite near the village of Ozernoye in the same area, so that the total mass of both fragments was about 3.66 kg. Both of them were transferred to the Ural Meteorite Commission for study, and in 2014 a small fragment from the first piece was already stored in the Ural Geological Museum (its authors studied it).

However, simultaneously with the second piece of Ozernoye chondrite, a larger fragment of a meteorite weighing 22.4 kg was discovered (in the same place – near the village of Ozernoye), but it was deliberately not handed over to specialists

for study. And in 2007, this fragment was already in Kurgan and was soon sold by the owner to the famous meteorite collector S. P. Vasiliev (living in Prague) – and with the permission of the Ministry of Culture of the Russian Federation (!) was taken to the Czech Republic… Our patriotic geologists [24] indignantly remind the reader of the complete illegality of this commerce, because according to Russian laws, "*extraterrestrial bodies that have fallen on the territory of the Russian Federation are the cultural heritage and property of Russia.*"

So, within the framework of our topic, ***chlorapatite, and especially merrilite, may turn out to be indicators of the extraterrestrial (meteoritic) genesis of the rock containing them.***

1.3. Sulfate and silica

Since one of the components included in the anionic part of apatite may be sulfate, some apatites contain sulfur. Interest in the entry of sulfur into apatite has increased markedly after the recent eruptions of volcanoes El Chicon (in Mexico) and Pinatubo (in the Philippines), whose lavas contained anhydrite, and large masses of sulfur were released into the atmosphere. Previously, anhydrite was not noted in effusions, since it was quickly dissolved by meteoric waters or disappeared even earlier - during post-magmatic hydrothermal processes. Therefore, a more stable early apatite is much more suitable for studying the magmatic geochemistry of sulfur.

In 2004, Hannoverian geochemists [119] made special experiments at 200 MPa and 800–1.100 ℃ with glass imitating the composition of rhyolite ($SiO_2 = 77.34$, $Na_2O = 4.24$, $K_2O = 4.85\%$), but without apatite components. 4 weight % apatite was added to the melt of this glass. ($CaO = 55.80$, $P_2O_5 = 42.10$, $Cl = 0.04$, $F = 3.22$ %). Subsequent addition of up to 0.5% S to the system under oxidizing conditions increased the solubility of apatite in the melt, since part of the Ca was bound to sulfur. If in the experiment the sulfur content in the melt was reduced, then with a decrease in temperature, the sulfur content in apatite also decreased. The molar coefficient of sulfur distribution between apatite and the melt $\mathbf{Kd_s}$ increased from 4.5 to 14.2 with a decrease in temperature under conditions of anhydrite undersaturation. However, in the supersaturated anhydrite melt, at 800 ℃, the $\mathbf{Kd_s}$ was lower – about 8. Thus, the $\mathbf{Kd_s}$ value depends not only on the temperature, but also on the sulfur content in the melt. As a result, these first experiments showed that, according to the sulfur content in apatite, it is possible to judge the evolution of sulfur contents in magmatic systems under oxidizing conditions.

In 2011, Italian volcanologists studied 14 samples from the lavas of two historical eruptions of Vesuvius – 1631 and 1872. It was possible to identify 5 varieties of apatite, each of which not only differs in association with other minerals, but also has clear differences in color, structure and composition [123]. For example, apatites of type-1 (yellow) and type-4 (green) are associated with large-crystalline

clinopyroxene and phlogopite, and apatites of type 2 (transparent and colorless) – with microcrystalline minerals of the cancrinite group, feldspar and opaque ore. On Si–S–P/100 triangles, these types form almost non-overlapping fields. For example, the poorest in silicon and the most sulfurous are apatites of type 3 (transparent and colorless), and the most siliceous are apatites of type 5 (aquamarine color). So, quite noticeable admixtures of silicon and sulfur, replacing phosphorus, allow us to distinguish well between different types of apatites from volcanic eruptions.

In 2013, Yekaterinburg geologists [1] described the Middle Devonian epidote-containing porphyries of trachyandesite-trachydacite composition forming a dike field in the zone of the active continental margin of the Middle Ural segment of the Ural folded belt. *A remarkable feature of these rocks is the presence of sulfur-containing apatite and igneous anhydrite*. Apatite has an oscillatory type of zoning for sulfur and progressive for fluorine. The SO_3 content varies from 0.5 to 1.5 wt. % in cores and from 0.05 to 0.2 wt. % in the borders of apatite phenocrysts. It is believed that the crystallization of sulfur-rich apatite occurred at 850–800 °C and 10^{-8} kbar. Poor in S apatite in paragenesis with anhydrite was formed at 725–700° and 7.5^{-6} kbar. The initial magma was very rich in water, sulfate-saturated and oxidized with oxygen fugacity = 0.5–1.5 log units above the NNO buffer. The source of sulfur could be both sulfide-enriched rocks of the lower crust and emanations of mantle fluids separating from mafic magmas.

In the work of Ural geologists [73] it was noted that the rocks of the Late Paleozoic Khudolazov complex, specialized for Cu-Ni mineralization, are characterized by apatites with the highest contents of sulphate sulfur (up to 0.65 wt.%), isomorphic with phosphorus in the composition of the anionic complex $(PO_4)^{3-}$. These apatites have a reduced fluorine content (< 2 wt.%) with a noticeable chlorine content (up to 1.50 wt.%). *Such a character of the ratio of halogens and sulfur in apatites can be recommended as one of the most effective indicator signs of specialization of Late Paleozoic accretion-collisional gabbrodolerites of the Western Magnitogorsk zone of the Southern Urals for Cu-Ni mineralization*. An additional criterion for such specialization is the presence of sulfide minerals rich in Cu, Ni and Co in rocks.

According to the review of Novosibirsk chemists [75], the substitution of the phosphate group with the SiO_4^{4-} silicate group gives the surface of hydroxyapatite (HAP) new properties, therefore, such Si-HAP is widely used in medicine for coating implants, synthesis of biocompatible ceramics, production of medicines and cosmetics, etc. [75, p. 478]:

"The high surface activity of Si-HAP <...> is associated with the formation of silanol groups -SiOH <...> on the surface of the material. Due to differences in the sizes of terahedral anions (distances Si–O = 0.166 nm, P–O = 0.155 nm), the substitution of phosphate ion for silicate is accompanied by microstresses in the structure of apatite. As a result, silicate ions are segregated on the surface of the particle".

During the mechanochemical synthesis of Si-HAP in a planetary mill, where monetite $CaHPO_4$, CaO and amorphous silica gel of the composition $SiO_2 \cdot nH_2O$ ($n = 0.59–0.71$) were mixed, followed by annealing at 1000 °C in a chamber electric furnace, a product with the formula was obtained: $Ca_{10}(PO_4)_{6-x}(SiO_4)_x \cdot OH_{2-x}$ where x was set equal to 0.1, 0.2, 0.4 and 0.8. For example, GAP-08 was obtained mechanochemically according to the equation:

$$5.2\ CaHPO_4 + 4.8\ CaO + 0.8\ SiO_2 \cdot 0.71\ H_2O = \\ Ca_{10}(PO_4)_{5.2}(SiO_4)_{0.8}(OH)_{1.2} + 2.568\ H_2O$$
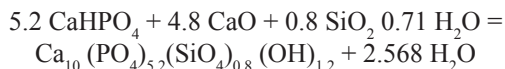
1.4. Carbonate

Carbonate radicals CO_3^{2-} can form already in bioapatite (hydroxyapatite), where they can replace both OH^- and PO_4^{3-} in the lattice. Carbonate reduces the crystallinity of apatite and makes it more amorphous and brittle. Carbonate apatites are particularly characteristic of bone tissue. In tooth tissues, they are formed in the immediate vicinity of the enamel-dentine border due to the production of anions by HCO_3^- pulp cells (odontoblasts). The formation of HCO_3^- is possible as a result of the metabolism of the aerobic microflora of plaque. The accumulation of carbonatapatite over 3-4% of the total mass of hydroxyapatite contributes to the development of caries. With age, the amount of carbonatapatites in the teeth increases.

During the formation of most *phosphorites*, carbonate-apatite (*francolite*) is formed in diagenesis, as the sediment is buried and removed from the "bottom water/sediment" boundary. In this process, as shown by V. S. Savenko and his daughter A.V. Savenko [56], there is an increase in the carbonate alkalinity of pore waters, as a result of which the initially formed precipitate of calcium phosphate begins to dissolve and return the phosphate group PO_4^{3-} to the pore waters (and then to the bottom water – *"phosphorus respiration of the sediment"*), which is replaced by the carbonate group CO_3^{2-}.

In turn, if phosphorites formed in diagenesis sink into the catagenesis zone, then as our most prominent experts Yu. N. Zanin [25] and V. Z. Bliskovsky [9] have shown, a strong decrease in carbonate content occurs in the composition of francolites, with a corresponding removal of strontium.

So, in the aspect of our topic (apatite as an indicator), the content of the CO_3^{2-} group in apatite can serve as an indicator:

(a) the mineral belongs to bioapatites;

(b) mineral formation in diagenesis;

(c) mineral changes in catagenesis.

In addition to the well-known phosphorite deposits, where the phosphate mineral is represented by diagenetic francolite, it is necessary to emphasize the ***enormous resources of francolite in the weathering crust of carbonatites of the***

unique Russian Tomtor deposit – with complex niobium-rare earth-scandium ores. The deposit is located in the north of Yakutia and is associated with one of the world's largest carbonatite complexes (Ş=300 km2) with the most significant carbonatite manifestation (12 km^2). The massif has a rounded shape in plan and a concentric zonal structure – carbonatites form its central core, and alkaline and nepheline syenites, occupying most of the area of the massif, make up the marginal zone; carbonated iyolites, significantly inferior in area to syenites, are present in the form of a crescent-shaped body separating the syenite marginal zone from the carbonatite core of the massif. Within the Tomtor massif, an indigenous iron ore deposit with resources of more than 1 billion tons has been preliminarily estimated. ***Francolite ores with P_2O_5 resources of about 500 million tons have been identified in the weathering crusts of carbonatites with average phosphorus pentoxide contents of about 17%.*** However, the main wealth of Tomtor is its unique complex rare-metal ores, which contain more than two and a half dozen components in the ore complex and which significantly exceed in their parameters the ores of the richest developed foreign rare-metal deposits of the weathering crust of Arasha and Mount Weld carbonatites.

2. CATIONIC ELEMENTS-IMPURITIES IN APATITES

As indicated in the Irish review [130], the admixture elements of igneous apatite have been successfully used as a petrogenetic tool. Very commonly used «biplots» – binary graphs where characteristic relationships are laid down along the axes, for example:

- La/Lu,
- La/Sm,
- the sum of all REE (ΣREE),
- the ratio "light REE /heavy REE" (LREE/TREE), where light REE includes elements from lanthanum to praseodymium, and heavy REE - from terbium to lutetium,
- the ratio "light REE /medium REE" (LREE/MREE), where the average REE includes elements from neodymium to gadolinium,
- Th/U,
- Sr /Y

and a number of others, in particular, the Sr/Y – LREE biplot is promoted, on which 6 fields are allocated with mutual overlaps not exceeding 15% of the field area.

2.1. REE, their "spectra" and characteristic relations

Rare earth elements (REE in English literature) are the most important impurity elements in the cationic part of apatite. They are usually divided into groups of light (LREE, La–Nd or sometimes wider, La–Gd), medium (MREE, Pm–Ho) and heavy (HREE, Er-Lu).

In the Russian literature, according to D. A. Mineev [45], a slightly different division of lanthanides into groups is accepted, used, for example, in V. V. Gordienko's article on granite pegmatites [12]. REE are divided into cerium – **ΣCe** (from La to Nd) and yttrium **ΣY** (Eu–Lu). Moreover, yttrium REE are divided into two subgroups – Y1 and Y2. It is obvious that those REE, which in the West are called "average" (MREE), in terms of Mineev are REE of the group Y1, and "heavy" – Y2.

Graphs ("spectra") have received the widest application, where the REE symbols are located along the abscissa in order of increasing their atomic number (from La = 57 to Lu = 71), and according to the ordinate – their contents in apatite, normalized most often by chondrite, and less often by "shale", that is, by the average composition of post-Archean clay shale (PAAS), calculated at the time by S. Taylor and S. McLennan [64]. Another normalization was proposed by D Piper [121] according to the composition of the "middle shale" (AS) N. America, Europe and the USSR. Normalization is usually represented by the lower index N, for example, LaN or SmN.

The REE contents used for normalization are shown in Table 1.

*Average REE contents (ppm) in chondrites and two
average "shales" used for normalization*

REE	La	Ce	Pr	Nd	Sm	Eu	Gd
Chondrites	0.3	0.5	0.1	0.6	0.2	0.08	0.4
AS	41	83	10.1	38	7.5	1.61	6.35
PAAS	38	80	8.9	32	5.6	1.1	4.7

REE	Tb	Dy	Ho	Er	Tm	Yb	Lu
Chondrites	0.05	0.35	0.07	0.2	0.04	0.2	0.035
AS	1.23	5.5	1.34	3.75	0.63	3.53	0.61
PAAS	0.77	4.4	1.0	2.9	0.4	2.8	0.43

With a strong predominance of light REN over medium and heavy, the broken curve connecting the points of the contents of individual lanthanides is strongly "upturned" on the left; with comparable contents of LREN with SRZEN + TRZEN, the curve is "flat", approaching the horizontal, and with increased contents of SRZEN, the curve in its middle part is convex - "bell-shaped". Therefore, the shape of the "spectra" (along with numerical indicators La/Lu, La/Yb or La/Sm) serves as an important element in describing the distribution of REE in apatites – and, accordingly, one of the criteria for the genetic diagnosis of apatites and their host rocks.

For example, the analysis of bioapatites of the Upper Frasnian and Lower Famenian conodonts of the Southern Urals performed by the ISP-MS method with laser ablation [30], after normalization of REE contents by PAAS, showed a bell-shaped "spectrum" shape, meaning the accumulation of average REE. The reason for the difference of the "spectrum" from the typical one for phosphates formed in equilibrium with seawater is considered to be "lithogenic effect – diagenetic enrichment of REE by bioapatite from the host sediments.

Widely used indicators, called Cerium and Europium anomalies, denoted as **Ce^A** = Ce/Ce* and **Eu^A** = Eu/Eu*, require separate consideration.

Cerium anomaly **Ce^A** = Ce/Ce*

The cerium anomaly is calculated as the ratio of analytically determined chondrite-normalized cerium (Ce$_N$) to the calculated value of Ce*, which is a "weighted" sum of normalized lanthanum and neodymium contents (i.e., as it were, the "theoretical" cerium content):

$$Ce^A = Ce_N/Ce^*, \text{ where } Ce^* = 1/3 \, (1.44La_N + 0.66 \, Nd_N).$$

Thus, $Ce^A = 3Ce_N/(1.44La_N + 0.66 \, Nd_N)$ The coefficients 1.44 and 0.66 correspond to the ratio of lanthanum, cerium and neodymium in the composite (combined sample) North American shale NASC (La = 31 ppm, Ce = 67, Nd = 34). Although there can be no negative values here, in the literature, the values of $Ce^A > 1$ are usually called "positive", and the values of CeA < 1 are "negative". It is more correct, of course, to call them excessive and deficient. However, there are works in the literature <...> in which the value of the Ce anomaly is calculated differently, according to the formula $Ce^A = \log \, [3Ce_N \, / \, (2La_N + Nd_N)]$. In this form, it can really be both negative and positive (without quotes).

As is known [80, pp. 277–288], cerium is the only element from the lanthanide group that, at Eh values characteristic of aerated waters, is able to oxidize from the form of Ce^{3+} to the form of Ce^{4+}. In this form, it is easily hydrolyzed, captured by Fe-Mn hydroxides and removed from the water. In this process, the curve of the normalized REE distribution there is a characteristic minimum of the cerium – oxygen indicator facies characteristic of modern well-aerated ocean <...>.

In 1983, by comparing the precision of the definitions of REE in surface and deep (2500 m) waters of the Atlantic and Pacific was reliably proven that with the depth of content of LREE (Ce, La, Nd, Sm) decreases, and the heavy (Eu, Gd, Dy, Er, Yb) – increasing. At the same time, among the LREE, the decrease in Ce is most sharply manifested, for example, in the North Atlantic, it decreases from 120x10-7 to 24x10-7 ppm. This global oceanic phenomenon is due to the absorption of LREE from seawater on a suspension of Fe-Mn hydroxides generated by the discharge of underwater hydrotherms. Even at a distance of up to 1400 km from the axis of the East Pacific Uplift, 90% of all manganese is in water in the form of suspended particles with a dimension of <0.4 microns <...>. As can be seen from these data, the Ce content can vary fivefold, therefore, the value of the Ce anomaly is a sensitive indicator of the fine redox zonality of the water column <...>.

In oxygen-depleted (suboxide) water the Ce/Ce* index is ~0.6–0.9, and in oxygen-free water it can reach a value of 1.0. Thus, the value of the cerium anomaly in minerals formed in former seawater is an important "paleomarine" indicator of redox conditions, i.e. conditions that existed in ancient seas, and allows us to judge the depth of apatite formation.

Europium anomaly $Eu^A = Eu/Eu^*$.

The europium anomaly is calculated as the ratio of analytically determined chondrite-normalized europium (Eu_N) to the calculated value of Eu*, which is a half-sum of the normalized contents of the neighbors of europium – samarium and gadolinium (i.e., as if the "theoretical" content of europium): $Eu^A = Eu_N/Eu^*$, where

$$Eu^* = \tfrac{1}{2} \, (Sm_N + Gd_N) \text{ Thus, } Eu^A = 2Eu_N/(Sm_N + Gd_N)$$

Although there can be no negative values here, in the literature, the values of **Eu^A** >1 are usually called "positive", and the values of **Eu^A** <1 are "negative". It is more correct, of course, to call them excessive and deficient.

Like cerium, trivalent europium – Eu(III) can also change its valence, but not oxidize, but recover to Eu(II). However, the current redox conditions of the ocean are such that even in an anoxic environment, the Eh values of seawater are not low enough to reduce europium. Therefore, both in seawater and in autigenic minerals in equilibrium with it, the value of Eu/Eu* is close to 1.

Nevertheless, there are rare cases when significantly reduced values of the Eu/Eu* index were observed in autigenic minerals, proving that the reduce of europium still took place. Such cases were noted in autigenic apatites formed not just in anoxic, but in hydrogen sulfide ("euxine") environments of diagenesis. An additional sign of such situations is not only the absence of a negative Ce anomaly, but sometimes even a positive value of the Ce/Ce* value. However, more often such cases are explained not by diagenesis, but by the penetration of reduced underwater hydrotherms into the marine sediment.

As for detritus apatites from igneous rocks, the value of Eu/Eu*<1 was observed much more often for them, since in the reducing conditions of hot magmatic melts, europium is reduced and the resulting Eu^{2+} is absorbed by the rock-forming plagioclase (where it replaces Ca^{2+}), which leads to a sharp depletion of the accessory apatite formed later by europium. ***Thus, the "negative" value of the europium anomaly in apatite indicates either detrital magmatic apatite formed in magmas with low oxygen fugacity, or (much less often) – newly formed low-temperature autigenic apatite formed in euxine (hydrogen sulfide) medium of diagenesis.***

From the literature on REE in apatites, not covered by the Irish review [130], several works, both domestic and foreign, deserve attention.

In 2013, a major Novosibirsk geochemist, German Kolonin, performed (in collaboration with G. P. Shironosova) thermodynamic modeling of the association of apatite with monazite, which is important for petrogenesis. The authors wrote [78, p. 455]:

"A close association of apatite with monazite has been noted, while either monazite inclusions are observed in fluorapatite, or fluorapatite crowns sometimes with xenotime and allanite are the result of monazite substitution <...>."

Their calculations, in accordance with the data of their predecessors, showed that dark apatites with monazite inclusions are formed at 300-400 ° C.

In 2007, R. Kolonin and co-authors [32] studied a heterogeneous collection of monazites (including our Timan ones, from the collection of I. V. Shvetsova). Comparing the composition of monazites with the known thermodynamic data on the solubility of monazite and xenotime, he came to the conclusion that mona-

zites crystallized from acidic fluids (in which the REE content can be two orders of magnitude higher than in alkaline ones) and especially from low-temperature ones can be highly enriched with yttrium and heavy lanthanides [32]. ***Thus, the accumulation of yttrium and heavy REE in monazite may indicate its low-temperature nature and the acidic nature of the hydrothermal fluid.***

As shown by the Moscow region mineralogists who conducted experiments in "crustal" conditions, i.e. at P = 0.5 GPA, and T = 1200 °C, for the elements REE, Y, Th (as well as Cu and W), the coefficient of distribution D between apatite Apt and carbonate melt L_{carb} exceeds one [11]:

"Therefore, compared to the carbonate melt, Apt is a more efficient concentrator for the elements."

At the same time, a remarkable difference was found in the behavior of light and heavy REE – namely, the different dependence of their D on the atomic number (i.e., on the atomic weight): for light REE (from La to Eu), the D numbers increase with growth, and for heavy REE they decrease!

2.2. Strontium and manganese

As shown in the Irish review [130], the "Sr – Mn" biplot in detrital magmatic apatite is useful for determining both the degree of fractionation of the parent magma and for assessing the oxygen fugacity in the former melt. Usually, the Sr/Mn ratio of magmatic apatite makes it possible to distinguish three situations:

(1) the value of Sr/Mn is very low; such is apatite from highly fractionated melts due to the increased content of manganese (up to 1 wt.% or even more);

(2) the value of Sr/Mn is close to unity (1:1); such is apatite from igneous granitoids of type I, where the contents of both Sr and Mn are tens or several hundred ppm;

(3) the value of Sr/Mn is very high; such is apatite from mafic melts, in which the Sr contents reach several thousand ppm (i.e. 0.n%!), which was shown in particular in one of the works of E. A. Belousova and colleagues [85], while detrital apatite from ultrabasic rocks can be easily distinguished from apatite basites, since the former is much richer in strontium and extremely depleted in relation to severe REE.

Of the works not covered by the Irish review, one can note the recent acutely critical article by Jeffrey Bromley [86], "*Do concentrations of Mn, Eu and Ce in apatite reliably record oxygen fugacity in magmas*?" He came to the conclusion that Eu and Ce are not suitable for this, but the content of apatite manganese can be used with caution as a redox-sensitive indicator.

The correlation of the manganese distribution coefficients between apatite and the host rock as a function of the silicity of the rock (and the parent magma, respectively), for which the ASI alumina indices and polymerization indices were calculated, allows us to propose a model in which the Mn content in apatite largely

depends on the structure of the melt. In more developed magmatic systems, a decrease in the availability of non-conjoining oxides in silicate melts transforms Mn from an incompatible element into an increasingly compatible element in apatite.

2.3. Uranium and thorium

In the article of the Chinese team [127], the **Th/U** ratio in the bioapatite of conodonts was used together with the value of **Ce^A** to assess redox conditions in ancient seas on the territory of Southern China. As is known, uranium has two different states: under oxygen conditions, U^{6+} is stable and highly soluble, but it turns into insoluble U^{4+} in oxygen-free waters, while the solubility of Th is not affected by redox changes. This leads to an increase in the **Th/U** ratio in anoxic facies. If the degree of oceanic anoxia becomes significant, as it was assumed for the early Triassic, then the uranium reservoir in the ocean will be depleted, which will lead to an increase in the **Th/U** ratio.

From other works, where the uranium content in apatite is given, the unique deposit of metalliferous (uranium-rare earth) bone detritus Melovoye, located within the Southern Mangyshlak (Kazakhstan), is of particular interest [7]. Here, native minerals of uranium and rare earths were recorded as part of bone bioapatite: uraninite UO_2, coffinite USO_4, ningioite $(U, Ca, Ce)_2[PO_4]_2(1–2)H_2O$, otenite $Ca_2[UO_2][PO_4]_2(8–12)H_2O$ and cherchite $YPO_4(2H_2O)$.

The deposit, formed in the Oligocene–early Miocene, was a series of bed-like deposits consisting of bone detritus of fish (ichthyolites) and marine animals with abundant inclusions of iron sulfides and admixture of terrigenous material. The phenomenon of accumulation of a colossal mass of biogenic phosphate material enriched with rare metals at the bottom of a reservoir is of interest from the point of view of the evolution of biogeological systems. The accumulation of uranium and REE in this and similar deposits occurred in several stages due to a series of reducing and oxidizing episodes during the formation of ore layers. The circulation of thermal metalliferous solutions coming from deep horizons of the sedimentary strata could also have a certain effect on the ore process.

It should be noted that according to the estimates of foreign experts [79], the extraction of uranium from phosphate fertilizers is not only economically justified, but also environmentally important, since it cleanses them from undesirable impurities. It is noted that, depending on the origin of phosphate minerals, the concentration of uranium can vary from 150 mg/kg (francolite in sedimentary rocks) to 220 mg/kg in ores of volcanic origin. From phosphate ores, which have reserves in dozens of countries around the world, it is possible to extract from 9 to 22 million tons of uranium. This would make it possible to ensure the supply of uranium for nuclear power for 440 years at the price of uranium obtained from traditional sources. Technologically, the extraction of uranium from mineral raw materials during the production of phosphate fertilizers is not very difficult. In a number

of countries, including the USA and Germany, uranium was obtained from phosphate ores in significant quantities as long as it was economically feasible. For all countries with reserves of phosphate minerals, it is important to understand that the use of uranium extracted from ore in the production of phosphorus fertilizers will make it possible to use cleaner fertilizers, and therefore will help prevent contamination of the soil, natural reservoirs and the atmosphere.

2.4. Other elements-impurities in apatites

In 2013, Russian geochemists discovered that native gold particles of 5-30 microns in size, with a probity of 875-990 are visible on the surface of biogenic apatite from the reference sections of the Lower Paleozoic of Sweden, the southern coast of the Gulf of Finland and the Ladoga region. [65]. Data are presented that indicate the redistribution of Au in the thickness of the Lower Paleozoic sediments of Baltoscandia, followed by sorption on biogenic apatite under the influence of a slightly acidic fluid with a temperature below 80 °C. The $^{87}Sr/^{86}Sr$ value of such a fluid was significantly lower than the values characteristic of the Early Paleozoic oceanic reservoir, which, taking into account the absence of sedimentary carbonates with low $^{87}Sr/^{86}Sr$ values in the Phanerozoic section in the northwest of the East European Platform, may indicate the juvenile nature of the fluid.

The American team analyzed 171 apatite phenocrystals from 4 consecutive layers of K-bentonites from outcrops in the north of the Mississippi Valley in the Caradoc Decor formation [99]. Each grain was analyzed at several points from 3 to 6 times for REE and other impurity elements. The contents of magnesium and manganese were the most variable. According to them, a diagnostic graph was constructed in the coordinates Mg (0.01–0.18 %) – Mn (0.0–0.08 %). In this graph, the of dots of each bentonite formation (in the amount from 29 to 47) differed well. Thus, it was proved that the composition of apatites can be used for stratigraphic correlation of bentonites.

3. ISOTOPIC RATIOS IN APATITES

The components of apatite with the general simplified formula $Ca_5[PO_4]_3$ (OH, F, Cl) may have isotopic variations carrying important genetic information. In particular, isotopic ratios were studied:
– rock-forming Ca;
– rock-forming O;
– a small element Sr, isomorphically substituting Ca;
– rare lanthanide Nd, isomorphically substituting Ca.
But if only a few papers have been devoted to the isotopy of Ca in apatites, then dozens of studies have already been devoted to the isotopy of phosphate O and Sr, and recently work on the isotopy of Nd has also increased dramatically.

3.1. Calcium

It is known that with the "classical" mechanism of growth from a solution of Ca-containing crystals, the solid phase is enriched with a light isotope of calcium – ^{43}Ca. If crystallization occurs according to a "non-classical mechanism", in particular, when whole clusters are captured on the active growth surface, then it can be expected that no significant fractionation of Ca isotopes will occur. This idea was tested in experiments carried out in 2018 by Catherine Schilling and colleagues [124], using the most modern, extremely fine methods - with mineralogical characterization and nanoscale visualization of growth features to determine the high-speed fractionation of Ca isotopes during the seed growth of hydroxyapatite (HAP) with the participation of a precursor – octacalcium phosphate (OCP). It turned out, in particular, that the growth rates are greatly weakened with an increase in pH, because the binding of OH ions of Ca2+ prevents the precipitation of phosphate. Nanoscale images of the surface topography showed direct deposition of primary particles on the surface of micron HAP crystals after steady growth, ***visually proving the dominance of the non-classical hydroxyapate growth pathway.*** At the same time, as expected, the difference in the isotopic composition of Ca between the initial solution and the precipitated phases of phosphates turned out to be insignificant – within the limits of the analysis error.

3.2. Strontium

As is known, the method of strontium isotope chemostratigraphy is based on the fact that the $^{87}Sr/^{86}Sr$ ratio is currently homogeneous in the World Ocean, which has been the case throughout the entire existence of the oceans. The fact is that the residence time of Sr in the ocean exceeds the time of complete mixing of all the sea waters of the Earth, which leads to the homogenization of the isotopic composition of strontium in seawater

In the geological history of the Earth, the isotopic composition of strontium in seawater has changed. The $^{87}Sr/^{86}Sr$ ratio in seawater is controlled by mixing the following sources:

1) continental runoff resulting from the weathering of the earth's crust by surface and river waters;

2) hydrothermal flow arising from the interaction of seawater with volcanic rocks in the area of mid-Oceanic ridges (MOR);

3) the flow resulting from the dissolution and recrystallization of marine carbonate sediments.

Strontium chemostratigraphy of pelagic sediments is based on the determination the age of sediment by the ratio of strontium isotopes ($^{87}Sr/^{86}Sr$) in biogenic foraminifera carbonate or bone detritus apatite. In the pelagial of the ocean, fossilized remains of fish (ichthyolites) preserve the isotopic composition of strontium of ocean waters at the time of fish life, therefore, the isotopic composition of strontium of ichthyolites can be used to determine their age.

As an example of the successful application of the strontium method, we can name the precision work of Russian geochemists dedicated to determining the age of only two ichthyolites, 34.7×30.3×6.2 mm and 40.2×26.5×9.5 mm in size, sealed in the Cape Basin in the southern part of the Atlantic Ocean [59]. The age of the tooth enamel of sample 2188/5 was 6.6±0.3 million years, and sample 2188/4 was 5.2±0.2 million years. Thus, the use of a complex (mechanical and chemical) technique for cleaning tooth enamel from the nuclear part of the Fe-Mn nodules of the Cape Basin from Fe and Mn oxyhydroxides made it possible to reliably determine the isotopic composition of Sr in biogenic apatite.

Some materials on the isotopy of phosphate strontium were contained in our 2011 book (all references made there are replaced here with angle brackets <...>. In particular, it was reported [80, pp. 99, 439] that a molar of a terrestrial mammal (Gomphotera) was found in the pebbles of Miocene sandstone south of Stockholm. Isotopic analysis of the elements of the phosphate substance of enamel (C, O, Sr, Nd) was compared with that of the host rocks and with analyses of other bone residues of the same age in Sweden and the Center. Europe. The value $^{87}Sr/^{86}Sr$ (0.71592) is typical for ancient rocks and is significantly higher than in the teeth of phosphate residues from the Center. Europe (from 0.70650 to 0.71063, according to 17 analyses). The value $^{87}Sr/^{86}Sr$ (0.71592) is typical for ancient rocks and is significantly higher than in the teeth of phosphate residues from the Center. Europe (from 0.70650 to 0.71063, according to 17 analyses).

The general conclusion is as follows: in the Miocene in Scandinavia there were terrigenous deposits with mammalian fauna that were eroded during the Pleistocene glaciationδ). In particular, it was reported [SK-2011, pp. 99, 439] that a molar of a terrestrial mammal (Gomphother) was found in the pebbles of Miocene sandstone south of Stockholm. Isotopic analysis of the elements of the phosphate substance of enamel (C, O, Sr, Nd) was compared with that of the host

rocks and with analyses of other bone residues of the same age in Sweden and the Center. Europe. The value 87Sr/86Sr (0.71592) is typical for ancient rocks and is significantly higher than in the teeth of phosphate residues from the Center. Europe (from 0.70650 to 0.71063, according to 17 analyses).

Since modern autigenic francolites show exactly the same $^{87}Sr/^{86}Sr$ ratio as in seawater (0.70916), it is logical to assume that ancient phosphorites also inherit the isotopic ratio of the age-appropriate seawater. At the same time, ***it turns out that during metasomatic phosphatization of limestones, primary carbonate strontium is completely exchanged for strontium of seawater***. This means that the $^{87}Sr/^{86}Sr$ value in phosphorites, compared with the "standard geochronological curve" constructed from carbonate rocks, can date phosphorites. So, phosphates desert Sechura in Peru showed the age 11.8 ± 0.5 million years, offshore Namibia – 1.15 ± 0.25 million years, at an underwater ridge Chatham – 4.90 ± 0.35 million years, which is consistent with other (independent) age <...>.

There are examples of using isotope of strontium and for high-temperature magmatic and hydrothermal apatite. Thus, Murmansk geologists [40] determined the isotopic composition of strontium hydrothermal apatites and francolites formed in the post-carbonatite stage of development of the Kovdorsky foscorite-carbonatite complex. The values of $^{87}Sr/^{86}Sr$ obtained by them were 0.7036-0.7059, whereas the known average value for carbonatites is 0.7043. Values below the "middle carbonatite" (characteristic of the calcite stage of the Kovdorsky complex) are treated as mantle, and those above (characteristic of the later dolomite stage of the Kovdorsky complex) are treated as typical of the crust.

3.3. Oxygen

As you know, the Cenozoic was a period of gradual transition from greenhouse conditions to glacier conditions, and this process was not smooth, but was interrupted by sharp cold spells. Two such breaks occurred at the boundary of the Eocene and Oligocene and in the Middle Miocene. Both were found to be associated with the growth of the East Antarctic ice sheet.

Cenozoic climate changes were intensively studied mainly from the archives of deep-sea sediments using the value $\delta^{18}O$. Most of these determinations were made using the $\delta^{18}O$ data in benthic foraminifera carbonate. However, these values of $\delta^{18}O$ reflect only the temperature of the ocean bottom waters, as well as the salinity and volume of ice. The oscillation amplitudes do not always correctly reflect the change in air temperature on the surface of the continent.

Therefore, the method of climatic reconstructions by the value $\delta^{18}O$ of bones and teeth of herbivorous mammals was proposed and successfully used, because it reflects the composition of drinking water of these animals, which, in turn, was closely related to the air temperature on the continent. The obvious disadvantage of this method is the comparative rarity of finding the remains of large mammals, moreover, concentrated in a relatively short period of time.

In this sense, the technique of paleoclimatic reconstructions according to $\delta^{18}O$ of rodent teeth has obvious advantages. An example is the work on Southern. Germany with an abundance of such localities, which made it possible to give a paleoclimatic reconstruction covering the period from the Late Eocene to the Miocene [106]. The authors managed to show that the air temperature in the South. Germany in the period from the late Eocene to the beginning of the Late Miocene ranged from 12 °C to 25 °C, and at the Eocene/Oligocene boundary, the average decrease in air temperature was either ~2 °C (taking into account classical biostratigraphy) or ~6 °C (taking into account the revised biostratigraphy).

Changes in the humidity of the climate on the territory of Chad (Central Africa) were tried to clarify with the help of oxygen isotopy in the apatite of tooth enamel of freshwater fish, during the Upper Miocene – in Messinian, covering the period between $7,246 \pm 0.005$ million and $5,332 \pm 0.005$ million years ago [117]. It turned out that the most open habitat of fish, with a lower content of $\delta^{18}O$ in *Hydroconus* teeth, existed in four Chadian vertebrate localities – Toros-Menalla, Kossom-Bugudi, Kolle and Koro-Toro, dated respectively 7.04 ± 0.18 Ma, 5.26 ± 0.23 Ma, 3.96 ± 0.48 Ma and 3.58 ± 0.27 Ma. The value of $\delta^{18}O$ increases by ~2 in two locations corresponding to the age of the Messinian; there is also a slight increase by ~0.6 in three Pliocene locations. These results reflect a change in the precipitation regime in the Center. Africa during the Late Neogene.

Oxygen isotopy in the bioapatites of ichthyolites and conodonts in the lower carboniferous layers on the Northern Ireland made it possible to confirm the data on permocarbon glaciation [83]. Compared with normal seawater, the values of $\delta^{18}O$ phosphate oxygen were shifted by +2.4%. This was the result of an increase in the volume of ice during a cooling of 4.5°C on the surface of the equatorial sea between the beginning of the Asbian and the middle of the Brigantine time of the late Vise. It is shown that the $\delta^{18}O$ apatite of conodonts and ichthyolites reflect the stabilization of the climate of the "ice house" during the Brant-Serpukhov time. The Visean cooling revealed on the basis of $\delta^{18}O$ is consistent with global glacioeustatic data.

Positive excursions of isotopic characteristics were recorded in the phosphate of ***conodonts of Mississippian age***: $\delta^{18}O$ to +2 and up to +1.5 - for late Tourne and Serpukhov, and in carbon $\delta^{13}C_{carb}$, respectively, to +6.5 and up to +5 [89]. This ratio may mean that the Serpukhov cold snap occurred before the accumulation of carbonaceous precipitation (i.e., the latter was not the cause of the cold snap?). In general, these isotopic data indicate that the first big cold snap began already in the tour (even with possible glaciation?), the first known glaciation manifested itself in the Vise, and the second – in Serpukhov Oxygen data are interpreted as direct indications of cooling and an increase in the volume of ice. Carbon data (both S_{org} and S_{carb}) can be associated with the burial of S_{org} in black shales, which lowers the CO_2 content in the atmosphere and, as a result, causes cooling.

As is known, in Pennsylvania–early Permian there was a high-latitude glacia-

tion in Antarctica and the adjacent continents of Gondwana. The beginning of glaciation dates back to the Serpukhov-Bashkir century, and the first maximum glaciation reached in the Moscow century. In the Gzhel century, the area of glaciation decreased, but increased again in the early Permian, reaching a second maximum in the Assel-Sakmar time. The study of the Pennsylvania sediments showed frequent cyclical expansion and contraction of the Gondwanan cover glaciers, which generated corresponding fluctuations in sea level.

In 2006, German authors [108] studied the oxygen isotopy in the bioapatite of Midcontinent conodonts to assess glacio-eustatic sea level fluctuations in Pennsylvania (Middle-Late Carboniferous). It is known that in the Pennsylvanian time, the ocean covered most of the Midcontinent. The northern and central part of the Midcontinent basin was relatively shallower, and the basin deepened to the south. This pool was open to the Pantalassa Ocean to the Z and NW. The Pennsylvania deposits of the Midcontinent are represented by a cyclic alternation of thin layers of transgressive limestones, offshore gray to black phosphate shales and thicker layers of regressive limestones. These cycles are underlain and overlapped by coastal or terrestrial shales with paleosols and coals. ***Glacioeustatic fluctuations in sea level are considered as the main cause that generated cycles.***

$\delta^{18}O_{phosph}$ were obtained in comparison with the Vienna Standard of Mean value for seawater (VSMOW): The following average values of $\delta^{18}O_{phosph}$ were obtained:

black shales = 20.1 ± 0.5%,
gray shales = 20.5 ± 0.5%,
regressive limestones = 21.0 ± 0.3%,
transgressive limestones = 21.1 ± 0.6‰,

The maximum difference of values $\delta^{18}O_{phosph}$ for individual data between shales and limestones is 1.7%. This difference compares well with the difference obtained for Pleistocene equatorial intraglacial and interglacial shallow-water foraminifera, which confirms the reliability of the figures obtained from conodont phosphate. However, since the Pennsylvanian glacial maxima are represented by terrestrial facies that are not documented by conodonts, glacio-eustatic sea level fluctuations in Pennsylvania were probably greater than 120 m, reached in the Pleistocene.

Some materials on the isotopy of phosphate oxygen were given in our 2011 book (all references made there are replaced here with angle brackets <...>).

In particular, there was shown, that with $\delta^{18}O_{phosph}$ of fossil bone remains it is possible to judge the climate in which mammals lived $\delta^{18}O_{phosph}$ of hydroxylapatite of their bones and teeth, in particular tooth enamel (in which fluorapatite is also present) is very informative. And since the value of $\delta^{18}O_{H2O}$ depends on the climate, it is indicated there [80, p. 165] that important climatic information can be obtained by the value of $\delta^{18}O_{phosph}$ of biogenic phosphates, since the oxygen-isotopic composition of the water that terrestrial mammals drink (and herbivores, in addition, receive as part of the green mass they eat) directly affects the value of <...> $\delta^{18}O_{phosph}$, significantly less than the first [80, p. 166].

The reason for these differences is the determining influence of the mountain barrier on the humidity of the climate. Despite seasonal complications, the Sierra Nevada ridge with an average height of 2800 m clearly divides the humid climate area to the west, at a distance of about 300-350 km to the Pacific coast – from the arid climate area to the east of the ridge. This is because the winds that carry masses of moist air from the Pacific Ocean to the east, reaching the barrier of the Sierra Nevada, lose up to 90% of moisture in the form of precipitation. Direct measurements of the isotopic composition of precipitation showed that to the west of the Sierra Nevada, the values of δO_{H2O} (SMOW) are – (3–10), on the ridge itself they drop sharply by 6–7 % and further east at a distance of 400–1100 km from the coast they remain at the level of –(12–16) % <...> δO_{H2O} (SMOW)) in precipitation (in the form of rain or snow.

This phenomenon has received the beautiful name of the isotopic "rain shadow" The higher the barrier, the stronger its isotopic "rain shadow". On average, for our planet, the gradient of decreasing magnitude is is –0.28 % for every 100 m of increase in the height of the mountain barrier.

Analysis of the isotopic composition of phosphate oxygen from the famous location of Neogene mammals in southern Germany [80, p. 221] allowed us to make amazing reconstructions: to determine what water (lake or rain) lake turtles, small and large terrestrial mammals drank – Table 2

Table 2.

Isotopic composition of phosphate oxygen of paleontological remains of Lake Steinheim and its probable interpretation Compiled according to T. Tuetken et al., 2006. <...>

Objects	Number of analyses	$\delta^{18}O_{phosph} = \delta^{18}O_{H2O}$, ‰ SMOW	Interpretation
The bones of the shell of fresh-water turtles	6	+2.0 ± 0.4	Such was the isotopic composition of oxygen in the lake water
Tooth enamel of small mammals	7	+2.7 ± 2.3	Such water was drunk by small mammals; therefore, they drank lake water
Tooth enamel of large mammals	31	–5.9 ± 1.7	Such water was drunk by large mammals; therefore, they did not drink lake water, but rain water

Measurements of the value of δIn the carbonate substance of phosphate-bearing carbonaceous diatoms on the shelf of Namibia [80, p. 329], the value of $\delta^{18}O_{phosph}$ (Holocene-Pleistocene nodules, bones of fish and marine mammals) give temperatures in the range from 10.9 to 14.8°C, which is also quite plausible for

upwelling zones with their cool waters $\delta^{18}O_{cars}$ (SMOW) is 30.4 %, which fully corresponds to the temperature of surface waters equal to 18.8 <...>.

A comparison of the values of $\delta^{18}O_{phosph}$ in two types of Upper Cretaceous and Paleocene/Eocene phosphate fossils of Tunisia – in shark teeth and in coprolites – showed that, on average, the phosphate oxygen of the former is about 0.4 % lighter than the latter: 19.2–20.5 % vs. 20.4–21.2 % [80, pp. 377-378]. This small but significant shift reflects the temperature difference of the bathymetric facies in which the phosphate was located: coprolites were formed mainly in the higher warm layers of the water column, whereas shark teeth were buried mainly in the pelagial, where the phosphate reached isotopic equilibrium with colder waters <...>.

Autigenic phosphate mineralization in carbonaceous silts of Peruvian upwelling shows values of $\delta^{18}O_{phosph}$ in the range of 20.2-24.8 % [80, p. 453]. At the same time, phosphates formed from an "impersonal" phosphorus resource near the water boundary/sediment, have values of $\delta^{18}O_{phosph}$ equilibrium with seawater, whereas phosphates in deeper sediment horizons, genetically related to the P_{org} that entered the pore waters from the organic matte are more or less disequilibrium in terms of values of <...>.

However, in ocean sediments to the north of Africa, disequilibrium is established, on the contrary, in the surface layers. Although there is no unambiguous interpretation of the discovered phenomenon, among the possible factors is the sedimentation rate, when bacterial phosphate consumption does not keep pace with its release from the buried organic matter <...>. If this version is true, then the isotopic composition of phosphate oxygen could serve as an indirect characteristic of the subtle features of diagenesis.

In the siliceous-phosphate black shales of the Chatkalo-Naryn structural zone of the North the Tien Shan, the oxygen isotopic composition of carbon-siliceous-phosphate nodules was found to be facilitated, in which the average value of $\delta^{18}O$ is +15.6 %, whereas in the host silicites this value is significantly higher than +(26-27) %. It is believed that the oxygen relief of autigenic phosphate and flint is directly related to the intensity of diagenesis, since the value $\delta^{18}O$ positively correlates with the phosphate content in the studied nodules/

Finally, the data [80, p. 334] on the development of the so-called phosphate paleothermometer are very interesting. When phosphate is deposited in equilibrium with seawater, isotopic exchange is possible according to the scheme: $H_2^{18}O$ + 1/4 $[P^{16}O_4]^{3-}$ (water) $\Rightarrow H_2^{16}O$ + 1/4 $[P^{18}O_4]^{2-}$ (phosphate). After a series of not entirely successful experiments, A. Longinelli was still able to establish a linear relationship between temperature and the value of the isotopic densification $\delta^{18}O$:

$$T°C = -80.0 - 4.8 \ (\delta^{18}O_{phosph} - A).$$

Thus, if syngenetic carbonates and phosphates are present in the rock (or, better, if phosphate forms an impurity in the carbonate), then the use of two independent thermometers seems to allow an absolute estimate of the paleotemperature.

At the same time, the isotopic shift in the formation of phosphate is greater than in the formation of carbonate and averages 12%. This situation, apparently, only favors an increase in the accuracy of paleothermometry. Unfortunately, as R. Bowen points out <...>, isotopic measurement of phosphate oxygen is a very difficult task, since natural phosphates contain impurities of non-phosphate oxygen in the form of OH and CO3. Nevertheless, R. Bowen (who was only aware of the preliminary results of A. Longinelli's work) optimistically assessed the possibilities of the phosphate thermometer <...>

3.4. Carbon

Using the isotopy of phosphate carbon of conodonts, it was possible to confirm the global nature of the Late Ordovician cooling [98]. The samples of marine phosphates represented the section interval of the late Ordovician corresponding to ~10 million years before the Hirnant glaciation. The authors found out whether the climatic fluctuations of the orbital scale controlled the growth and melting of continental glaciers, which led to glacial-eustatic changes in sea level and the development of widespread marine sedimentary cycles. The values of $\delta^{18}O$ of conodont apatite from 14 cycles of the Late Ordovician (Catian) vary from ~17 to 21. Isotopic indices are minimal in deep-sea facies and maximal in shallow-water facies, which confirms the hypothesis that glacioeustasy was the dominant factor in controlling the depth of the sea. The measured intracycle changes in $\delta^{18}O$ (0.7–2.5%) were controlled by changes in ice volume (sea level changes <60 m), sea surface temperature (<5 °C) and potentially a local increase in seawater evaporation during drier and/or windier glacial stages. These isotopic interpretations confirm recent interpretations of the dynamic and long transition of the Ordovician greenhouse (greenhouse) to the glacier (ice house).

Permafrost conditions in the northeastern regions of Siberia allowed the remains of large mammals that lived in these territories in earlier Cenozoic epochs to be preserved here. Horse mummies are quite rare among them, but bone remains are ubiquitous. In 2013, a predominantly Russian team of authors [17] performed complex isotopic studies of five mummies and several bones of Late Pleistocene horses found in the north of Yakutia. The obtained results suggest that the carbon isotopic composition of carbonate hydroxyapatite of Yakut horse bones can be used as a paleoclimatic indicator.

It was established in which climatic conditions the horses lived (warm or cold, wet or dry), the remains of which were investigated. According to preliminary data, the habitat conditions of Late Pleistocene horses of Yakutia and Zap. Europe was close. The authors cite the graph "Evolution of the carbon isotope composition of hydroxyl-apatite carbonate of the bones of large herbivores of Northern Yakutia in the late Pleistocene", where the values of $\delta^{13}C_{carb}$ in the range from –11 to –16 % are plotted on the abscissa, and three "*marine climatic stages*" are plotted on the ordinate, up to 12 (?) thousand years ago (1), up to 25 thousand years

(2) and up to 50 thousand years (3). Note that no trend is visible on the graph. The authors themselves interpret the graph as follows [17, p. 98]:

"A possible conclusion is the instability of the Late Pleistocene climate of Northern Yakutia, which was expressed in sharp short-term (500–2000 years) irregular episodes of relatively mild climate, having the rank of interstadials in intensity".

3.5. Neodymium

Recently, the rare-earth element neodymium has become extremely popular, according to the ratio of isotopes of which the value of "epsilon neodymium" – εNd is calculated. The neodymium isotope ^{143}Nd is formed as a result of alpha decay of ^{147}Sm, with parameters $= 6.54 \times 10^{-12}$, $T1/2 = 10.06 \times 10^{11}$ years.

The isotopic composition of neodymium is usually depicted εNd – the $^{143}Nd/^{144}Nd$ (R) isotope ratio normalized by chondrite:

$$\varepsilon Nd = (R_S / R_{CHUR} - 1), \text{ in ten thousandths.}$$

Here R_S is the $^{143}Nd/^{144}Nd$ in the sample, and R_{CHUR} is the value of $^{143}Nd/^{144}Nd$ in CHUR – "chondritic uniform reservoir", which is assumed to be **0.512638**.

Since the continental crust has a smaller Sm/Nd ratio than the mantle, the mantle (and its young magmatic derivatives) has a $^{143}Nd/^{144}Nd$ ratio higher than the Earth as a whole – and, accordingly, negative values of εNd

On the contrary, ancient crustal rocks have $^{143}Nd/^{144}Nd$ lower than in the Earth as a whole, and positive values of εNd – the more negative the older the rocks

As G. Faure writes in his remarkable book [66, p. 223]:

"The model assumes that the terrestrial Nd evolved in a homogeneous reservoir, the Sm/Nd ratio in which is equal to this ratio in chondrite meteorites. The current value of $^{143}Nd/^{144}Nd$ in this reservoir is 0.512638 relative to $^{146}Nd/^{144}Nd =0.7219$.

The current ratio ($^{147}Sm/^{144}Nd$) in CHUR is 0.1967. This information allows us to calculate the ratio $^{146}Nd/^{144}Nd$ in CHUR at any other time t in the past <...>".

It should be noted that at present, the literature on the use of the value "epsilon neodymium" for the diagnosis of the petrofund of marine sediments has become so extensive that it can be considered practically unlimited.

Without fear of seeming immodest, it can be noted that one of the good reviews can be found in our book-2011 [80, p. 100–102] (we omit references to the literature used here and replace them with angle brackets). In this case, the value εNd is often used in conjunction with the value ISr = $^{87}Sr/^{86}Sr$.

In the stratigraphic sequence, examples of such use relate to Precambrian sediments <...>; Paleozoic, in particular, Cambro-Ordovician and Upper Ordovician carbonates and phosphates <...>; Mesozoic, including for the Upper Cretaceous

anoxic event OAE-2 <...>; Cenozoic, including for young sediments of the Labrador Sea <...>, the Indian Ocean <...>, the flysch strata of Kamchatka and the South of the Koryak Ridge <...>, for alluvial sediments of the Indo-Gangetic plain <...>, young sediments of the Central Basin of the Indian Ocean <...>.

In the aspect of this review (apatite as a geological indicator), we note that there are data in this book [80] directly related to our topic – on the use of *εNd* in the apatite of conodonts. In particular, it is noted that the comparison of two remote sections of Upper Ordovician carbonates – in Saskatchewan and Iowa – showed synchronous fluctuations in the value of *εNd*: the alternation of two characteristic maxima and minima in seawater <...>.

These fluctuations, thus acquiring important stratigraphic significance, are explained by the changing contributions of two provenance with significantly different isotopic characteristics: (a) low-lying Precambrian basement, in the rocks of which value of *εNd* ranges from –22 to –15, and (b) young the high-altitude Taconian orogen with *εNd* in the range from –6 to –9.

The expansion of the transgression of the epicontinental Ordovician sea (and, accordingly, in carbonates) increased; regression led to the opposite result

The Upper Cretaceous and Cenozoic strata of the Kamchatka flysch and the south of the Koryak Ridge had at least two petrofunds. One of them was juvenile – suprasubduction volcanic complexes, to a lesser extent basalts of MOR or back-arc basins. This petrofund is characterized by low $^{87}Sr/^{86}Sr$ ratios and high values of *εNd(T)* <...>

Another source was apparently represented by complexes of ancient continental crust. This petrofund is characterized by the accumulation of radiogenic ^{87}Sr and negative values of *εNd* <...>.

Good results were obtained when using the value *εNd* in combination with the value *εHf* <...>. So, isotope diagram in the coordinates *εHf* (in the range from –35 to +25) – *εNd* (in the range from –25 to +15) – good differs some genotypes of marine sediments – Fe-Mn nodules, clayey silts and sands <...>.

In addition to its value as a great indicator of petrofond of rocks and sediments, the value of *εNd* is an excellent tracer of ocean circulation.

This property discovered in the study of the modern ocean, has been successfully used for paleogeographic reconstruction of the Iapetus ocean in the territory of the Eastern United States and to the Upper Devonian sediments of Morocco and Poland <...>.

Like other REES, neodymium accumulates in phosphates. Therefore, ***the study of such biogenic phosphates as conodonts or ichthyolites allows us to judge the isotopic composition of seawater of the corresponding epochs, which makes it possible to make completely non-trivial paleogeographic reconstructions.***

For example, the study of isotopic geochemistry of conodonts and their host limestones in precisely dated (~454 million years) the interval of sections of the Upper Ordovician on the territory of the East. Laurentia (from Iowa to

Pennsylvania) showed that the values of εNd and (to a lesser extent) $\delta^{13}C_{carb}$ showed strong variations depending on the reconstructed paleogeography of the epicontinental "Mojave Sea", which represented the northwestern (shelf) part of the ancient Iapetus Ocean. On the territory of the Midcontinent – in the western part of the sea fed by the terrigenous material of the ancient Canadian shield, the value of Sm/Nd in conodonts is low, on average 0.19 ± 0.01; the values of εNd are strongly negative,$–15 \pm 2.6$ (from $–12$ to $–19$); the values of $\varepsilon^{13}C_{carb}$ are also negative, on average $–0.6 \pm 1.3$. It is obvious that the composition of seawater in this part of the sea was affected by the ancient acidic petrofund and the flow of isotope-light carbon from the river runoff. In the southeastern facies zone and in the extreme east of the sea – in the Taconian Foreland, isotopic characteristics $\delta\varepsilon^{13}C_{carb}$ are positive, on average $+2.2 \pm 0.2\%$. This was clearly affected by the influence of the basite petrofund eroded in the young Taconian orogen at the boundary of the shelf sea with the Iapetus Ocean <...>.

These results are important for the correct interpretation of isotopic data. The fact is that, as you know, the vast majority of the stratosphere is composed of shallow-sea strata – the former sediments of epicontinental seas. Consequently, the detected isotopic variations (primarily εNd) sensitively reflecting the individual characteristics of inhomogenized water masses of ancient seas (= facies zones!), should not be uncritically transferred to the global level of the World Ocean. And indeed, in this case, the values of εNd of the water of the Iapetus open ocean ranged from $–5$ to $–0.6$ (!), i.e. they were strikingly different from the values for the facies zone of the Midcontinent <...>.

Another example of the effective application of the value εNd is the analysis of conodonts from the Upper Devonian sections in Morocco and Poland, representing both the shelf of Gondwana and Euramerica, and deeper sediments of the Variscian Ocean that separated these continents.

It turned out that the shelf sediments were characterized by low values of εNd εNd from $–7$ to $–12$, while the ocean sediments showed less negative values of εNd, from $–7$ to $–1$. This means that the waters of the shelf could not freely mix with the surface waters of the open ocean, which is possible only under conditions of predominance of low sea level. And only in the sediments of the *semihovae* conodont zone (zone No. 11), the transgression turned out to be powerful enough for the surface waters of the ocean to penetrate the shelf: in this interval of all sections, the values of εNd fall into the "ocean" interval from $–6$ to $–2$. At the same time, it turns out that according to the values of εNd the ancient Variscian Ocean is more similar to the modern Pacific Ocean than to the Atlantic and Indies that emerged later in its place

In the ichthyolites from the Upper Cretaceous black shales on the Demerara underwater ridge (opposite the coast of Suriname, the extreme west of the equatorial Atlantic), two opposite anomalies of magnitude εNd (T) are recorded: <...> 1) very low background values for ocean sediments from $–14$ to $–16.5$; 2) an un-

usually sharp and powerful positive excursion εNd, up to 8! It corresponds to the very beginning of the Cenomanian-Turonian OAE-2, covers a column interval of about 1.6 m (which corresponds to only 120–160 thousand years) and completely coincides with the positive excursion of $^{13}C_{org}$ (shift by +8 %). If the first can be explained (with reservations) by the local influence of a terrigenous source – a close Guianan shield composed of ancient metamorphites and granites with a magnitude of εNd (T) up to –30, then the second is more difficult to explain. The most plausible idea is the powerful influence of mantle basalt volcanism - the "trigger" of OAE-2. Thus, the basalts of the Great Caribbean Volcanic Province have values of εNd (T) equal to +10.

It has already been noted above that the values of εNd should be inversely correlated with the values of $I_{Sr} = {}^{87}Sr/{}^{86}Sr$. Indeed, in the works of recent years, both indicators are used together. These are, in particular, examples of a very successful decoding of the petrofund of alluvial sediments of the Indo-Gangetic Plain <...>, the Tibetan Plateau <...> and young pelagic sediments of the Central Basin of the Indian Ocean <...>.

Among the more recent works (not included in the review of the book-2011), we will name the study of apatite shells of neogene phosphate brachiopods (Lingulidae and Discinidae) from the South. parts of the North Sea, Center. Parathetis and the Atlantic coast of Europe – as a paofacial indicator [109]. Here the value of εNd is used in conjunction with the value of $\varepsilon^{18}O$ of phosphate oxygen. The shells of the genus Glottidia of the North Sea showed a low value of εNd and a high value of $\varepsilon^{18}O_{PO4}$ during the Mio-Pliocene, which indicates the cold temperature of the brachypod habitat, where the local seawater corresponded to the water of the Atlantic Ocean. On the contrary, brachypods of the genera *Lingulidae* and *Discinidae* of Parathetis in the Middle Miocene inhabited warm subtropical sea waters with a possible influence of the Indian Ocean (via the Mediterranean), which is confirmed by their average value of εNd –8.3. Combined geochemical data support thermal and marine separation of Parathetis from the North Sea without direct connection or significant exchange or significant water exchange. The temperature in Parathetis was very similar to that derived from the data of the Middle Miocene brachiopods West. France, but the value of the sea water's εNd here is identical to the same age in the Atlantic Ocean. Late Miocene lingulids from the South. Portugal has a high value of $\varepsilon^{18}O_{PO4}$, similar to specimens studied from the North Sea. This reflects either the deep-sea habitat of the lingulids, or the situation after the onset of global cooling, which ended with an increase in the value of $\varepsilon^{18}O_{PO4}$ of seawater.

As another example of using the value of epsilon neodymium (not specified in the book-2011), we can name an article where the calcium isotopy in apatites was considered together with the data on the εNd (T) – to clarify the conditions of global phosphogenesis at the turn of the Cretaceous and Eocene [128]. It was shown that the values of εNd (T) and $\delta^{44}Ca$, as well as the accumulation rates

of P and Ca, experienced clear changes. In particular, the sharp increase in the *εNd* (T) after the Cenomanian period is explained by the increased penetration of Pacific waters enriched with radiogenic neodymium, which was caused by global sea level rise at the end of the Cretaceous period, the emergence of a link between the North and South Atlantic, global post-Santonian cooling and the gradual expansion of the Caribbean threshold, all this combined significantly enhanced the Tethys circular current (TCC). This also reflects the weakening of the continental Nd signal due to a decrease in open landmasses caused by increased flooding of continental shelves. High values of $\delta^{44}Ca$ at that time also indicate a decrease in Ca^{2+} fluxes during weathering and the expansion of carbonate deposits on the shelves, which enriches seawater with isotopically heavy Ca^{2+}.

The study of bioapatite of Devonian ichthyolites in the Escuminac formation of Quebec (Canada) can serve as an example of using the value of epsilon neodymium in close connection with the $^{87}Sr/^{86}Sr$ index [115]. The values of **$^{87}Sr/^{86}Sr$** in biopatite range from 0.70804 to 0.70845, which overlaps the values for sea water of the Frasnian time. Although a small part of the values fall within the "Frasnian sea water interval", most of them are shifted towards more radiogenic continental (freshwater) values. This trend seems to be due to the postmortem exchange between fossils and a fluid isotopically different from seawater. All bioapatites are enriched with REE and for values normalized by shale, they show depletion of HREE and some enrichment by MREE. The values of the *εNd* (T) *for rocks* in the range from –4.8 to –6.4 are consistent with the post-Taconic Appalachian provenance. By contrast, *for bioapatites*, the values of *εNd* (T) are more radiogenic: from –2.6 to –4.6. This difference between rocks and fossils means the presence of of a secondary, diagenetic Nd reservoir. It is assumed that part of this reservoir was seawater. The neodymium similarity between the Escuminacian fossils and the Upper Devonian conodonts of Poland indicates a close connection between the Devonian Rheic Ocean and the Escuminac Formation basin.

4. IGNEOUS AND METAMORPHIC APATITES

The dominant factors controlling the solubility and crystallization of apatite in igneous rocks are the concentrations of SiO_2 and P_2O_5 in the melt and the melt temperature. The solubility of apatite strongly correlates with the degree of assimilation by the melt of the host rocks, and apatite in anatectic melts has much greater solubility than apatite in basaltoid magmas. Therefore, accessory apatite may be absent in some S-type granitoids, since apatite dissolved in the initial magmas, and phosphorus went into P-containing K-feldspar. The water content, pressure and Ca concentration in the melt are not important factors determining the solubility of apatite.

The possibility of using accessory apatite as an indicator mineral in 2002 was for the first time reliably proved in the article by E. A. Belousova and her Australian colleagues [84]. It is no coincidence that the text of this article is almost literally reproduced in the Irish Review [130].

First, the authors introduce a useful designation for stable indicator accessory minerals, which they call RIM – resist indicator mineral. Such RIMs include: garnet of mantle origin, pyroxene, chromite and Mg-ilmenite, rutile, magnetite, tourmaline. The necessary conditions for the use of RIM are: (1) wide distribution in the appropriate rock types, (2) a range of composition that is sensitive enough to the crystallization medium to carry significant genetic information, (3) the ability to survive weathering and transportation in a surface environment, and (4) relative ease of recognition, separation and analysis. Since the accessory apatite satisfies all these conditions– it should also be rightfully attributed to the number of such RIM. Indeed, apatite is a widespread accessory mineral; its content directly depends on the phosphorus content in the rock and is inversely proportional to the silicic acid content of igneous rocks.

The content of apatite can reach several percent in phosphorus-rich alkaline lavas poor in silica, while apatite is rarely found in phosphorus-poor (0.01% P_2O_5) rhyolites. The crystallization of phosphate phases is an important process in natural systems, since phosphates contain characteristic impurity elements such as U, Th, Sr and REE, the content of which is controlled by the melt/phosphate mineral equilibria. Moreover – we have already seen that apatite can carry a high proportion of the gross contents of REE, Sr, U and Th. Therefore, the distribution of impurity elements in apatite may be a sensitive indicator of magmatic crystallization processes. Variations in the content of impurity elements in apatites are associated with the parameters of the entire system – such as the activity of SiO_2, fO_2, total alkali content, aluminum saturation index (ASI).

As noted by Ural geologists [73, p. 190],

"apatite, through the specifics of its composition, with a wide range of isomorphic substitutions in the composition of cations and anions, carries information about the composition, nature and oxidative regime of the initial magmas, their fluid regime and metallogeny."

Based on these (already known) data, E. A. Belousova and colleagues [84] tried to solve two main issues: 1) is it possible to recognize individual types of rocks by the composition of their apatite; (2) to what extent does apatite reflect parameters such as fractionation and degree of oxidation related to ore mineralization processes? To answer these questions, the authors, using modern laser ablation (LA) techniques with ICP-MS analysis, analyzed more than 700 (!) grains of apatite for 28 elements, representing endogenous formations in a wide range of their composition, including also apatites from some industrial types of phosphate-containing iron ores.

As a result, it was shown that the slope of the normalized chondrite curves of the REE "spectra" varies systematically from ultramafic to mafic and intermediate and to highly fractionated types of granitoid rocks. Ratio $(Ce/Yb)_N$ is very high in apatites from carbonatites and lherzolites of mantle origin (more than 100 and more than 200, respectively), while the values of $(Ce/Yb)_N$ in apatites from granite pegmatites are usually less than 1, which reflects both the enrichment of HREE and depletion of LREE.

Within a large sample of apatites from granitoid rocks, the chemical composition was closely related to both the degree of fractionation and the degree of oxidation of magma. Since apatite can accept high concentrations of transitional and chalcophilic elements and even As, this makes it possible to recognize apatite associated with certain types of mineralization.

Based on multidimensional statistical analysis, the authors proposed a user-friendly scheme for recognizing apatites from various types of rocks by the contents of Sr, Y, Mn and total REE content, the degree of enrichment of LREE and the numerical value of the Eu anomaly. The authors recommend using this scheme to recognize apatites from certain types of rocks or types of mineralization, so that it is possible to determine the origin of apatite grains in heavy mineral concentrates.

Below we give examples of some other works showing the use of apatite for the recognition of specific igneous rocks

4.1. Hyperbasites and basites

In the Irish review [130], on the logarithmic "biplot" LREE – Sr/Y, apatites from pyroxenites and lherzolites fall (together with carbonatites) into the "ultramafic" UM field – with maximum values of the Sr/Y magnitude and sufficiently high values for the LREE abscissa.

According to the data of the Ural geologists [73, p. 190], the mantle type of the initial basaltoid and andesitoid magmas is indicated by the enrichment of apatites

with chlorine (up to 1.0–1.5%), which is always accompanied by the accumulation of siderophilic and chalcophilic elements in them. The informativeness of binary graphs was found out, where the contents of U (ppm) are deposited along the abscissa, and the contents of W, Bi, V, Th (ppm) are deposited along the ordinate. On such graphs, it was possible to identify fields (with minor overlaps) corresponding to (1) gabbroids and pyroxenites with Ti-Fe-V mineralization, (2) gabbroids and granitoids with large scarn-magnetite mineralization, (3) granitoids with Cu-porphyry mineralization and (4) granitoids with Au-sulfide mineralization in quartz veins. In general, the new analytical data obtained by them convincingly indicate that the composition of apatite is an important indicator of the metallogenic specialization of mantle and crustal magmas, their composition, oxidative and fluid regimes.

In two almost identical articles in 2015, with only some rearrangement of co-authors, V. V. Kholodnov et al. present data on the contents of halogens and sulfur in apatites as criteria for predicting Si-Ni, Fe-Ti and Au mineralization in accretion-collision gabbro-dolerites of the Western Magnitogorsk zone of the Southern Urals [71; 72]. The F–Cl and F–SO$_3$ graphs show fairly clear clusters corresponding to individual magmatic complexes. In particular, the authors conclude that the rocks of the Khudolazovsky complex, specialized in Cu-Ni mineralization, are characterized by apatite with the highest contents of sulphate sulfur (up to 0.65 wt. %), isomorphic with phosphorus in the composition of the anionic complex (PO$_4$)$^{3-}$. This apatite has a reduced fluorine content (< 2 wt. %), with a significant content (in olivine gabbro) and chlorine (up to 1.50 wt. %). Such a nature of the ratio of halogens and sulfur in apatite can be recommended as one of the effective indicators for Cu-Ni mineralization. Apatite in the gold-bearing Ulugurtau dyke complex has a moderately elevated chlorine content and a low content of sulphate sulfur. The appearance of apatite-rich late calcite segregations here characterizes the composition of the late magmatic fluid.

In 2016, new data were added on diorite intrusions of the Voznesensky and Elenovsky deposits and the Kutuyevsky ore occurrence of the copper-porphyry type [70]. In the apatites of the studied objects, elevated chlorine and sulfur contents were found, characterizing the fluid regime of copper-porphyry ore-magmatic systems and the manifestation of liquid immiscibility in the composition of ore-forming fluids. These data confirm the possibility of using concentrations of halogens and sulphate sulfur in apatites to substantiate the prospects of intrusions of increased basicity for the search for porphyry copper mineralization.

The same Ural petrologists in 2018 [50] repeated data on accessory apatites of four gabbroid complexes D$_3$-C$_1$ of the Western Magnitogorsk zone of the Southern Urals. According to the contents of halogens and sulfur, 3 groups of apatites were identified: 1) high-fluorbearing apatites with a moderately increased amount of chlorine and a small amount of sulfur; 2) high-fluorbearing apatites with a reduced amount of chlorine and a small amount of sulfur; 3) low- fluorbearing and low-chlor-

bearing apatites with an increased amount of sulfur. Based on these data, the authors concluded that the studied complexes have a low potential for Ti-Fe ore content.

In the North Karelia, the Early Proterozoic stratified ultramafic-mafic Kivakka intrusion, which is part of the Olang group, has a rounded shape (about 3 km across), a substantially peridotite-gabbronorite composition and lies in the rocks of the Archean basement of the Paanayarva synclinorium, the Baltic/Fennoscandian shield [3]. A zone of low-sulfide EPG-containing mineralization called "Kivakka Reef" has been identified here. This zone is located in olivine gabbronorites, olivine-plagioclase-orthopyroxene cumulates containing, on average, about 50–55 vol.% orthopyroxene, 30–35% plagioclase (cumulus An 79-81 and intercumulus Ab), up to 10 vol.% olivine (Fo79) and clinopyroxene (augite–diopside). In particular, significant variations were found in the compositions of intercumulus apatite grains with a dimension from 5–10 to ~50 microns. The maximum Cl contents are inherent in the apatite of the EPG mineralization zone and the overlying level directly adjacent to this zone. Significant variations of Cl are noted both in the compositions of different grains and in grains that are heterogeneous in composition and do not show any "correct" (regular) zonality. The Cl content in apatite systematically decreases upwards, with a tendency of parallel increase of F, the maximum concentrations of which are inherent in relatively large (0.2−0.3 mm) subidiomorphic crystals in pegmatoid gabbronorites of the upper stratigraphic level. The increase in the dimension of apatite grains is primarily explained by the relative increase in the concentration of P during magma crystallization. At the same time, the revealed variations indicate more complex isomorphism schemes involving apatite and OH, in addition to Cl and F. The Russian authors [3] believe that the variations they have identified are quite consistent with observations on other stratified intrusions, both very large (Stillwater and Bushveld complexes) and relatively small intrusions of the Karelo-Kola region, in which the enriched Cl apatite is localized in the early (high-magnesian) cumulates of the lower stratigraphic level.

E. V. Lobova studied the compositions of amphibole and apatite from rocks of the Reftin magmatic complex (Eastern zone of the Middle Urals) [41]. She found that during the evolution of the complex, amphibians are characterized by a decrease in the contents of Al_2O_3 and TiO_2, which indicates a decrease in the RT parameters of rock formation. A diagram was used where the contents (wt. %) were deposited by abscissa, in apatites F, and by ordinate – Cl, with a range of 0–4 and 0–%, respectively [41, p. 86]:

"In the rocks of the first phase, from gabbro to diorites, then to quartz diorites, the chlorine content decreases markedly, and fluorine on the contrary increases <...>. As for the rocks of the second phase, they are also characterized by a decrease in chlorine and an increase in fluorine with an increase in the silicic acid content of rocks from quartz diorites to tonalites."

4.2. Kimberlites

Kimberlites are tubular magmatic bodies in a diatreme, usually underlain by coherent rocks of the root zone and associated dike/sill complexes. In a recent work on the classic Kimberley district in the South. In Africa, the questions of the genesis of kimberlites were tried to clarify by studying the composition of accessory apatite - both from the diamond-bearing kimberlite itself and from its accompanying dikes/sills [126].

Early minerals (olivine, spinel, Mg-ilmenite) in the rocks of dikes/sills and the root zone have an indistinguishable composition and, therefore, crystallize from similar primitive melts. Conversely, the compositions of apatite, as a rule, are different in dikes/sills (low Sr content, high and variable Si content) and in kimberlites of the root zone (high and variable Sr content, low Si content). The enrichment of Si apatite in dikes/sills is explained by the conjugate substitution of the PO_4^{3-} ion with CO_3^{2-} and SiO_4^{4-} ions, reflecting a higher CO_2 content in the initial melts and the accumulation of silicon in kimberlite magma due to the predominant crystallization of carbonates compared to mica/monticellite. The low Sr content in apatite from dyke/sill rocks reflects the equilibrium of apatite with melt – for carbonate and silicate melts, while the increased Sr content in apatite from kimberlites of the root zone requires crystallization with a reduced CO_2 content in the melt. The relative enrichment of CO_2 in dikes/sills is evident from the abundance of carbonates, the presence of dolomite inclusions in mesostasis and calcite in some samples and the concomitant decrease in the proportion of other phases of the main mass (for example, serpentine, mica, monticellite). During the late modification of dike/sill rocks, monticellite is usually replaced by carbonates, while olivine and pleonast are relatively stable. This means that the melts forming dikes/sills evolve at higher CO_2/H_2O ratios.

It is unlikely that these two different evolutionary paths were caused by the assimilation of the host rock material by kimberlite melt or the breakthrough of kimberlite magma to the surface, since assimilation processes are not reflected in the isotopic composition of O and Sr of late olivine crusts or carbonates. The authors suggest that higher concentrations of CO_2 are preserved in kimberlite dikes/sills of higher pressures – without their degassing in near-surface conditions. On the contrary, the release of CO_2 from the melts of the root zone of kimberlites increased the ratio of H_2O/CO_2 in the melt and contributed to the crystallization of mica and monticellite due to dolomite and calcite. It is believed that apatite compositions can help in distinguishing kimberlites from lamproites (higher LREE, Sr, F, and S contents, lower Si content) and carbonatites (higher LREE, F, Cl, and S contents, lower Fe content). However, the compositions of kimberlite apatite overlap the compositions of apatite from ailikites, probably due to similar compositions of the melt at a late stage.

Recently, Russian geologists have also studied apatite from the Middle Paleozoic kimberlite Monchary tube in the Khompu-May field of Central Yakutia [47]. The mineral turned out to be F-apatite, and in general, the study confirmed the already known patterns showing that apatite has a late magmatic nature, therefore its composition is associated with the influence of fluids enriched with F and Sr. At the same time, certain differences between the studied apatite and apatites from diamond-bearing kimberlite bodies, carbonatites, xenoliths of peridotites and eclogites of South Africa, Canada and China were revealed. A trivial conclusion is made that the impurity composition of apatite can be used in the comparative study of kimberlite and other rocks.

4.3. Granitoids

As can be seen from the Irish review [130], apatite from anatectic S-type granites is depleted by light rare-earth elements (LREE) and Th, while apatite from younger igneous granites of I-type ("mafic granites") generally contains similar (or even higher) chondrite normalized REE contents compared to medium rare-earth elements (MREE), as well as more U. On the logarithmic "biplot" LREE – Sr/Y, apatites form two separate fields: IM and S. The IM field (median, intermediate values on both axes) includes granodiorites and "mafic" I-granites with low values of the ASI index. The S field includes anatectic granites of the S-type, as well as "felsic" granites of the I-type, with a high value of the ASI index. With some average values for the LREE abscissa, they are clearly distinguished by the minimum values for the Sr/Y ordinate.

Since in rocks with a high ASI index (ASI >1.1), monazite crystallizes as the primary phase, taking the main amount of REE from the melt, acid melts that generate S-type anatectic granitoids poor in alkalis and calcium ***are characterized by a gentle appearance of the apatite "spectrum" of REE normalized by chondrite***. This is due to the depletion of apatite by the light REE (LREE), which monazite absorbed. Consequently, the observed pattern can be explained by simultaneous or later crystallization of apatite with respect to monazite, which reduces the amount of Th and LREE available for apatite. In particular, since La goes into monazite much more vigorously than Sm, the reduced La/Sm ratio in monazite-cogenetic apatite can be used to recognize such acid magmas.

Since the solubility of apatite strongly depends on the degree of assimilation by the melt of the host rocks, it is quite possible that the composition of the REE of igneous apatite may be associated not only with ASI, ***but also with the sequence of crystallization of apatite relative to K-feldspar***, which takes a significant amount of P, Sr, La, Ce, Pr and Eu from the melt. Therefore, in very acidic melts, where the phosphorus-bearing K-feldspar $KAl_2[PSiO_8]$ was formed, accessory apatite turns out to be either highly depleted of La and Ce (as well as Sr), or, due to its high solubility in the initial melts, it does not crystallize at all.

In a recent collective work [138], the characteristics of igneous apatites of two regions of the granite belts of the Northern and Eastern parts of China – the Luming and Lower Yangtze – were studied in order to study their potential in petrogenesis, mineralization and tectonic evolution of granites. Apatites from those and other granites are mainly fluorapatites, and show strong negative anomalies of Eu, indicating the crystallization of plagioclase earlier than apatite. The negative correlation of Eu/Eu* (δEu) – Mn, δEu – δCe and δEu – Ga in apatites means that the initial magmas of both granites were moderately reduced. The Sr/Y ratios of apatites with respect to δEu also show that both granites are not adakitic in nature, which is consistent with the non-adakitic composition of the host rocks.

Apatites of the Lower Yangtze containing more chlorine (0.02–1.45 wt.%) and less fluorine (1.1–3.85 wt.%) are associated with the dehydration of slabs, whereas apatites from Luming having a lower Cl content (0–0.04 wt.%) and a higher F content (3.36–5.29 wt.%), suggest an association of granites with partial melting of the juvenile crust material. Based on the positive correlation in SO_3 – Li granites, $(La/Sm)_N$ – $(Yb/Sm)_N$ and obvious variations $(La/Yb)_N$ compared to Eu/Eu*, it is concluded that these host rocks must be ore-bearing.

In addition, the geochemical characteristics of apatites from Luming show low F/Cl ratios, stable La/Sm ratios, low values of δEu (0.04–0.43, on average 0.21) and high values of δCe (0.96–1.12, on average 1.02), indicating that the magmas of these granites are associated with plate dehydration and are associated with Cu–Mo–W mineralization caused by the mutual effect of subduction of the Paleoceanic Plate and intraplate expansion. For comparison, rather high ratios of F/Cl, La/Sm, low values of δEu (0.12–0.23, on average 0.16), high values of δCe (0.98–1.09, on average 1.04) and low Sr/Th ratios in luminescent apatites indicate that granites containing Mo–W mineralization arose as a result of partial melting of juvenile crust material.

E. A. Belousova and co-authors studied apatite from granitoids associated with the famous Australian giant – the Pb-Zn-Cu deposit of Mount Isa ores [85]. It was found that the distribution of REE, Sr, Y, Mn and Th in apatite correlated with parameters such as the SiO_2 content, the degree of iron oxidation, the total amount of alkalis and the aluminum saturation index (ASI). The relative accumulation of Y, HREE and Mn and the relative depletion of Sr in the studied apatites reflect the degree of fractionation of the host granite. Apatites from highly oxidized plutons tend to have higher concentrations of LREE compared to MREE. Manganese concentrations in apatite are higher in the reduced granitoids because Mn^{2+} directly replaces Ca^{2+}. The La/Ce ratio of apatite correlates well with the content of K_2O and Na_2O in the whole rock, as well as with the degree of oxidation and the value of ASI. The authors conclude that since the composition of the impurity elements of apatite reflects the chemical composition of the entire rock, it can be a useful indicator mineral for recognizing ore-mineralized granite series, where certain mineralization styles are associated with granitoids that have specific geochemical signatures.

Detection by cathodoluminescence of a clear zonality in apatites from granite Shap in the North. In England, it was a real gift for petrologists who previously did not have a suitable tool for judging the evolution of granite magmas [95]. Grains of accessory apatite were analyzed for REE and other impurity elements by the LA-ICP-MS method. Based on the obtained figures, diagnostic graphs were constructed: Sr (0–500 ppm) – Y (0–600 ppm), Ce (0–6000 ppm) – U (0–50 ppm), as well as the normalized chondrite "spectrum" of REE. In general, it is possible to see 3 distinct zones in apatite crystals: a small core, a thick mantle and a thin shell. In the Sr – Y graph, the cores contains less Sr than the shell. On the Ce – U graph, the core is very variable, with a large spread of points, whereas the points of the mantle and shell are located compactly in the center of the graph with some trend repeating the trend of the rock – decreasing uranium and REE as crystallization. The "spectrum" of REE is quite flat, although it shows enrichment with light REE, with a very small negative anomaly of europium. The contents of all REE in the mantle of zonal crystals are much less variable than in the cores and shells.

As a result, the following general conclusions were made.

1. Cathodoluminescent images of zonal apatite in combination with the analysis of trace elements by the LA-ICP-MS method provide powerful tools for deciphering the processes of crystallization of granites. Usually, the long history of apatite crystallization, combined with the absence of subsequent changes in the mineral, allows us to recreate a complete picture of the evolution of the magmatic system.

2. Many apatite crystals from the Shap granite contain texturally identifiable cores that have variable composition and show numerous evidences of partial dissolution, reflecting an early magmatic evolution dominated by magma mixing. A lot of inherited cores were found in apatites from the Shapsky granite. The recognition of such inheritance has serious implications for the interpretation of the REE profiles of granite rocks.

3. The later growth of apatite (mantle formation) occurred in a relatively stable medium with a constant magma composition and records the history of crystallization in gradually more isolated melt foci.

4. There are no signs of rapid volumetric diffusion in these apatites, and the zones differ in different contents of impurity elements, including Sr and REE.

5. The growth and preservation of apatite is strictly controlled by the crystallization of biotite in granite.

Fluid inclusions in minerals are a valuable tool for judging the composition of ore-forming fluids that have retained their primary composition. The Chinese team of authors [131] applied a new subtle method of microanalysis - X-ray fluorescence analysis induced by synchrotron radiation (SRXRF) to study both apatite itself and fluid inclusions in it. Prismatic crystals of accessory apatite from the Mesozoic Yuerya granite, with which gold deposits are associated, were analyzed. Chondrite-normalized REE "spectrum" shows that granite belongs to the S-type.

It has been shown that the main components of fluid inclusions in apatite are Zn, Cu and Cl. According to the authors, this proves the relationship between the mineralization of gold and the evolution of granite magma.

4.4. Alkaline rocks

In the Irish review [130], on the logarithmic "biplot" LREE – Sr/Y, alkaline rocks form a separate ALK field. This is the rightmost field on the biplot, with maximum values on the LREE abscissa, but with wide (non-diagnostic) variations of values for the Sr/Y ordinate.

Although the ***Khibiny apatites*** have been studied for a very long time, only in recent years have there been studies performed by modern methods. Among a number of works, we can name one of the relatively recent ones (2013), which provides data on the zonality of the Khibiny massif with respect to the content, morphology and composition of accessory and rock-forming fluorapatite [35]. The authors showed that the amount of Na, REE and Si impurities in the composition of apatite consistently decreases in the direction from the massif to the Main ring structure composed of melteigite-urtites and rischorrites. Within the same ring structure, the purest apatite is characteristic of rich ores of large deposits, where it is freed not only from Na and REE, but also from Sr in favor of Ca. The fractal dimension of fluorapatite aggregates in all textural types of apatite-nepheline rocks (ores) corresponds to the dimension of various fractured structures, which, along with the mineral composition of apatite-nepheline rocks and data on the zonality of the host foidolites, indicates the superimposed nature of apatite mineralization.

In O. B. Dudkin's summary [20], taking into account new geological materials, variations in the composition of apatite in a number of Khibiny deposits of different structures are traced. Basically, the composition of apatite is linked to the composition of rocks. Generalization made it possible to identify an age range of deposits in which younger and younger magmatic processes are consistently increasing.

Academician Lilia Kogarko (maiden name Basilevich) emphasized a long-known fact: Khibiny fluoro-apatite is extremely rich in strontium (on average 4.5 wt. % SrO) and REE, the content of which reaches 8891 ppm. The absence of the Eu anomaly means the residual nature of the Khibiny alkaline magma and indicates that the differentiation of primary olivine-melanefelinite magma developed without the fractionation of plagioclase, which is the main mineral concentrator of Sr and Eu in basalt magmatic systems [31].

Nepheline syenites of the Pilansberg alkaline complex (South Africa) underwent extensive subsolidic balancing and alteration under the influence of a late fluid rich in Cl and Na [111]. As a result of the substitution of primary aluminosilicates, rinkite, eudialyte and fluorapatite, complex complexes of secondary minerals were formed. The composition of minerals of the apatite group formed

during these processes of change reflects the content of Sr- and REE, the ratio of Na/Cl and pH of secondary fluids. The minerals of the apatite group were formed in the following sequence:

igneous fluorapatite ☐ *strontium britolite-(Ce)* ☐ *strontium fluorapatite* ☐ *Sr-apatite* ☐ *rich in Sr, Na and REE minerals approaching by stoichiometry to belovite-(Ce) and deloneite(Ce)* ☐ *britolite (Ce).*

The increase in the alkalinity of secondary fluids is reflected in the increase of Sr replacing Ca in apatite, and culminates in the formation of Sr-apatite containing 62.1 wt.% Sro (~4.17 f.e. Sr).

4.5. Carbonatites

Carbonatites are genetically closely related to alkaline rocks. Although the full reality of carbonate magma has already been proved experimentally, the genesis of some carbonatites remains a subject of debate, since they are considered metasomatic (for example, some South Ural [38]).

On the logarithmic "biplot" LREE - Sr/Y [130], carbonatites fall into the "mafic" UM field together with pyroxenites, lherzolites and "mafic I-granites with a low ASI index. For this field, the highest values for the ordinate Sr/Y and moderately high values for the abscissa LREE are characteristic.

In carbonatites (as in some granite pegmatites), phosphate minerals can be so abundant that they become rock-forming. In addition, they have very characteristic differences from other igneous apatites. In this regard, the review of the international team on the composition of apatite carbonatites published in 2017 is of great value, based on ~600 electron probe and 400 laser-ablation mass spectrometric analyses of apatites in 80 samples from 50 localities around the world [91].

Most *igneous apatites* from the rocks under consideration are Cl-poor fluorapatite or F-rich hydroxyapatite ($\geq$ 0.3 f.e. fluorine) with 0–4.5 wt.% $LREE_2O_3$, 0–0.8 wt.% Na_2O, and relatively low concentrations of ions replacing Ca (up to 1000 ppm Mp, 2300 ppm Fe, 200 ppm Ba, 150 ppm Pb, 700 ppm Th and 150 ppm U), none of which shows a significant correlation with the type of host rock. Silica, $(SO_4)^{2-}$ and $(VO_4)^{3-}$ anions replacing $(PO_4)^{3-}$, as a rule, are found in greater quantities in crystals from calcite carbonatites than from dolomite ones – up to 4.2 wt.% SiO_2, 1.5 wt.% SO_3 and up to 660 ppm V.

Hydrothermal apatite in carbonatites is formed as a replacement product of primary apatite or is deposited in cracks and pores in the form of euhedral crystals and aggregates associated with typical late-stage minerals (for example, quartz and chlorite). This apatite is usually depleted in Sr, REE, Mn and Th, but enriched with F (up to 4.8 wt.%) compared to its magmatic predecessor, and also differs from the latter in at least some key REE ratios (for example, shows $(La/Yb)_N$ $\leq$25 or negative anomaly Ce). The only significant exceptions are replacement zones rich in Sr ($\pm$ REE, Na) and new formations of igneous apatite in some dolomite-

containing carbonatites. Their crystallization conditions and initial liquid were apparently very different from the more common strontium- and REE-depleted rocks.

Based on the new data presented in this work, the distribution of trace elements between apatite and carbonatite magmas, the solubility of phosphates in these magmas and the change in the composition of minerals of the apatite group from spatially bound carbonatite rocks are critically overestimated.

In 2020, a Chinese team studied apatites from three Chinese REE deposits associated with carbonatites: Shasyundun, Miaoya and Bayan Obop [114]. ***Magmatic apatite***, which occurs mainly in samples from Shasyundun, is euhedral and usually shows a growth zone with a yellow-green luminescent core and a purple luminescent rim. Euhedral to subhedral ***metasomatic apatite*** from Miaoi and Bayan Ob is characterized by a cloudy appearance, while most grains are associated with dissolved monazite. ***Hydrothermal apatite*** from Bayan Obo, usually occurring in the form of aggregates in close connection with fluorite and barite, is anhedral, with green or light purple luminescence. Apatites, differing in color and structure, are characterized by different compositions of impurity elements.

Magmatic apatite contains the highest concentrations of Mn (on average 457 ppm) and Sr (on average 18285 ppm) and is characterized by a steep slope, the curve of the "spectrum" normalized by chondrite. Metasomatic apatite, which has undergone repeated precipitation-dissolution, contains lower concentrations of Mn (on average 272 ppm) and Sr (on average 9945 ppm). It is characterized by highly variable REE spectra with the La/Sm$_N$ ratio varying from 0.13 to 5.61, and lower average values of La/Yb$_N$, La/Sm$_N$ and Sr/Y (46, 2.2 and 18, respectively) than magmatic apatite. Hydrothermal apatite is characterized by convex upward normalized chondrite curves of the "spectrum" of REE with the lowest ratios of La/Yb$_N$, La/Sm$_N$ and Sr/Y (13, 0.69 and 5.8, respectively). The average concentrations of Mn and Sr in this apatite are 270 and 6610 ppm, respectively.

An important problem of REE mineralization associated with carbonatites on cratonic margins and in orogenic belts is the late metasomatic and hydrothermal processing of minerals, erasing their primary geochemical marks. In 2020, a Chinese team tried to clarify the role of late metasomatosis using the isotopy of strontium and carbon in calcites and apatites of the already known Miaoi carbonatite deposit located in the orogenic belt of Southern Qinling [135]. Calcite carbonatites in Miaoi are usually found in the form of rods and dikes embedded in syenite, and can be subdivided into equal-grained (type I) and uneven-grained (type II).

Calcite in type I carbonatite is characterized by the highest concentrations of Sr (up to 22000 ppm) and REE (195–542 ppm) with low values (La/Yb)$_N$=2.1–5.2. Here the values of $^{87}Sr/^{86}Sr$ = 0.70344–0.70365 and $\delta^{13}C_{carb}$ = 7.1–4.2 ‰ are also recorded here, which is consistent with the mantle nature of carbonatite.

In type II carbonatite, calcite is poorer in strontium (Sr = 1708–16322

ppm) and REE (67–311 ppm), having variable values $(La/Yb)_N$=0.2-3.3 and $(La/Sm)_N$=0.2–2.0. Here $^{87}Sr/^{86}Sr$ and $\delta^{13}C_{carb}$ vary greatly: from 0.70350 to 0.70524 and from 7.0 to 2.2, respectively.

Fluorapatite in carbonatites of types I and II is characterized by similar trace element and isotopic compositions. Both demonstrate variable LREE concentrations, and at the same time, relatively stable almost chondrite Y/Ho ratios. Fluorapatite is characterized by constant isotopic compositions of Sr with a corresponding average ratio of $^{87}Sr/^{86}Sr$ equal to 0.70359, which suggests that the mineral remained relatively closed with respect to contamination.

Taken together, these data suggest that the fluids dissolved in carbonatite, together with the possible assimilation of syenites during Mesozoic metasomatism, left an imprint on the original trace element and isotope signatures created in early Paleozoic magmatism. Hydrothermal processing led to the dissolution-redeposition of calcite and fluorapatite, which served as the dominant source of REE mineralization during a much younger metasomatic activation.

In the study of carbonatites in Malawi [87], the analysis of apatite from five carbonatites with magmatic textures. allows you to outline the contours *of the field of primary magmatic apatite (PIA)* with $\delta^{18}O$ = +2,5 – +6,0 (VSMOW), comparable to the compositions *of primary igneous carbonate (PIC)*. In 10 samples of carbonatite from Songwe Hill, paired values were obtained – both $\delta^{18}O$ CARB and $\delta^{18}O_{phosph}$. Values like $\delta^{18}O_{carbs}$ in carbonates (as well as the value of $\delta^{13}C_{carb}$) show a general growth trend from the beginning to the end of evolution – from +7.8 to +26.7% (VSMOW). The value of $\delta^{18}O_{phosph}$ shows the opposite trend, decreasing from the PIA field to negative values: from +2.5 to -0.7% (VSMOW). These contrasting results are interpreted as the result of the interaction of minerals with the fluid at different temperatures and compositions.

The simulation allows for the possibility of exposure to both carbon dioxide fluid and the mixing of meteoric and magmatic waters. As a result, a model is proposed in which brecciation leads to depressurization of the ore system and rapid precipitation of apatite. It is assumed that a convective cell interacting with meteoric water is formed in carbonatite. REE is likely to be transported into this convective cell and precipitate due to a decrease in salinity and/or temperature.

In 2012, the Ukrainian team [19] studied TR-apatites with determination of the content of Ca, P, Si, Na, Sr, TR and other elements from the tweitosite-pyroxenites, ringites and beforsites of the Chernihiv carbonatite massif. Apatites of the studied rocks turned out to be quite different. *Apatites of tweitosite-pyroxenites and ringites* are characterized by an inhomogeneous structure of the apatite matrix. In the latter there are areas enriched and depleted by TR and Si. The isomorphic entry of TR together with Si into the structure of such apatites occurs according to the britolite scheme. In addition, these apatites contain numerous inclusions of newly formed minerals resulting from the decay of primary TR-apatites. Such

inclusions of exolution minerals are more often represented by britolite and bast-nesite. ***Apatite from beforsites*** is characterized by a homogeneous grain structure and an increased concentration of TR, Na and Sr. Such apatites are characterized by a belovite isomorphism scheme. The revealed differences in the structure of apatites from the mentioned rocks and the values of the concentration of impurity elements in them are explained by the different chemical composition and physico-chemical conditions of crystallization of the host rocks.

In 2011, Yekaterinburg student E. Krestyaninov [38] studied apatite from the Mauk manifestation of carbonatites, located in the Chelyabinsk region on the Southern. The Urals. The genesis of these carbonatites (as well as other South Ural ones) is the subject of discussion. Apatite turned out to be quite chloride (F/Cl = 2.1–2.6, F = 1.7–1.8%, Cl = 0.7–0.8%), moderately rare-earth (ΣREE = 740 ppm). The relatively low value of La/Yb = 4.3 gives rise to a flat appearance of the "spectrum" of REE normalized by chondrite. After making a number of comparisons with apatites from other carbonatites, the author leaned towards the idea of the metasomatic nature of Mauk carbonatites, which (among other things) makes them promising for the detection of gold mineralization.

As noted by Ural geologists [36], in the apatites of the "oreless" calcite carbonatites of the South Urals, the REE content is very low, 4-48 ppm, they are also poor in Sr, Y and Zr content. However, in the dolomite variety of these carbonatites, the amount of REE (about 800 g/t) and the contents of Sr, Y, Zr (respectively 370, 177 and 70 ppm) are significantly higher.

A decisive contribution to understanding the genesis of carbonatites was made in 2017 by Siberian geologists who studied the carbonate and apatite-fluorite association in the lamproite series rocks of the high-potassium intrusive Ryabinovy massif that this mineralization was formed during silicate-carbonate liquation with the separation of P, F and SO_3-containing carbonatite melt, which, in turn, then divided into immiscible sulfate-carbonate and sulfate-phosphate-fluoride fractions.

During the silicate-carbonate liquation in the ultrabasic lamproite system, the carbonatite melt concentrated LREE, U, Th, Ba and Sr with the participation of P and F, and Ti, Zr, Nb, Ta went into the silicate melt. Apatite, like biotite, has an inverse zonality in the content of F. Apatite inclusions from olivine-diopside-phlogopite and diopside-phlogopite lamproites differ in significant enrichment of LREE, as well as Th and U in comparison with apatite from minette and syenite porphyries; the difference in HREE contents is insignificant. When the "primary" carbonatite magma is divided into pure carbonatite and phosphate-fluoride fraction, apatite-fluorite veins with rare-earth apatite, carbonates and fluorocarbonates with LREE are formed. As a result of the removal of the so-called salt fraction, pure calcite-dolomite carbonatite, depleted by scattered elements, is formed.

4.6. Pegmatites

Following the predecessors, the St. Petersburg mineralogist V. V. Gordienko [12] considers 6 formations of granite pegmatites in descending order of their formation depth:

(1) ceramic $\Rightarrow$ (2) mica-bearing $\Rightarrow$ (3) rare-metal-rare-earth-$\Rightarrow$ (4) rare-metal ceramic .$\Rightarrow$ (5) rare-metal-rare-earth-amazonite (6) $\Rightarrow$ crystal-bearing

All these formations contain accessory apatite, although in varying amounts [12, p. 114]:

"The content of apatite in various types of pegmatites varies widely (from 0.05 to 0.2%, sometimes reaching 1.5%), and apatite of the crystalline formation is characterized by the greatest"

In general, these formations also differ in the composition of apatites [12, p. 116]:

"The vast majority of granite pegmatite apatite belongs to F-apatite (F-minal content from 65 to 8%), with a variable amount of Mn. The variations of the latter are quite significant (from 0.1 to 10% MnO)".

Mn contents consistently increase from primitive pegmatite formations to highly specialized ones. The contents of REE will change more difficult, differing in the generation of apatite [12, p. 118]:

«From early to late generations of apatite, the content of ΣREE and Y decreases, and the most recent generations of apatite (V and VI) also obey this trend».

Strontium behaves differently and even accumulates in late generations, reaching a maximum (up to 0.3%) in generation apatites V. Gordienko explains this in terms of thermodynamics [12, p. 118]:

"Such a feature finds a good explanation based on the average values of «ΔZ SrO (137.3 kcal/mol) and CaO (144.5 kcal/mol), which indicates an energetically unfavorable isomorphic substitution of Ca for Sr in oxygen compounds."

Apatites of the formation (5) occupy a separate position [12, p. 118],

"where, in addition to the usual mango-fluoro-apatite, silicate-apatite (the britolite–abucumalite group) is found, characterized by an abnormally high content of ΣREE and Y (ΣREE and Y more than 40%) and a reduced content of F-minal (<...>. Both of these varieties of apatite are at the same time close to each other in Mn content (0.9–4.0% MnO) and correspond to that in apatites from the pegmatite formation (4)".

In general, as we can see, granite pegmatites are distinguished by a special peculiarity of the geochemistry and mineralogy of phosphorus. Firstly, phosphates can be so abundant here that they no longer become accessory, but rock-forming minerals. Secondly, other phosphates are often formed here instead of calcium phosphate of apatite – for example, iron-manganese.

One of such minerals is Ca-Mn phosphate **beusite CaMn$_2$[PO$_4$]$_2$**, named after our famous geochemist and mineralogist A. A. Beusa. In Polish pegmatites, beusite was described in association with the equally unusual manganese fluorapatite [120]. An association of phosphate minerals, including beusite, high-manganese fluorapatite, chlorapatite, hydroxylapatite and an admixture of alluadite and mitridatite, usually accompanied by high-manganese oxides, also enriched in Ba, Ca, Mg, Ni, Bi, Pb, is found in granite pegmatites localized in serpentinites of the Shklyary massif in Lower Silesia. These pegmatites are a subclass of muscovite-rare metal pegmatites. Beusite is usually developed here in the form of a substantially manganese, Ca-Fe-Mg phase, devoid of the usual lamellar accretions with triphylin or sarcopside, which becomes more and more manganese in the course of the process. In terms of its manganese content, beusite from Shklyar is on a par with beusite from Cross Lake pegmatites in Canada, considering as an example of the richest manganese phosphate in the world. Apparently, high-manganese fluorapatite containing up to 19.3 wt.% MpO, and a mineral of the apatite group with a dominant Mp (up to 31.5 wt.%MpO) are two types of apatite, which are also record manganese,

Nodules were found in the outer parts of the granite pegmatites of Cema (San Luis province, Argentina), very exotic Fe-Mn phosphates [122]. Two complexes of phosphate associations were identified here. The first Association – bauset of willeit-siclari with tanecetum and farolitos among the major products of substitution values of Fe/(Fe+Mn) from 0.46 to 0.48 for sclerite and MgO content up to 2.14 wt.%. The second association is lithiophilite-siclari with farolitos and guerolito among the major secondary products, with low values of Fe/(Fe+Mn) of the order of 0.37–0.39 for lithiophilite and low MgO content of about 1 wt.%.

As can be judged by the composition of these Fe-Mn phosphate nodules, the first association had higher crystallization temperatures. The enrichment of Mn apatites observed in these pegmatites with low differentiation can be explained by the early crystallization of other Fe-enriched minerals, such as sherl, in the nearband parts of pegmatites. Crystallization of this silicate leads to depletion of Fe activity in residual pegmatite melts.

Equally surprising, Al-Li-Be-Ca-Sr secondary phosphates have been described in lithium rare-metal pegmatites of Eastern Argentina [103]. Dendritic montebrasite secretions in albite are widespread here, mainly in the northern parts of the bodies, while lepidolite is widespread in the south. Dendritic secretions are confined to block pegmatites at the boundary with the quartz core. They have been substantially changed. 3 stages were identified: 1 – two generations of secondary montebrasite in fusion with hydroxylherderite, augelite and fluorapatite (acidic

aqueous fluids, 450-420 °C, 2 kbar); 2 – gojacite-crandallite and hydroxyapatite formed when equilibrium is reached between pegmatite and host rocks during the arrival of Ca, Sr and S from host rocks when cooled to 300°C; 3 – at low temperatures, the remains of montebrasite and all its products of change are a source of leaching and phosphorus scattering and Si introduction. Pseudomorphoses are formed, consisting of kaolinite, quartz, lithium muscovite, feldspar (adular) and microliths of previous stages.

Even more exotic phosphates can be formed by hydrothermal and hypergenic alteration of granite pegmatites, especially those whose parent granites belong to anatectic granites of the S-type. In the high-alumina primary melts formed from metapelites, apatite was highly soluble - better than in low-alumina, due to Ca deficiency, which goes into plagioclase. Therefore, there are so many non–calcium phosphates in the residual (pegmatite) melts that arose from the original high-alumina ones, in particular, iron-manganese ones, as can be judged from the data of Spanish geologists who studied tin-tungsten deposits associated with the pegmatites of the Halama batholith near Salamanca [113]. There are almost 2 dozen such rare fofats in the tablet they gave! In the hydrotherms following the pegmatites, these rare phosphates are transformed and other equally rare ones are obtained, such as **montebrasite $LiAlPO_4(OH)$ and childrenite $Fe^{2+}AlPO_4(OH)_2 \cdot H_2O$**.

In the Danilovsky manifestation of rare-metal granite pegmatites in the Altai Mountains, most of the REE is contained in orthite, monazite and xenotime, therefore, in fluorapatite, the amount of REE is small (about 350 ppm), with a predominance of light among them [15].

4.7. Metamorphites

During the metamorphism of rocks, as detailed in the Irish review [130], the composition of accessory apatite undergoes serious changes. The authors separately consider low-graded metamorphites (mainly green shale facies) and high-graded (up to granulites), where apatite changes are especially significant. On the logarithmic "biplot" LREE – Sr/Y, the compositions of metamorphic apatites form two disjoint fields: LM and HM.

The LM field (a wide, non-diagnostic range of values for the Sr/Y ordinate and minimum values for the LREE abscissa) are low- and medium-graded metamorphites, which are characterized by dissolution and re-deposition of apatite – with a corresponding loss of REE.

The HM field (low values of Sr/Y and LREE content greater than 1000 g/t) are high-grade metamorphites and metasomatites; here are also the compositions of anatectic metamorphite leukosomes. An increase in the temperature of metamorphism up to anatexis reduces the REE content in primary magmatic apatites and lowers Sr/Y – due to a simultaneous increase in Y concentrations and a decrease in Sr concentrations.

The works not covered by the Irish review include many articles by domestic geologists, as well as a number of foreign studies.

Voronezh geologists [58] studied mineral parageneses, morphology and composition of apatites from iron-siliceous formations of different ages (FSF) Voronezh crystal massif. Two generations of apatite, differing in composition and morphology, have been established in Mesoarchean FSF. At the peak of metamorphism of the Mesoarchean FSF (more than 900 ° C), fluorapatite-1 was stable, preserved in the form of small crystals enclosed in large secretions of ortho- and clinopyroxenes. The metamorphic fluid was characterized by sufficiently high HF fugitives. Apatite-2 crystallized during the second and/or third less thermal (700 °C) metamorphic events. It is present in the development sites of later minerals – garnet, grunerite, chlorite. The composition of apatite-2 corresponds to hydroxyapatite with an admixture of chlorine, which indicates the water-salt composition of the equilibrium fluid. This is confirmed by the finding of pseudo-toxic water-salt fluid inclusions with low concentrations of 1.9-4.9 wt.% NaCl eq. In magnetite quartzites of the Neoarchean and Paleoproterozoic FSF fluorapatites are stable. In general, a decrease in fluorine fugitivity in the metamorphic fluid from the Mesoarchean to the Paleoproterozoic was found, which is due to a decrease in the amount of apatite in the rocks of the Neoarchean and Paleoproterozoic ferruginous-siliceous formations relative to the Mesoarchean.

Deposits of Fe-Ni ores representing metamorphosed former laterites have been described in Northern Greece [97]. Among the accessory minerals, chlorine–free fluorohydroxyapatite with an average composition (wt. %) CaO = 51.35, FeO = 2.80, P_2O_5 = 41.4 and (F + H_2O) = 5 is described. The mineral occurs in small grains (from <10 to 50 microns) scattered in an ore matrix composed of goethite, hematite, magnetite, shamosite and quartz, or forms an intermediate zone in zonal chromite crystals (strongly enriched with Mn, Ni and Co) – between the chromite core and the magnetite shell. Structures of plastic and brittle deformations are visible in apatite. Quartz and magnetite inclusions are found in the poikyloblastic grains of apatite. All these data together prove that apatite is metamorphic, formed during the gradual dissolution of the primary apatite of laterites, approximately simultaneously with the rock-forming minerals of ores.

The newly formed fluorapatite is described in the metamorphites of the Alps foundation, which is part of the remarkable "crowns" growing on monazite-1 and consisting of allanite and fluorapatite, which are considered by the authors [102] as products of the "decay" of primary monazite-1. These "crowns" contain monazite-2 growths – as evidence of polymetamophism. The authors write [102, p. 1102]:

"From a geological point of view, this means that polymetamorphic monazite-containing rock will become the most suitable for the growth of new monazite when it passes a phase of strong regression between P-T peaks. In the case of orogenic events separated by large time intervals, such periods of low temperature will usually be usually located between the peaks of metamorphism".

Among the characteristic minerals of metamorphites can be called **goyazite SrAl$_3$(PO$_4$)(PO$_3$OH)(OH)$_6$** aluminum and strontium phosphate from the crandallite group. Although the findings of gojacite in pegmatites were previously known, but in 2017 Ural geologists discovered it in metamorphic paraslates (and propylites formed from them) in the folded Pre-Jurassic basement of the West Siberian Plate [23]. According to the authors, primary feldspar and monazite served as the source of the substance for goyazite.

Finally, the appearance of an association of florencite and crandallite, described, in particular, by Bulgarian mineralogists, can be attributed to the characteristic relatively low-temperature metamorphic transformations of igneous apatite [105]. They described the transformations of igneous apatite, which in the processes of argillization of the epithermal sulfide Cu-Ag Chelopech deposit at temperatures of 200–300 oC turned into an association of florencite and crandallite.

Florencite (Ce,La,Nd)Al$_3$(PO$_4$)$_2$(OH)$_6$ and **crandallite CaAl$_3$(PO$_4$)$_2$(OH)$_5$·H$_2$O** are the extreme aluminum members of the group of aluminum-sulfate phosphates (APS), which, in turn, is part of the supergroup of alunite. This supergroup contains more than 40 mineral species with the general formula **DG3**(TO$_4$)$_2$(OH, H$_2$O, F)$_6$, where **D** – major cations (K$^+$, Na$^+$, NH$_4$+ , H$_3$O$^+$, Ag$^+$, Pb^{2+}, Ca^{2+}, Ba^{2+}, Sr^{2+}, Bi^{3+}, REE^{3+}) with coordination numbers greater than or equal to 9;

G – Al^{3+}, Fe^{3+}, Cu^{2+} or Zn^{2+} in octahedral coordination;

T – is basically S^{6+}, P^{5+} and As^{5+} in tetrahedral coordination.

Minerals of the APS group are formed in endogenous and hypergenic processes, as products of Al-containing minerals changes in relatively oxidizing environments with an abundance of S and P, in a wide temperature range of 15–400 $^{\circ}$C. And depending on the situation, solid solutions are formed in the minerals of the APS group. Some varieties of these minerals are characteristic of high-sulfur epithermal systems, where they are formed as a result of either endogenous (magmatic-hydrothermal) or hypergenic processes of change with gradual heating. The initial phase for the formation of florencite and crandallite was igneous apatite. It turned out to be unstable under conditions of low pH and oxidizing environment of the formation of these ores.

Detritus apatites (as well as sphenes-titanites and zircons) of Archean age in tuffs (near the famous Oklo river!) in Gabon, underwent a low-temperature hydrothermal change in the chlorite facies of metamorphism somewhere at the end of the Ediacaran (approx. 560 million years). At the same time, the contents of Ti, Al, Fe, Ca, REE, U, Pb in titanites (sphenes) and zircons underwent a strong change (in–out), while the grains of accessory apatite turned out to be quite stable. Trying to understand what is the matter, the French-Japanese team of authors [107], relying on the redistribution of REE, U and Pb in titanite and zircon, came to the conclusion that the processes of hydrothermal change occurred in an alkaline environment, at pH >8.

Ukrainian authors who studied the contents of paramagnetic centers (PC) in 11 groups of metamorphic (including metasomatic) rocks obtained valuable data on the dependence of the content of PC on the conditions of crystallization (recrystallization) of apatite [28, p. 61]:

"Samples from metamorphic rocks are characterized by high values of O-centers in the absence of Mn^{2+} ions in the cationic positions of M(1) <...>. In samples from metasomatic granites <...>, F-O-F-centers are significantly (about 50 times) smaller, OH-containing PC are absent, with a high content of Mn^{2+} ions in both structural positions <...>. The low concentration of O-centers is most likely due to the presence of H2Ostr molecules."

By the method of ICP-MS with laser ablation, Buryat geologists [76] studied the compositions of two morphological varieties of rock-forming metasomatic apatite from amphibolized gabbro of the Oshurkovsky massif in the South of Transbaikalia. Here apatite ranges from 2–3 to 6–10 wt%, and in the zones of hydrothermal change reaches 40–45 wt%. High concentrations (ppm) of REE (8156–9546), with sharp enrichment with LREE, weak europium anomaly (Eu/Eu* = 0.85–0.90), strong accumulation of Sr (9844–11567) with moderate concentrations of Mn (440–491), Y (138–160), U (5.9–6.6) and Th (19–22).

Irkutsk geologists [55] studied apatite from apatite-phlogopite-ribekite near-contact metasomatites associated with calcite and dolomite-ankerite carbonatites of the Onguren dyke-vein complex in the Western Near-Baikal region. These metasomatites are characterized by high concentrations (ppm) of LnCe (up to 11200), U (23), Sr (up to 7000), Li (up to 400), Zn (up to 600), Th (up to 700). REE concentrators in alkaline metasomatites are fluorapatite containing up to 2.7 wt. % $(Ln_{Ce})_2O_3$, as well as monazite-(Ce), cerite-(Ce), ferriallanite-(Ce), eshinite-(Ce).

5. HYDROTHERMAL AND ORE-BEARING APATITES

In 2012, Ukrainian authors [18] assessed the feasibility of using REE in apatites of endogenous deposits of the Ukrainian Shield as an indicator mineral of ore formation conditions. Apatite from arrays of gabbro-syenite and alkaline-ultramafic formations of the Ukrainian Shield, as well as from P-Fe-Ti deposits within anorthosite-rapakivi granite plutons, apatite-bearing metagabbroids and calcifyres were analyzed. It is shown that apatite from deposits of different formation affiliation differs significantly in the concentration of impurity elements and the form of chondrite-normalized REE spectra. According to the authors [18], the values of Sr, REE, Y concentration, values (La/Yb)N and Eu/Eu* in apatite obtained by them can be used to diagnose the formation affiliation of apatite-bearing rocks, the type of their mineralization and conditions of mineral formation.

The interpretation of the processes of magmatic-hydrothermal ore formation is particularly controversial, as can be seen from the works of Ural geologists who studied the morphology and composition of accessory apatite in the granitoids of the Urals with quartz-vein gold mineralization [69]. The genetic concept proposed by them is striking in its complexity: according to the features of apatite, the authors try to judge the facies of the depth of granitoids, the P-T conditions of their crystallization, the compositions of magmas and their fluid regime! In particular, they studied in detail gabbro-tonalite-granodiorite-granite massifs (GTGG) of gold-metallogenic profile, as part of the granitoids of the plutonic group, which are suprasubduction formations of the active continental margin. The formation of such massifs began with water-based mantle magmatism, the products of which (gabbroids) in the conditions of the lower crust (at pressures of 6–8 kbar) were then subjected to partial melting (water anatexis) giving rise to the earliest members of the magmatic series – gabbro-tonalite-granodiorites, which are mantle by substrate, and anatectic by the mechanism of formation. And then the crustal anatexis of the rocks of these early series followed – with the formation of later adamellite-granite rocks, with which the golden and gold-sheelite mineralization is associated in the Urals (Berezovseoe, Kochkarskoye, etc. deposits). During the evolution of this very long (60–80 million years) crustal water anatexis, there was a multiple redistribution of gold from melts and crystallizing rocks into a weakly chlorine-bearing ore-forming fluid enriched with sulfur and carbon dioxide. Therefore, in pre-ore apatites, the chlorine content is 0.1–0.2%, and in apatites from ores, the fluorine content increases greatly with a decrease in chlorine to zero values. The second important sign of apatites from ores and ore-bearing metasomatites –berezites) is a sharp increase in in their sulphate sulfur content to 1% by weight.

5.1. Platinum-metal deposits

In 2018, the outstanding Moscow mineralogist Ernst Spiridonov, in collaboration with A. A. Serova, presented a detailed picture of the formation of Norilsk sulfide ores with PGE – based on the study of the composition of accessory apatites of three generations [60]. The authors assumed that apatite concentrates F and Cl, which play an important role in the formation of pneumatolite minerals of platinum group elements.

Apatite I, whose composition evolved from hydroxychlorapatite to chlorapatite, is common among the sulfide bodies of massive Norilsk ores and in the fringes of fluid action over sulfide droplets in interspersed ores. ***Apatite I*** is associated with Ti biotite, titanomagnetite, ilmenite with baddeleyite lamellae, anhydrite, low-titanium kersutite, chlorine-containing hastingsite and edenite, jerfisherite and bartonite, EPG and gold minerals. Apatite I contains up to 2.3 wt.% lanthanides, mainly Ce, La, Nd. Apatite I increases and replaces it with ***apatite II***, the composition of which has evolved from hydroxychlorofluorapatite to fluorapatite. Apatite II also composes numerous isolated crystals in the mass of sulfides. The lanthanide content in apatite II is up to 0.9 wt.%. Pneumatolite chlorapatite and fluorapatite contain ~0.5% SiO_2.

The composition of apatite testifies to *the discrete evolution* of fluids released during the crystallization of Norilsk sulfide melts: at the first stage from water-chloride to chloride, in the second stage from water-chloride-fluoride to substantially fluoride. Lanthanides released during the replacement of chlorapatite I with fluorapatite II were probably part of the pneumatolite *zonal orthite-(Ce)*. In the areas of late metamorphism in the prenite-pumpellite facies among metamorphosed sulfide ores, apatite I and apatite II are partially or completely replaced by apatite III, whose composition varies from hydroxychlorapatite to hydroxyapatite, and which is poor in fluorine and lanthanides. Lanthanides released during the substitution of apatite I and II with metamorphogenic hydroxyapatite III are probably fixed in metamorphogenic *nonzonal orthite-(Ce)*.

In 2015, Voronezh geologists, using the chlorine content in excessory apatites from the section of the stratified Kivakka intrusion in north Karelia, proposed a new criterion for searching for zones of platinum-metal mineralization, to which they gave the name "Kivakka Reef type" [3]. They claim that the identification of the stratigraphic level with the maximum chlorine content, as well as the most significant range of changes in the chloricity of apatite, may correspond to the level of development of the Kivakka Reef mineralization zones containing Cu-Ni and EPG, especially Pd and Pt. The proportion of sulfide mineralization in rocks, distributed very heterogeneously, varies from the first% to 10%; on average, within the exposed part of the vertical section, about 3-5 vol.%. Sulfide minerals are represented by an association of pyrrhotite, chalcopyrite, pentlandite, with local de-

velopment of bornite, secondary and rare pyrite, sphalerite, galenite, AuAg alloy,
secondary violarite and chalcosine. EPG minerals are represented by members of
the merenskite-moncheite ($PdTe_2$–$PtTe_2$), kotulskite (PdTe) and sperrilite (PtA_{s2})
series. The ore zone is characterized not only by the maximum concentrations of
Cl in apatite (> 6 wt.%), but also by the most significant range of detected varia-
tions. Along the section of this intrusion, significant variations in the composition
of the rock-forming plagioclase and accessory apatite are also observed.

5.2. Kiruna type deposits

As noted in the article by Buryat geologists [51], not so many apatite-magne-
tite deposits are known in nature. Some of them belong to the apatite-containing
titanomagnetite type associated with gabbroids (for example, Volkovskoye in the
Urals). The other part, described under the name nelsonites, contains increased
amounts of silicate minerals and is a product of differentiation of alkaline rocks.
The third group represents **the Kiruna type**. In addition to Sweden (Kirunavara,
Luosavara, Grangesberg, etc.), such deposits have been established in China
(Meishan), Iran (Bafc, Esford), South America (El Laco) and Chile. For the ore
regions of Russia, this type of deposits was previously considered not characteris-
tic. Only later the Markakul and Kholzun manifestations of Altai were attributed
to this type. Apatite-magnetite deposits of the Kiruna type are usually large objects
in terms of reserves. The specific features of such deposits, in addition to the pres-
ence of apatite in the ores, are increased concentrations of REE, sharp contacts
with host rocks and insignificant scale of near-ore changes.

So, Kiruna-type ore deposits are characterized by a sulfide-poor mineral as-
sociation of low-titanium magnetite, fluorapatite and actinolite, and varies from
giants with hundreds of millions of tons of high-grade ore to small vein and veined
manifestations. Both tend to riftogenic structures – either marginal (back-arc) or
intracontinental (anorogenic). Facially, the deposits are confined either to deposits
of shallow-sea basins or to subaerial ones and are accompanied by manifestations
of volcanic-plutonic activity and the strongest fluid influences expressed in albiti-
zation.

The genesis of these deposits is fiercely debated, and the proposed mechanisms
vary from magmatic (liquation) to exhalative-synsedimentation and to epigenetic
hydrothermal. However, in recent years, the concept has prevailed that ***Kiruna-
type deposits are the final member of an extensive group of Fe-oxide-Cu-Au
deposits designated as IOCG***. This idea is supported by the similarity of tectonic
settings, the abundance of early magnetite, the presence in massive magnetite ores
of small amounts of late pyrite and chalcopyrite ± Au ± REE and some com-
mon secondary and vein minerals, especially actinolite and apatite. ***It was proved
that evaporites participated in the formation of ores*** – they served as a source of
chlorine and sodium, which caused typical albitization for ores, and a high degree

of oxidation of ores due to large-scale circulation of basin brines, enhanced by intrusive magmatism.

Apatite-magnetite ores of the Kiruna type are described in the Ningwu volcanic basin in eastern China – **in the Meishan deposit** [137]. Here, massive and brecciated ores are isolated in the main ore body located at the contact between gabbro-diorite porphyry and biotite-pyroxene andesites, as well as subeconomic stockwork and scattered ores. There are 4 stages of mineralization, the features of which can be judged by the composition of apatite. At the first stage (in massive magnetite ore) apatite associates with magnetite, andradite and quartz, and at the second (in scattered magnetite ore) – with magnetite and siderite.

Accessory apatites in modified gabbro-diorite porphyry have a mixed OH-Cl-F anionic composition, whereas apatites from ores are much more polarized – up to the terminal members, F- and OH-varieties. Low Mn contents in apatites are characteristic - usually less than 0.17%, which indicates a high oxidative potential of the hydrothermal fluid. This is consistent with the universally observed negative Eu anomaly in ore apatites enriched with light REE – and the absence of such in igneous apatites. As usual, such an anomaly of europium in ore apatite is explained by the extraction of Eu2+ by earlier magmatic plagioclase. In general, all the features of ore apatite confirm the genetic relationship of mineralization with altered gabbro-diorite porphyries.

In an older Chinese article with the same first author [136], almost the same ideas are presented, but as it was popular in those years, the main emphasis in the genetic interpretation of Kiruna-type ores is on the mechanism of liquid immiscibility. Figures were given here: early igneous apatites contain 3031–12080 ppm REE, whereas late hydrothermal ones contain only 1958 ppm REE. This means that the late ore-bearing fluids were depleted of REE compared to magmas.

As noted in the article of the Iranian-German collective [132], the Bafq ore province is located in Central Iran, where magnetite-apatite deposits of the Kiruna type with iron ore reserves (million tons) are located within the Cambrian volcanic-plutonic arc: Choghart (216), Chador-Malu (400), Se-Chahun (140) and Esfordi (17). In the latter, apatite reserves amount to 17 million tons (with 14% P_2O_5 and 17.2% Fe), and the REE content in certain areas of the deposit enriched with apatite reaches 2% by weight. Apatite here is low-calcium fluorapatite with a small admixture of hydroxyl and REE. The relic mineral has undergone a strong change with the removal of Na, Cl and REE. The extracted REE were mobilized and became part of the secondary monazite (by which the age of mineralization was determined), and also in a small proportion into allanite and xenotime, which either form independent crystals or are present as inclusions in apatite.

The time has passed when Kiruna-type ores were unknown in Russia, and in 2017, and according to a number of signs, ores of the North Gurvunursky metrogenition (Western Transbaikalia) were also attributed to this type. According to the description of Buryat geologists [51]. pink apatite (color from finely sprayed

hematite, up to 0.5-1 wt. % FeO), composes idiomorphic grains and prismatic crystals in ores, less often their segregation. The size of the crystals is usually 0.5-1 cm along the long axis. The mineral is distributed unevenly, usually in the amount of 1-3%, sometimes up to 10% of the ore volume. Part of the grains of apatite is crushed and cemented with fine-grained magnetite. The mineral belongs to fluorapatite (2.7-4.2 wt. %F), sulfur and chlorine are not characteristic of it. In apatite, there is an emulsion impregnation, and in some cases, larger monazite secretions and less often xenotima. The composition of impurities in the mineral contains strontium, yttrium (500–900 ppm), thorium, uranium, and the REE content reaches 1–1.5 wt. %, with a predominance of LREE. Within the areas with the release of emulsion inclusions of monazite, apatite is sharply depleted of REE, often less than 0.1 wt. %. In the "spectrum" of REE, the europium minimum is clearly expressed. The value of Eu/Eu* varies between 0.2–0.4, the REE differentiation index $(La/Yb)_N$ is low and ranges from 1.75–3.63 (average 2.58). Sometimes small grains of apatite are found in hydrothermal veins. This apatite-2 is devoid of impurity elements, including REE.

Altai geologists [14], who studied Kiruna-type deposits in the western part of the Central Asian folded belt on the territory of Russia, Kazakhstan and North China, noted that at the early stage of ore formation, there was a noticeable selection and enrichment of the entire REE group in the earliest generations due to the sharp depletion of REE fluids, which were significantly consumed during the crystallization of rare earth minerals proper (orthite, monazite, xenotim, cerium epidote) [14, p. 77]:

"This is clearly visible in the early and late generation of apatite. In the second generation of apatite, the concentrations of all REE are noticeably lower. In parallel, there is a decrease in the ratio of light to medium and light to heavy rare earths. The Eu/Eu* ratio in the second generation of apatite also decreases by almost an order of magnitude compared to the first".

5.3. Gold deposits

In order to clarify the genetic relationship of the Berezovsky gold deposit with the granites of the Shartash massif, Ural geologists in 2011 studied the composition of the volatile phase (F, Cl, S) of apatite from the granites of the Shartash massif, from the dikes of the granite porphyry of both the massif itself and the Berezovsky gold deposit, as well as from the berezites formed by these dikes – in polished sections according to the samples of S. V. Pribilkin [33]. On the graph constructed by the authors in coordinates P_2O_5, % (from 40.5 to 43%) by abscissa and SO_3,% (from 0 to 1.20%) by ordinate, the field of inverse correlation in apatites from granite porphyry and berezite dikes (where SO_3% is greater than 0.40%) is quite clearly distinguished, and in the lower part of the graph (where SO_3%

is less than 0.40%) there is an uncorrelated field for apatites from granite of the Shartash massif. The authors concluded [33, p. 135]:

"The data obtained indicate an increase in the sulfur content in apatites, in the process of formation of the Shartash massif – from granites of the main phase to vein series completing its formation, reaching the highest values in apatites of dykes of blue-ore granite porphyries of the Berezovsky formation and in apatites of berezites according to them <...>."

Thus, in apatites from medium-grained granites of the Shartash massif, the SO_3 content is 0.15–0.26%, in blue-ore granite porphyries 0.26–1.08% and in metasomatites (berezites) according to them – 0.44-1.05%.

Unfortunately, the Bengge polymetal gold deposit in syenites in the South of China is known to us only from the meager English abstract of the Chinese article of 2019 [139]. As can be judged by the extremely general, non-specific data of this abstract, the content of impurity elements in apatites can be used for genetic purposes. In particular, as the intensity of gold mineralization in apatites increases, the contents of Mn and Ga decrease and the contents of Cl and SO_3 increase.

The data on regular variations in the composition of accessory apatite in rocks and ores of the giant Precambrian Olympic Dam deposit in South Australia, where Fe-Si-Au ores form a hydrothermal halo around the Roxby Downs granite reef massif (RDG), about 1.6 billion years old, are very indicative [110]. Based on the data on the composition of zonal apatite, the authors evaluate the indicator possibilities of the morphology and composition of REE in apatite for judging the evolution of the ore-forming fluid - from early to late hydrothermal stages. Zonal magmatic apatite usually has REE-poor cores and REE-enriched grain edges. The nuclei are enriched with light REE (LREE) normalized by chondrite, with a strong negative Eu anomaly. In hydrothermal ores, *igneous apatite-1* disappears, replaced by hematite and sericite, and a newly formed *apatite-2* is formed, in which the "spectrum" of REE normalized by chondrite has a convex shape due to the relative accumulation of medium REE (MREE), with a weak negative anomaly of Eu. The grains of such apatite-2 contain abundant inclusions of florencite and sericite. In the high-grade bornite ores of the apatite deposit, an even higher concentration of MREE with a positive Eu anomaly is demonstrated. The latter is explained by alkaline fluid conditions. The U and Th contents in apatite generally repeat the REE distribution – they are highest in igneous apatite of granitoids and consistently decrease in hydrothermal apatites.

5.4. Other deposits

In 2018, Yekaterinburg geologists examined the distribution of mineralizing elements F, Cl, S in coexisting apatites, hornblende and biotites of diorites and granodiorites composing the main part of the East Verkhotursky massif, and in

diorites of dikes cutting them [37]. It was shown that the S and Cl ratios in these apatites are closest to the compositions of apatites of suprasubduction diorite-granodiorite-porphyry complexes accompanied by **gold-copper-porphyry** and **copper-molybdenum-porphyry** mineralization. The authors cautiously suggested that the reduced content of sulphate sulfur in apatites from diorite dikes dissecting intrusive rocks may indicate a decrease in the oxidative potential at the final stage of the formation of the East Verkhotursky massif, which eventually led to the imposition of mineralization in the form of native copper. **A new diagnostic triangle "F-Cl-S in apatites"** has been proposed, which which may be useful for a preliminary assessment of the ore prospects of magmatic complexes of different composition.

Yekaterinburg geologists [13] studied apatites from rocks containing **(Mo)-Cu-porphyry deposits** of the Urals. The average S content in apatite crystals from minimally modified dioritoids is 0.05-0.08 wt. %. Apatite from sericitized-propylitized granitoids of quartz-diorite composition of the two largest (Mo)-Cu-porphyry deposits of the Urals (Gumeshevsky and Mikheevsky) is also not rich in sulfur - usually 0.01–.03 wt. %. Thus, the amount of S in apatite of quartz-diorite magmatites does not depend on the scale of deposits, the nature of metasomatic changes in granitoids and the content of pyrite with a small amount of it (up to 1–3 wt. %). Slightly increased S contents are observed in all apatite crystals from everywhere propylitized and epidotized rocks of the extensive Sapov subvolcanic structure. Apatite from dolerites and diorite porphyrites that break through them, as well as highly pyritized dolerites (up to 15 wt. % pyrite), contains (0.05–0.08) ±0.01 wt. % S.

The maximum concentration of S in apatite (0.10–0.20 wt. %) is observed only in rocks (Cu)-Mo of the Talitsky deposit and the Verkhneuralsky ore occurrence. The highest concentration of S is observed in apatite from metasomatites formed during acid leaching. For example, in apatite from the apodiorite sericite-quartz metasomatite of the Vostochno-Artemovsky ore occurrence, the S content often reaches 0.04-0.07, and in individual crystals – 0.11–0.25 wt. %. The average S content in newly formed apatite crystals in pyrite-bearing metasomatites of the Gumeshevskoe deposit is usually 0.07-0.14 wt. %, and in two crystals – 0.24-0.53 wt. %. The authors conclude that the activity of S in the ore-forming fluid tended to increase with the acidic fluid alkalinization.

In the Streltsov *uranium ore field* of the Southern Transbaikalia [48], the Talan manifestation of phosphates is known, which belong to the complex of Precambrian metamorophytes developed in the Southern Baikal region, on the Aldan, in China, the DPRK, Tanzania and other regions of the world. Phosphates are represented here by francolite and fluorapatite. Francolite is metamorphosed Middle-Riphean phosphorites, and fluoro-apatite is igneous, from the Middle-Riphean moderately alkaline peridotite-gabbro-gabbrodiorite complex, an example of which is the large Seligdar deposit in Yakutia [81, p. 38, 39].

6. BIOAPATITES

Bioapatites are commonly called calcium phosphates, which compose the bones and teeth of vertebrates (including humans), as well as vertebrate bones buried in sedimentary rocks, ichthyolites (bone detritus and fish scales) and conodonts – the remains of the dental apparatus of some extinct animals.

Modern bioapatites are represented by weakly crystallized hydroxyapatites with a noticeable admixture of carbonate, which increases with diseases of teeth and bones (paradanthosis, coxoarthrosis). As for bioapatites of sedimentary rocks, they have undergone strong changes in diagenesis – and in this respect are similar to fluoro-carbonate apatites (francolites) of phosphorites.

As shown by Omsk mineralogists who studied the heads of human femoral bones affected by coxoarthrosis, removed during endoprosthetics, provided to them by doctors, the basis of the bones was poorly crystallized non-stoichiometric apatite. With coxoarthrosis, the content of PO_4^{3-} decreased in its structure and the content of CO_3^{2-} increased. [39].
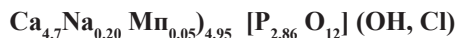
Yekaterinburg geologists [63] accidentally discovered fluorapatite shells of the Eifel-Zhivet foraminifera in thin sections of samples of carbonaceous-siliceous aleuropelites of the ore-containing thickness of the Safyanovsky copper-crusted deposit (Middle Urals). Since phosphate shells were unknown for the Devonian, it was assumed that apatite replaced the original calcite of the shells, but this could not be proved.

In 2007, Miass mineralogists [49] studied a mammoth tooth with a size of 9x12x22 cm and a weight of 2.1 kg found in the deposits of the above-floodplain terrace of the Borya river in the Chita region and gave 7 analyses of the tooth material (plates and cement with the same composition of hydroxyapatite, CaO/P_2O_5 = 1.35) and 2 analyses of the substance of the altered tooth. From the first, we chose analysis No. 8) with an ideal sum of cations equal to 5.01, and from the second, an analysis with such an amount equal to 4.95:

Apatite-1 unchanged tooth:

$$(Ca_{4.7}Na_{0.12}Fe_{0.16}Mn_{0.03})_{5.01} \ [(P_{2.74}S_{0.07})_{2.81} \ O_{12}] \ (OH, F, Cl)$$

Apatite-2 altered teeth:

$$Ca_{4.7}Na_{0.20} \ Mn_{0.05})_{4.95} \ [P_{2.86} \ O_{12}] \ (OH, Cl)$$

The authors concluded [49, p. 142]:

"Thus, in the bone tissue of a mammoth tooth <...> there is some phosphorus deficiency compensated by sulfur."

In the Lower Kellovian clays on the left bank of the Sola near the village of Kargort (Komi Republic), a bone layer with scattered fragments of highly pyritized skeletons of marine lizards – ichthyosaurs and plesiasaurs was found.

According to the study of Syktyvkar geologists and chemists [42], the K = CaO/P_2O_5 modulus for 7 bone samples was 1.16–1.35, which differs from the value of 1.31 pure francolite [42, p. 12]:
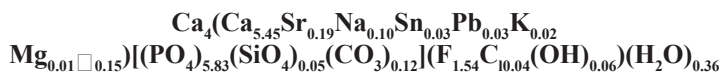
"Reduced values of the K modulus in the range 1.16–1.30 indicate a CAO deficiency in the structure of apatite and isomorphic substitutions of it with other elements: Si, Fe and TR."

Judging by not very reliable analyses, the SiO_2 and Fe_2O_3 contents in bones are 0.00–12.40 and 1.43–13.53%, and according to semi-quantitative spectral analyses by T.I. Ivanova, the contents (ppm) of Y, La, Yb are 40–200, 40–90 and 4–30, respectively.

According to the evidence of St. Petersburg crystallographers [67], the fossil remains of conodonts (conodont elements) were first discovered in 1856 in the Lower Ordovician deposits of St. Peteburg province and described by Ch. Pander, one of the founders of embryology and paleontology in Russia. He suggested that microscopic fossilized remains, which he called "*cone-shaped teeth*" – conodonts (Lat. conus – cone; Greek. Odus – genus, ontos – tooth), represent teeth and/or jaws of one of the unknown species of ancient fish. Since then, the systematic position of conodonts has been the subject of discussion for more than 150 years.

Their study of the Middle Frasnian conodonts by single-crystal X-ray analysis and energy-dispersive X-ray spectral microanalysis showed that they are an organo-mineral composite in which phosphate is fluoro-hydroxyatite. The content of carbonate ions replacing PO_4^{3-} anions is very insignificant (~1 wt. %).

The channels of the structure also contain F^- and OH^- ions of ions (in a ratio of 3:1), partially replaced by water molecules. As a result , the following phosphate formula with a molecular weight of 1001.35 was proposed:

$$Ca_4(Ca_{5.45}Sr_{0.19}Na_{0.10}Sn_{0.03}Pb_{0.03}K_{0.02}$$
$$Mg_{0.01}\square_{0.15})[(PO_4)_{5.83}(SiO_4)_{0.05}(CO_3)_{0.12}](F_{1.54}C_{10.04}(OH)_{0.06})(H_2O)_{0.36}$$

This formula reflects isomorphic substitutions of cations in the Ca2 position, as well as the presence of a cationic vacancy in the structure with f.e. = 0.15.

In 2015, the Chinese team [93] performed a fundamental study of the distribution of REE in the bioapatite of conodonts from the Lower Triassic sediments of the Southern. China. It turned out that, firstly, conodonts are more than 100 times enriched in REE compared to bioapatites of modern living organisms, and secondly, that the distribution ("spectra") The REE in conodonts are not at all similar to the spectra of seawater - although the sediments studied were undoubtedly normal marine. It became obvious that, in accordance with a number of previous studies, the processes of diagenesis played a decisive influence on the enrichment of REE conodonts (up to 1000 ppm), which led to adsorption (introduction) and

desorption (removal) REE in different phases of sediment, and to strong interelement fractionation of REE, depending strongly on the former redox conditions of the sediment pore waters. Remobilization of REE in sediment usually leads to interelement fractionation, which in different ways leads to enrichment or depletion of LREE, MREE and TREE. In addition, the remobilization of REE can be facilitated by changes in redox conditions, for example, by reducing the dissolution of hydroxides in suboxide and anoxide pore waters.

It was found that conodonts contain two diagenetic components of REE, one of which is characterized by a low value of ΣREE (100–300 ppm), high ratios of ΣREE/Th (>1000), strong enrichment with average REE and ratios of Eu/Eu* ~1.5–2.0, and the second – a high value of ΣREE (300–2000 ppm), low ratios of ΣREE /Th (~20-30), small or zero enrichment with average REE and ratios of Ei/Ei* ~1.0. The first component demonstrates the pronounced average convexity of the REE spectrum, which is an early diagenetic signature associated with suboxic conditions, possibly associated with the adsorption of REE on Fe and Mn oxyhydroxides in the shallow subsurface zone of the former sediment. The second component shows a flat distribution of REE, which is similar to solid rock, which indicates the receipt of REE from a terrigenous source (for example, from clay minerals), probably in the range of burial depths from small to large.

Thus, this study showed that ***the bioapatite of conodonts in no case can serve as a "paleomarine" indicator at the turn of the Permian and Triassic, since the distribution of REE in it was entirely determined by the processes of diagenesis.***

Using essentially the same technique, i.e. relying on cerium anomalies and the Th/U ratio in conodont bioapatite from the South. China, another Chinese collective went much further in the paleo-oceanic interpretation [127]. They claim that compared to other sources of bioapatite, such as ichthyolites, the albid conodont corona provides registration of cerium anomalies in the water column and the Th/U ratio, which are little affected by diagenetic changes. As a result, they built a detailed history of redox reactions. in the Paleocean Pantalassa and Paleothetis in a wider interval of geological time (20 million years): from the Late Permian to the Late Triassic. A well-known oceanic oxygen-free event (OAE) has been identified, coinciding with the extinction of species at the end of Perm. In addition, it was possible to find two more notable OAE – in the Early Triassic (the earliest smitium is the earliest spatium, and the middle spatium) and one weak OAE in the Middle Triassic (anisium).

7. APATITES OF PHOSPHORITES

As for the rock-forming apatites of phosphorites, in the Irish review [130] they are quite rightly called "autigenic" in order to distinguish them from accessory detritus apatites of "silicoclastic" (that is, clastic) sedimentary rocks.

Voronezh geologists tried to reconstruct the conditions of phosphorite formation based on the distribution of lanthanides in phosphorites [77]. In particular, they used the indicators La/Yb, La/Sm and Ce/Sm to diagnose topofations. It is believed that these indicators increase in coastal facies, while the indicators Yb/Sm, Y/Sm decrease. In pelagic facies, the behavior of these indicators is the opposite.

Thus, modern ocean phosphorites of the Mataiva Atoll have high values of Yb/Sm, Y/Sm compared to other phosphorites, as well as a low index of $\Sigma Ce/\Sigma Y$. It is believed [77, pp. 1105-1106] that this

"reflects the nature of lanthanide fractionation in sedimentation environments significantly remote from land."

In 2016, Ural geologist A.V. Maslov published a review of 49 papers with data on the geochemistry of REE in Neoproterozoic-Cambrian phosphorites [44]. It is characteristic that only 2 of them are Russian-speaking, including A.V. Ilyin's book [27] on ancient (Ediacaran) phosphorites. The purpose of the review was an attempt to use the data provided in it for the purposes of paleogeography. Maslov listed some more or less reliably established empirical patterns: 1) similarity of the REE "spectra" normalized for clay shale to the distribution of lanthanides in seawater with negative Ce anomaly and enrichment with heavy REE (HREE); 2) "shale" distribution of REE, characteristic of Miocene phosphate aggregates and younger formations off the coasts of South Africa and South America; 3) pronounced negative Ce anomalies and depletion of REE of almost all Pre-Mesozoic phosphorites; 4) phosphate crusts and The contractions associated with nodules and crusts of Fe-Mn may contain a positive Ce anomaly.

Nevertheless, it can be seen from this review that such commonly used indicators as ΣREE, $\Sigma LREE$ (sum of light REE), $\Sigma HREE$ (sum of heavy REE), $\Sigma MREE$ (sum of medium REE), ratios of LREE, MREE, HREE – relative accumulation or depletion (depletion) of them in phosphorites, the magnitude of Ce- and Eu anomalies, the ratio of REE with the isotopic composition of carbonates associated with phosphorites and organic matter – strongly vary. The noted variations are due to several factors, among which are:

- the composition of seawater of different epochs, which did not remain constant;
- sedimentation rate;

redox-sedimentation environment;

- the content and composition of the organic matter associated with phosphorites;

- content and composition of carbonates associated with phosphorites;

- diagenetic changes, among which poorly understood microbial processes played an important or even decisive role;

- complication of sedimentation by exposure to endogenous hydrotherms.

And although A.V. Maslov himself evaded certain conclusions of his review, in our opinion, the materials generalized by him make the use of apatite REE for diagnostic purposes a very dubious procedure, since it is not possible to separately assess the extent of the influence of individual factors. This assessment is not helped by the normalization of the REE content for the "shale", nor by the search for mutual correlations of indicators, for example, indicators of the isotopic composition of oxygen with the ratios of individual REE.

In general, A.V. Maslov came to approximately the same conclusions in 2017, having considered the distribution of REE in Pre-Ordovician phosphorites from different regions of the world [43]. Based on the analysis of a significant data bank, he showed that at present there are no universal parameters, guided by which it is possible to judge sedimentation and diagenetic conditions of phosphorite formation with any confidence, first of all, about redox conditions.

Any reconstruction of this plan requires a thorough analysis of both geological facts and extensive and diverse geochemical information. Approximately the same results were presented by A. V. Maslov in a 2016 article, but with a more optimistic assessment of the use of REE as a "paleomarine" indicator [44].

After G. N. Baturin discovered the process of modern phosphorite formation in carbonaceous diatom silts on the shelf of Namibia (southwest Africa) [5; 4], it was possible to think that the situation described by him is unique and has no analogues. Therefore, the Miocene nodules described by him in 2012 from the bottom of the Sea of Japan [6] proved to be an important confirmation of the reality of the open mechanism, but with characteristic differences.

The lithological and geochemical study of Miocene nodular phosphorites from four underwater uplifts of the Sea of Japan - Northern Yamato, Southern Yamato, East Korean and Krystofovich was performed using scanning electron microscopy, chemical and modern plasma (ISP-MS) analysis. The obtained data on the microstructures of phosphorites and the distribution of 57 macro- and microelements in them revealed their significant similarity with the late Quaternary granular phosphorites of the Namibian shelf and with phosphorites in general, which is evidence of their genetic similarity. But unlike the phosphorites of the Namibian shelf, traces of the influence of volcanogenic-hydrothermal activity have been found in the phosphorites of the Sea of Japan, as evidenced by examples of positive cerium anomaly in some samples and positive europium anomaly in others, as well as a slightly increased gallium content in phosphorite from the Chentsov

volcano (22 g/t Ga versus 2–6 ppm in other phosphorites).

Unlike many others, the phosphate of the zhelvak phosphorites of the Middle-Riphean Strelnogorsk formation of Eastern Siberia contains so little CO_2 (<1%) that it is certified not as francolite, but as fluorapatite, which proves that phosphorites pass the stage of deep catagenesis [26]. The authors explain the sharp negative anomalies in La and Yb by the same reason. Nevertheless, an abnormally high content of the amount of REE was recorded, reaching a record figure of 2978 ppm in one sample. The "spectrum" of REE normalized by the average shale has a bell-shaped shape, meaning the accumulation of average REE.

In the technological sample (weighing about 400 kg) of Fe-Mn crusts from the underwater Magellanic Mountains (NW of the Pacific Ocean), the share of the cementing phosphate fraction accounts for about 10%. The rest is made up of Mn and Fe oxides (21 and 19%, respectively) and silica (23.5%). As a thorough study of the phosphate fraction showed, the facets of apatite crystals were often covered with a thin **cerianite** rash **(CeTh)O$_2$** and less often – **parisite (Ce, La)$_2$Ca [CO$_3$]$_3$F$_2$**, with the size of the discharge in hundredths of a micron. It turned out [8, p. 924] that

"a significant part of the REE, primarily cerium, are part of cerianite, and not molecules of the apatite mineral."

Thus, important differences between the phosphates of these crusts and shallow shelf phosphorites were discovered [8, p. 924]:

"it is noteworthy that phosphates and carbonates of REE are formed in shelf phosphorites <...>, and in phosphorites of seamounts – mainly REE oxide (cerianite), i.e. the dependence of the nature of rare-earth mineralization on the facies situation is traced. It can also be assumed that the initial stage of REE accumulation is associated with their sorption from seawater by collomorphic phosphate, which, as they crystallized and self-purified, displaced them beyond their crystal lattice, where they formed autigenic minerals."

8. THERMOCHRONOLOGY OF APATITE – TRACK METHOD

Relatively recently, a completely new use of accessory apatite has appeared – the so-called track method, adopted not by mineralogists or geochemists, but primarily by tectonists! This method allows us to reconstruct the details of the geological history of sedimentary strata of entire regions - episodes of their immersion and uplift, up to "exhumation" (that is, reaching the daytime surface), as well as reliably reconstruct the stages of thermal metamorphism of strata (or intrusions) – their heating and cooling.

Since all this was completely unthinkable earlier, during reconstructions of the history of geological development, the new method gained enormous popularity in geology and, accordingly, generated an avalanche of literature numbering many hundreds of names

Below we will give a brief summary of the theoretical foundations of the track method, based on the doctoral dissertation of A.V. Solovyov, defended at the GIN RAS in 2005 [61], and we will give just a few randomly selected examples of its application – in different regions. A complete review of the existing (almost immense) literature is out of the question.

8.1. Theoretical foundations of the track method

According to the presentation in the abstract of A. V. Solovyov [61], in the early 1960s, American researchers developed a new method for determining the age of minerals based on calculating the density of tracks of fragments of spontaneous fission of uranium nuclei accumulating in the mineral during geological history <...>.

In the English literature, the method was called fission-track dating. It has been shown that counting tracks in minerals can be carried out using optical microscope, as their size can be increased by chemical etching in a certain reagent <...>.

Translated into Russian language method is called "Dating in the tracks of fission fragments of uranium" <...>. For brevity, A. V. Solovyov proposes to use the term fission-track Dating

Nuclear fission is one of the processes of decay of heavy radioactive nuclides. During fission, an unstable nucleus splits into two daughter fragments of approximately the same size. In this case, several neutrons are released, a significant amount of kinetic energy of two fragments of the nucleus, which scatter in the opposite direction at high speed and carry a high positive charge. When passing through a solid, a fast charged particle leaves a disturbance at the atomic level, oriented along the trajectory of its movement. These disturbances are called nuclear tracks (or tracks of charged particles), and the material in which the tracks are recorded is a detector.

The spontaneous fission tracks observed in natural materials were mainly formed due to the fission of ^{238}U. The other two isotopes of uranium and thorium have too low a content and/or a much longer half-life to produce a number of tracks comparable to the number of decay tracks of ^{238}U.

Tracks that have not been etched with a chemical reagent are usually called hidden, and their observation is possible only with an electron microscope at a magnification of 50000x<...>. For visual examination of tracks using an optical microscope, techniques for increasing the size of tracks or visualization have been developed. The most popular and widely used technique of chemical etching based on that hidden tracks are primarily dissolve chemically aggressive reagent <...>. In chemical pickling, the mineral is immersed in acid, which dissolves first and foremost places of defects and increases the size of the tracks (Fig. 2).

For dating using optical microscope (magnification 1250x and above). Track dating is based on the classical equation describing the decay rate of a radionuclide <...>..

The calculation of the track age is based on the measured number of spontaneous fission tracks and the number of atoms in a certain volume of matter. Determining the number of atoms is also based on counting tracks. To do this, the sample is irradiated in a nuclear reactor by a stream of thermal neutrons, resulting in induced fission of uranium atoms.

The development of isotope geochronology methods has led to the emergence of the concepts of true age, apparent age and closure temperature of the isotope system <...>.

The true age of a rock (mineral) corresponds to the time interval between its formation and the present time.

The apparent age is the age of a rock (mineral) obtained by some isotopic method and different from the true age.
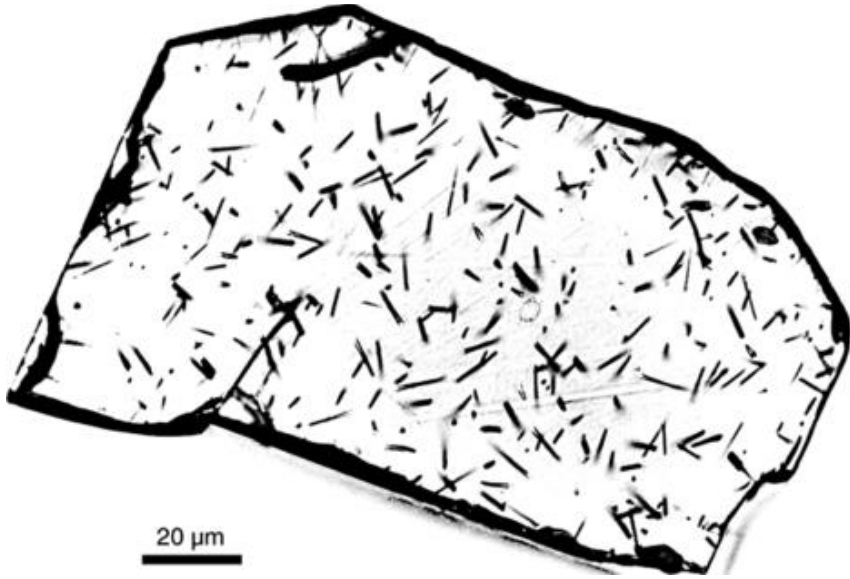
Figure 2. *Apatite crystal with ^{238}U spontaneous fission tracks*
enlarged by chemical etching. Taken from the Internet:
http://www.uib.no/en/project/tectonics/57161/thermochronology(University of Bergen)

The closing temperature (or blocking temperature) of an isotope system is the temperature at which the rate of loss of an isotope due to diffusion becomes insignificant compared to the rate of its accumulation <...>. The apparent age value measured during dating is the time interval from the moment when the mineral under study last cooled below the closing temperature of the isotope system, provided that from that moment the isotope system remained closed.

Various geological factors, such as temperature, time, pressure, hydrothermal action, ionizing radiation, can destroy tracks of spontaneous fission of uranium in crystals. The main one is the temperature. The effect of temperature on the annealing of tracks depending on the exposure time is described by Arrhenius lines. The longer the sample is kept, the lower the temperature at which the tracks are annealed. The disappearance of tracks does not happen instantly, the annealing of tracks is a gradient process.

The temperature range in which the tracks are annealed is called the partial annealing zone (PAZ). It is defined for zircons, sphenes and apatites. The thermal stability of the tracks increases in the following order: apatite $\Rightarrow$ zircon $\Rightarrow$ sphene <...>. The annealing properties of apatite are affected by its chemical composition. For example, tracks in chlorine-containing apatite are more stable than in fluorine-

containing <...>. During annealing, not only the density of tracks decreases, but their length also decreases. The study of track lengths in apatite is very important for the correct interpretation of data.

Track age, in physical terms– is the period of time during which the accumulation of tracks in the crystal occurred. It is necessary to keep in mind a clear distinction between the "physical measurement" and the "geological interpretation" of track ages. Interpretation of track ages is not always trivial and requires careful analysis of both the obtained material and consideration of various geological factors. Track dating is used to solve a wide range of problems in geology. As a traditional method of tephrochronology, track dating is used to determine the age of volcanic glasses <...>. The method is also actively used for dating impactites <...> and kimberlites <...>.

Dating of terrigenous deposits, correlation of sections, reconstruction of provenances.

Current research using fission-track analysis, aimed at determining the age of the cuts deprived of fauna, the reconstruction of the source rocks of terrigenous material, the study of exhumation of orogenic belts and the establishment of the thermal history of sedimentary basins <...>.

Fission-track dating is applicable to studying the dynamics of tectonic processes (accretion, collision, exhumation) by quantifying the time and the speed of their development <...>. Fission-track age reflects the time of cooling of the mineral below a certain threshold or temperature closure. In this sense, track ages correspond to the formation time for rapidly cooled volcanic rocks (age of eruption) or reflect the cooling time of rocks slowly rising from the depths (age of exhumation).

Detritus thermochronology is a technique that allows us to estimate the ages of rock cooling in provenances based on the study of track ages of detritus minerals from sedimentary sections. The main advantage of detritus thermochronology is that it allows you to trace in time the relationship between tectonic processes and sedimentation. Tracks in apatite are stable only in near-surface conditions (at temperatures below 60 °C), which limits the use of apatite in detritus thermochronology.

Study of exhumation rates of complexes of feeding provinces. One of the modern directions of track analysis is the dating of apatite and zircon from sections in order to study the exhumation of rocks in sources of terrigenous material <...>. This direction aims to study the temporal relationship between relief formation, erosion, climate and sedimentation.

Each feeding province (block, complex) supplies clastic grains with certain track ages to the adjacent basin, which depend on the thermal history of this province.

Study of the thermal history of sedimentary basins. The stability of tracks in minerals depends on temperature and time, which led to the use of track analysis for the reconstruction of the thermal history of sedimentary basins. *A large num-*

ber of studies are devoted to the study of apatite, since the temperature range of the partial annealing zone of tracks in apatite is very close to the temperatures at which liquid hydrocarbons are generated.

The formation of oil and gas in sedimentary basins is known to occur under certain temperature conditions. In particular, the formation of liquid hydrocarbons proceeds most intensively in the range from 60 ° to 130 ° C, and gaseous hydrocarbons – in the range of 130 °–220 ° C at a heating rate of 1–10 ° C /million years <...>.

The formation of methane from coal during coalification occurs in the temperature range of 80–230 °C, and the most intense generation of coal methane is characteristic of the range 150–230. Track analysis, unlike other methods (for example, vitrinite reflectivity analysis), makes it possible to trace the change in paleotemperature over time.

Study of the rates of uplift of orogenic systems. This is one of the important and complex problems of modern geotectonics. The formation and evolution of the relief depends on many factors, this system is the result of an integral interaction of endogenous (tectonic forces, magmatism) and exogenous (climate, erosion, sedimentation) factors. Since the track analysis provides quantitative information about the cooling processes, it can be used to estimate the rates of uplift, erosion and tectonic denudation.

Reconstruction of the structural evolution of complexes. Track dating is actively used to study the evolution of structural inhomogeneities of the earth's crust, for example, regional thrusts, discharges. A lot of complex studies based on structural analysis and track dating have been carried out to decipher the history of the evolution of metamorphic cores of the Cordillera type <...>. These studies make it possible to establish a link between deformation and denudation, to restore the time and speed of discharge movements.

Study of the tectonic evolution of accretion prisms. The formation of accretion prisms is a process leading to the buildup of the continental crust; the study of these structures is one of the fundamental problems of modern geodynamics. Using the examples of the accretion prisms of Shimanto (Japan) and Cascadia (North America), it is shown that the track dating of zircon and apatite can be successfully used to study the age of accreted sediments, the accretion time and the rates of removal of complexes to to the surface.

In addition to the above, we note that counting the number of tracks under a microscope is a tedious and very time-consuming procedure. Therefore, with the development of computer technology, the idea of automating this procedure arose, for which the University of Melbourne developed the Autoscan technique, hoping to save the geologist from unproductive mechanical work [100]. Unfortunately, this technique leads to big errors, because the machine does not know how to filter tracks of different genesis, so it requires mandatory correction of counting - manually, by the usual optical method.

8.2. Some examples

Out of many hundreds of works using track thermochronometry, we have arbitrarily selected only a few typical examples showing the solution of various geological problems.

In 2012, V. A. Soloviev and J. Garner demonstrated the effectiveness of the track method for sedimentary and volcanic-plutonic complexes of the North. Kamchatka [62]. Track dating of apatite from autochthonous, allochthonous and neoautochthonous rocks of the Lesnovsky thrust allowed us to conclude that in the process of collision of the Achaivayam-Valaginsky arc with the northeastern margin of Eurasia on the North. In Kamchatka, a thin allochthonous plate was pushed over the autochthonous deposits, which sank to the depths of the first kilometers (less than 4 km).

After the collision was completed, neoautochthonous volcanic-plutonic complexes of the Kinkil belt were formed, so that apatite in the upper parts of the autochthon was exposed to thermal effects 45–40 million years ago.

Then the ultra-slow post-collision exhumation began, in the period from 40 to 13 million years ago at a rate of 10–15 m/million years.

In 2013, Novosibirsk geologists, together with foreign colleagues, evaluated the history of the Mesocainozoic peneplain of the Eastern Sayan by the track method and received unexpected conclusions [2].

Unexpected because they are directly related to the genesis of weathering crusts – and hence related minerals. The largest relic of the leveling surface of this area is the Okinskoe plateau, separated from the xp. Kropotkin Okino-Zhombolok fault. The formation of peneplene in the area of the Okinsky plateau falls, according to track analysis, on the Late Jurassic-Early Cretaceous. This age is much younger than the age of the alignment surfaces preserved in the Tien Shan, Gobi and Mongolian Altai (early Jurassic), but older than the peneplain on the Chulyshman plateau in Altai (Late Cretaceous), which indicates the asynchrony of the formation of the ancient peneplain of Central Asia.

A similar story of exhumation of samples from the Okinsky Plateau and from the XP. Kropotkina testifies that these morphotectonic structures from the Jurassic to the end of the Miocene developed as a single block undergoing continuous slow denudation at an average rate of 0.0175 mm/year. In the late Miocene, active tectonic processes led to the destruction of the leveling surface and the elevation of its individual sections to different hypsometric levels. At the same time, an approximate estimate of the velocity of vertical movements along the Okino-Zhombolok fault for the Pliocene-Quaternary period was 0.046-0.080 mm/year, which is several times higher than the denudation rate in this area. The Okin plateau at the Pliocene-Quaternary stage did not undergo significant morphological changes due to its intermediate position between the summit and the base surface of the East.

Sayan and partial reservation by basalt lavas.

O. M. Rosen and A.V. Solovyov successfully applied the track method for dating apatites from the cores of deep wells that opened the foundation of the Siberian platform at a depth of 2–3 km [53]. Although accessory apatites were formed in the early Precambrian, they showed Mesozoic age values due to the cooling of the host rocks below 100 °C. Thermal events of Mesozoic age in the crystalline basement of the Siberian Platform have not yet been known. It is most likely that the annealing of the tracks occurred as a result of intensive heating of the sedimentary cover during the introduction of platobasalts.

In 2015, the international team [134] obtained the first data on decay tracks in apatites of the Khibiny massif aged 368±6 million years (according to U-Pb dating), taken in wells from a depth of 520 and 950 m. Cooling took place in three stages: 290-250 million years – rapid cooling from 110° to 70°-50°; 250–50 million years –stable stage and 50–0 million years - slow cooling to modern temperatures. The geothermal gradient over the last 250 million years was 20 °C/km, during which the massif was exhumed from a depth of 5–6 km.

In 2012, Pakistani geologists published in Russian (!) the results of an assessment using the track method of the time and level of introduction of the Silai Patti carbonatite complex in the North of Pakistan [68]. In the alkaline magmatic province of the Peshawar Valley of Northern Pakistan, this complex is represented by the second largest body of carbonatites. Carbonatites occur in the form of a formation intrusion 12 km long and 2–20 m thick, embedded mainly along the fault separating the meta-sediments and granitogneisses, but locally they also occur in metamorphosed sedimentary rocks. The age dating of carbonatites = 29.40 ± 1.47 million years was obtained by the track method. Comparison with other radiometric dating indicates the introduction of the Sillai Patti carbonatite complex into the upper horizons of the crust and its subsequent exceptionally rapid cooling to near-surface temperatures (<60 °C), necessary for the complete preservation of fission tracks in apatite. Comparison with the world data of denudation rates caused by uplift clearly indicates the presence in the region of a post-collision stretching situation south of the main mantle fault in the Oligocene time. This conclusion strongly rejects the idea of the predecessors about the formation of carbonatite complexes in the Lo Shilman and Sillai Patti areas along the upwelling in the Oligocene time.

A large Chinese team (8 co-authors) in 2012 proved that based on the materials of track chronometry, two successive stages of cooling of Cretaceous porphyry-like iron ores of China can be distinguished [112]. Apatites were studied at four deposits formed about 130 million years ago: Dongshan, the familiar Meishan (Ninu Basin), Nihe and Lohe (Luzong Basin). Apatites of these deposits have ages, respectively, 106.3±5.4; 94.2±4.0; 81.3±4.0 and 79.1±3.3 million years, decreasing with increasing depth of burial and approaching the age of mineralization, depending on the size of the uplift and the degree of post-ore denudation.

The simulation of the thermal history reflects two stages of cooling with a change of rapid cooling associated with the loss of a heat source, slow cooling due to an uplift. Judging by the temperature of the cooling rate change, it appeared at a depth of 1.7–1.8 km. It is shown that since 110 million years, the rate of uplift and denudation in the Ninu Basin has been significantly higher than those in the Luzong Basin. This led to less burial or exposure on the surface of the deposits of the Ninu basin.

Although with great delay, but in 2018 there was work with the use of a new (though not track) method of thermometry for apatite and in our Institute of Geology. This was a study by Yu. V. Denisova, who studied the thermal history of the Nikolaishor granite massif in the Circumpolar Urals, which had been studied by our petrographers for a long time and repeatedly [16]. To do this, she applied the so-called Watson saturation thermometry (with a clarifying Bea coefficient) for apatite. As a result, it was concluded that the crystallization of the rocks of the Nikolaishor massif occurred in a temperature range including two episodes (633.5–699.1 ° C and 751.2–77.4 °C). Yu. V. Denisova concluded that Watson saturation thermometry with the addition of Bea for apatite provides the same accurate information about the evolution of the temperature regime during the formation of granites as the evolutionary-crystallomorphological analysis of Pyupin and Turko for zircons (which was previously done by her).

The application of the track method to the Cenozoic strata of the North of Turkey made it possible in 2012 to draw non-obvious tectonic conclusions [90]. According to the tracks of apatite decay in Zap. 3 episodes of Cenozoic exhumation were identified in the Pontides, which correlate with the main supra-regional tectonic episodes. 1. The exhumation of the Paleocene-Early Eocene reflects the closure of the Izmir-Ankara Ocean. 2. The exhumation of the Late Eocene–the beginning of the Oligocene is a consequence of the resumption of tectonic activity along the Izmir–Ankara suture. 3. Exhumation of the Late Oligocene-Early Miocene records the manifestation of stretching of the north. parts of the Aegean region. Samples collected to C and Y from the tectonic contact between the forming Zap. The Pontides of the Istanbul and Sakari terranes record the same episodes of cooling, indicating that these terranes were amalgamated in the pre-Cenozoic time

Since the erosion of the High Himalayas ensures the flow of enormous volumes of sedimentary material to the shelf of the Indian Ocean, the reconstruction of the tectonic history of the Himalayas, made by the team in 2012, is important for recreating the details of Cenozoic sedimentation [129]. This paper presents the results of dating along the tracks of the decay of apatites and zircons from the rocks of the upper parts of the slopes of Mount Everest and along a number of valleys that are the catchments of Mount Everest and the Makalu massif, forming vertical intersections of a series of High Himalayas in the East. Nepal with a length of almost 8000 m. The age of apatites varies in the rocks of the Himalayan series

from 0.9±0.3 to 3.1±0.3 million years, systematically increasing from bottom to top along the section. The apatites of the Everest and Ordovician limestone series are much older and reach an age of 30.5±5.1 million years. The ages of zircons in the rocks of the Himalayan series range from 3.8 ± 0.4 to 16.3 ±0.8 million years.

The rates of brittle exhumation calculated on the basis of these data indicate that the rocks of the Himalayan series were exhumed from about 9 million years ago at speeds of 1.0–0.4 mm/year, and in the Pliocene the rate increased to 1.7 ± 0.3 mm/year. These values do not differ significantly from the estimate of the plastic exhumation rate (1.8 mm/year) established for metamorphic minerals that experienced decompression between 18.7 and 15.6 million years ago, but are noticeably lower than the rates determined on the basis of thermomechanical models. Higher exhumation rates are associated with increased erosion during glaciation of the High Himalayas in the Late Pliocene-Pleistocene.

In 2005, a thorough review of the application of the track method for the purposes of oil and gas geology was published [94]. The authors emphasized that exhumation, removal of overburden rocks as a result of the uplift of tectonic blocks from the maximum depth of burial, occur both regionally and locally in marine sedimentary basins and have important consequences for assessing the prospects of oil and gas basins. The issues to be solved by an oil geologist in these basins include: the time of thermal heating and cooling of blocks of oil-bearing rocks, lithogenetic restrictions imposed by the maximum depth of reservoir rocks, physical and mechanical characteristics of tire rocks during and after exhumation, the structural evolution of traps and the history of the placement of hydrocarbons in them. Central to solving these problems is the ability of a geologist to identify exhumation events, assess their scale and determine their timing.

GENERAL CONCLUSION

In the course of the presentation, some particular conclusions have already been made in this review; here we will try to bring them together and, if necessary, supplement them.

1. The widest distribution of accessory apatite in igneous rocks is explained by the properties of phosphorus – its extremely limited ability to enter into the composition of rock-forming minerals. In rocks with poor P2O5 contents (such are some granites and rhyolites), there is no apatite. Therefore, accessory apatite is both a concentrator and a carrier of rock phosphorus.

2. As a rock-forming mineral, apatite is present only in some cumulative and rare types of igneous rocks – some pegmatites, nelsonites and carbonatites, as well as in hypergenic phosphorites (the world's largest source of phosphorus for fertilizers).

3. Structurally, apatite $Ca_5(PO_4)_3(F,Cl,OH)$ is unique, because in its cationic and anionic parts, extremely diverse isomorphic substitutions are possible – both homo- and heterocharged.

Since these substitutions were defined in a variety of characteristics of the environment of formation of Apatite – Apatite makes it remarkable genetic "marker": the composition of Apatite could judge the TR-conditions in the magma oxygen fugacity in them, their alumina content, the sulfur content, the content of water, Halogens, sulphur, etc.

4. In the cationic parts of Ca2+ can replace Na^+, K^+, Ag^+, Sr^{2+}, Mn^{2+}, Mg^{2+} Zn^{2+}, Cd^{2+}, Ba^{2+}, Sr^{2+}, REE^{3+}, Y^{3+}, Sc^{3+}, U^{4+} and Th^{4+}. Of these, Mn, Sr, REE and U are of the greatest importance for the use of apatite as an indicator of geological processes. In addition, apatites are also a real raw material source of REE and U.

5. In the anionic part, phosphate, halogens and hydroxyl can be replaced by CO_3^{2-}, SO_4^{2-}, $Cr_2O_4^{2-}$, AsO_4^{3-}, VO_4^{3-}, BO_3^{3-}, JO_3^{3-}, CO_3F^{3-}, CO_3OH^{3-}, SiO_4^{4-}. Of these, carbonate and sulfate are the most important.

6. Isomorphic substitutions of Ca are further complicated depending on the position of Ca in the structure, since Ca enters both the phosphate skeleton of the structure (**Ca1** atoms) and the channels of the structure (**Ca2** atoms). The **Ca1** atoms are in 9-coordination, forming a regular trigonal prism of the $\mathbf{CaO_9}$ composition, while the Ca2 atoms are in 7-coordination, forming an irregular polyhedron of the $\mathbf{CaO_{6A}}$ composition, where **A** are oxygen-substituting anions, that is, halogens, CO_3^{2-}, etc.

7. The impetus ("trigger") for the compilation of our review was the recent (2020) generalizing publication on the composition of apatite, covering 147 works:

Gary O'Sullivan, David Chew, Gavin Kenny, Isadora Henrichs, Dónal Mulligan. *The trace element composition of apatite and its application to detrital provenance studies //* Earth-Science Reviews, 2020, vol. 201. 103044.

Since 4 of the authors of this review are from Dublin, and only Gavin Kenny is

from Stockholm, for simplicity it is called by us the "Irish review". The authors of the Irish review for the first time covered all known applications of the composition of accessory apatite to indicate the conditions in which host (or associated) rocks or ores were formed. As a result of thorough consideration of various diagnostic graphs, the authors especially recommend the logarithmic "biplot" LREE - Sr/Y, in which the important diagnostic value of the Sr/Y value was justified by E. A. Belousova. The authors focused on detrital accessory apatite of igneous and metamorphic rocks (falling into terrigenous sedimentary rocks) and much less on apatite of phosphorites, which they call "autigenic".

As in the West in general, Russian-language works remained out of the sphere of attention of the authors of the Irish review. The only exception concerns the works of our outstanding geologist E. A. Belousova, but only because these works are English-language.

8. The formation of bioapatite, which largely consists of the bones and teeth of vertebrates (including humans) is a complex, stage-by-stage process. Under natural conditions, biogenic **hydroxyapatite $Ca_{10}(PO_4)_6(OH)_2$** is not formed immediately, but is preceded by biophosphate-1 – or **octacalcium phosphate $Ca_8(HPO_4)_2(PO_4)_{4.5}H_2O$**, or **brushite $CaHPO_4 2H_2O$**, and with particularly strong supersaturation of the saline solution – **amorphous Ca-phosphate $Ca_xH_y(PO)_z$ nHO**(n = 3–4.5). Thus, hydroxyapatite turns out to be biophosphate-2, it is formed only by the substrate of biophosphate-1, most often – octacalcium phosphate.

9. In 2014, it was possible to prove experimentally that in urolithiasis (nephrolithiasis), the formation of calcium oxalate monohydrate of vevellite **$CaC_2O_4 \cdot H_2O$,** which has long been known to urologists, is closely related to the earlier formation of hydroxyapatite. Model experiments have clarified why vevellitis in the renal tissue, as a rule, grows on the so-called Randall plaques - areas with disperced hydroxyapatite.

10. Both Russian and foreign petrologists have reliably proved that the ratio of halogens in apatite is an excellent indicator of the fluid regime in petro- and ore genesis. Two trends of magmatic differentiation of basaltoid magmas are known: (1) tholeiitic – the evolution of the melt towards the accumulation of iron – with the formation of ferruginous gabbroids, with which titanium-magnetite ores are associated, and (2) calcareous-alkaline – the evolution of the melt towards an increase in its silicic acid and alkalinity, which is associated with scarn-magnetite mineralization. These trends are well documented by the content of chlorine and fluorine in apatites. Comparison of the ferruginous index of melts f (f = Fe/(Fe + Mg), at.%) with the content of halogens in accessory apatites showed that chlorine in apatites exhibits pronounced ferrophilicity, and fluorine - magnesiophilicity.

11. Ural geologists who have studied fell near Chelyabinsk chondrites "Chelyabinsk", "Ural" and "Lake", confirmed that the characteristic phosphate chondrites is **merrilite $Ca_9Na[Fe,Mg][PO_4]_7$** – anhydrous end member in a series of 14 solid solutions merrilite – whitlockite.

12. Apatity may contain sulfur from the substitution of the anion phosphate anion sulfate. The content of S in apatite is directly dependent on the former content of S in the melt. Experimentally, it was possible to show that the introduction into the rhyolite melt under oxidizing conditions up to 0.5 wt. %S dramatically increased the solubility of apatite in the melt. As proved by Ural geologists, high-sulfur apatites (up to 0.65 wt. %S) are good indicators of the prospects of gabbro-dolerites for Cu-Ni mineralization.

13. Francolite $Ca_{10-a-b}Na_aMg_b[PO_4]_{6-x}(CO_3)_{x-y-z}(CO_3F)_y(SO_4)_zF_2$, a low-temperature fluorocarbonatapatite (often referred to simply as carbonatapatite), is the main mineral of hypergenic phosphoric ores - phosphorites. As proved by Russian geochemists from Moscow State University – V. S. Savenko and his daughter A.V. Savenko, *francolite is formed in the diagenesis of sea silts* – as the sediment is buried and removed from the section "bottom water/sediment". In this process, the carbonate alkalinity of the pore waters increases, as a result of which the initially formed calcium phosphate precipitate begins to dissolve and return the phosphate group PO_4^{3-} to the pore waters (and then to the above-bottom water – "phosphorus respiration of the sediment"), which is replaced by the carbonate group CO_3^{2-} in the sediment.

However, *some carbonatapatites have a primary biogenic nature*, being formed, in particular, in dental tissue, where CO_3^{2-} radicals can replace both OH– and PO_4^{3-} in the lattice of biogenic hydroxyapate

An important discovery of recent years is the discovery of huge resources of francolite not in marine sedimentary rocks, but in the ***weathering crust of carbonatites*** of our unique rare-metal Tomtor deposit, which has no world analogue in its size and composition

14. The value of the ***cerium anomaly*** $Ce^A = Ce_N/Ce^*$, where $Ce^* = 1/3$ $(1.44La_N + 0.66 Nd_N)$ in apatites is an important diagnostic tool. Since in the modern aerated ocean (most likely also in the oceans of the Phanerozoic) the value of $Ce^A < 1$ (which is commonly called "negative"), then apatites formed in equilibrium with seawater should also have a "negative" value of the cerium anomaly. Accordingly, any increase in the value of Ce^A indicates the formation of apatite either in deep suboxic waters (where the Ce content is greatly reduced), or in anoxic waters, where Ce (III) is not oxidized at all, so that the value of Ce^A in such apatites is close to unity.

15. The value of the Europium anomaly $Eu^A = Eu_N/Eu^*$, where $Eu^* = ½ (Sm_N + Gd_N)$ in most low-temperature apatites is close to 1 - as in seawater. However, in some igneous apatites, the value of Eu/Eu*<1 was noted, which indicates the occurrence of the reduced Eu^{2+} in an earlier plagioclase. Despite the theoretical impossibility of restoring Eu in hypergenesis, Eu/Eu* <1 values were occasionally observed in sedimentary apatites of hydrogen sulfide ("euxine") facies; thus, the value of Eu^A can serve as an indicator of such facies.

16. The often observed close association of fluorapatite with monazite reflects

the *history of polymetamorphism*. Usually monazite is formed before fluorapatite, taking the REE resource from the medium. However, when the temperature decreases, monazite becomes unstable, reacting with the host silicates and dumping the REE contained in it. This leads to an increase in the primary monazite-1 of remarkable "crowns" consisting of fluorapatite and allanite, in which, with a new episode of a decrease in the temperature of metamorphism, growths of newly formed monazite-2 appear.

17. Along with REE, *strontium and manganese* are very informative elements of the cationic part of apatites. The *Sr/Mn* ratio was proposed in one of the works by E. A. Belousova and colleagues, and then successfully used on the *Sr/Mn* (ordinate) – *LREE* (abscissa) biplot designed by the authors of the Irish review, where LREE contained 7 lanthanides from La to Gd. Note that only two fields contoured by the authors need an abscissa axis: the minimum LREE contents for the LM field (low-grade metamorphites and metasomatites) and the maximum for the ALK field (alkaline magmatites). For the remaining 4 fields, the LREE parameter "does not work", and they are quite satisfactorily (with overlaps not exceeding 15% of the area) recognized by a single Belousova's parameter *Sr/Mn*.

18. The actinides *uranium and thorium* in the cationic part of apatites can also be used for diagnostic purposes. Uranium has two different states: U6+ compounds are highly soluble in oxygen conditions, and U4+ oxide is insoluble in oxygen-free waters. At the same time, the solubility of Th is not affected by redox changes, which leads to an increase in the *Th/U* ratio in anoxic hydrophations. If the degree of oceanic anoxia becomes significant (as, for example, it was assumed for the early Triassic), then the uranium reservoir in seawater will be depleted, which will lead to an increase in the *Th/U* ratio in apatite.

19. In addition to using uranium as a geochemical indicator (for the diagnosis of sedimentation hydrofacies), *apatites are a real raw material source of uranium*. From phosphate ores, which have reserves in dozens of countries around the world, it is possible to extract from 9 to 22 million tons of uranium. This would ensure the supply of uranium for nuclear power for 440 years.

20. The isotopic ratio $^{87}Sr/^{86}Sr$, which has found the widest application for dating carbonate sedimentary rocks, has become actively used for phosphate strontium - for dating apatites. In the pelagial of the ocean, fossilized remains of fish (ichthyolites) preserve the isotopic composition of strontium of ocean waters at the time of fish life, therefore, the isotopic composition of strontium of ichthyolites can be used to determine their age.

21. The isotopic ratios $\delta^{18}O$ in the oxygen of apatites and $\delta^{13}C$ were as widely used as the value $\delta^{87}Sr$ –- to assess the climate of the sedimentation epoch. Phosphate of bones and teeth of terrestrial animals, phosphate of ichthyolites have been studied, but *the isotopic analysis of oxygen and carbon of conodonts should be recognized as the most promising*. It is this method that has become the most widespread in recent years.

22. Isotopic analysis of neodymium using the value *εNd* – "epsilon neodymium" has found enormous application. i.e., the isotope ratio R = ^{143}Nd/^{144}Nd normalized by chondrite:

$$εNd = (RS/ RCHUR – 1), \text{ in ten thousandths.}$$

Here R_S is the ^{143}Nd/^{144}Nd in the sample, and R_{CHUR} is the value of это ^{143}Nd/^{144}Nd в образце, а R_{CHUR} – значение ^{143}Nd in **CHUR** – (chondritic uniform reservoir), which is assumed to be **0.512638**.

Since apatites concentrate REE in their cationic part (including neodymium), it is apatite that seems to be the most convenient object for using the value *εNd* for diagnostic purposes – namely, ***for the diagnosis of the petrofund*** from which detritus apatite was deposited. The fact is that the mantle (and its young magmatic derivatives) has a ratio of ^{143}Nd/^{144}Nd higher than the Earth as a whole – and, accordingly, ***positive values of εNd***. On the contrary, ancient crustal rocks have ^{143}Nd/^{144}Nd lower than in the Earth as a whole, and accordingly, ***negative values of εNd***, the more negative the older the rocks. These data make it possible to determine the petrofund with great reliability by the value of *εNd* in apatite.

23. Another remarkable property of the value of *εNd* in apatite (in particular, in the phosphate of conodonts) allows ***it to be used for the reconstruction of paleogeography*** details, since, as shown for the modern ocean, the value of *εNd* in seawater is a remarkable tracer of ocean circulation.

24. ***Apatites from igneous rocks of ultrabasic and basic composition***, with which deposits of Ti-Fe-V ores are genetically related, have the highest values of the Sr/Y index at low LREE contents. The most chlorinated apatites were identified by Russian geologists in stratified mafic-ultamafite intrusions with zones of low-sulfide EPG-containing mineralization. As the process of magmatic differentiation of basaltoid magmas from gabbro to diorites and quartz diorites develops, the content of Cl in apatites decreases, and fluorine increases. With further differentiation up to tonalites, the chlorinity of apatites continues to decrease, and the fluorinity increases.

25. ***Apatites from kimberlites*** contain silicon, which is explained by the conjugate substitution of the PO_4^{3-} ion with CO_3^{2-} and SiO_4^{4-} ions, reflecting a higher CO_2 content in the initial melts, as well as the accumulation of Si in kimberlite magma due to the predominant crystallization of carbonates compared to mica/monticellite.

26. ***Apatites from granites*** on the logarithmic graph LREE – Sr/Y form two separate fields: IM and S. The **IM field** (median, intermediate values on both axes) includes apatites from granodiorites and "mafic" I-granites with low index values ASI = Al/(Ca+Na+K). Fluorapatites from anatectic granites of the S-type, as well as from "felsic" granites of the I-type, with a high value of the ASI index, fall into the **S field**. With some average LREE abscissa contents, they are clearly distinguished by the minimum values for the Sr/Y ordinate.

27. Detection by cathodoluminescence of a clear ***zonality in apatites*** from granite Shap in the North. In England, it was a real gift for petrologists who previously did not have a suitable way to judge the evolution of granite magmas. Cathodoluminescent images of zonal apatite combined with the analysis of trace elements by the LA-ICP-MS method provide powerful tools for decoding the crystallization of granites. Prolonged crystallization of apatite, which has not undergone secondary changes, allows us to recreate a complete picture of the evolution of the grant magmatic system.

28. ***Apatites from alkaline rocks*** are known to have strong concentrations of REE. Therefore, on the logarithmic graph LREE – Sr/Y, they form the rightmost field of **ALK** with the maximum digits on the abscissa LREE, but with wide (non-diagnostic) variations on the ordinate Sr/Y.

29. ***Apatites from carbonatites*** on the same LREE – Sr/Y graph fall into the "ultramafic" **UM field** together with pyroxenites, lherzolites and "mafic" I-granites with a low ASI index. This field is characterized by the highest values for the Sr/Y ordinate and moderately high values for the LREE abscissa.

30. The geological evolution of carbonatites and associated mineralization is extremely complex - multi-stage, Based on the composition of apatites, apparently, Siberian geologists made a decisive contribution to understanding the evolution of carbonatites and their successor metasomatites and hydrothermalites in 2017.

31. ***Apatite of granite pegmatites*** is distinguished by its exceptional originality, especially in the pegmatites of anatectic granites of the S-type. The fact is that in the initial high–alumina melts that arose from metapelites, apatite is highly soluble - better than in low-alumina melts, due to Ca deficiency, which goes into plagioclase. That is why there are so many non-calcium phosphates in residual (pegmatite) melts. The presence of unusual phosphates (Li, Fe, Fe-Mn and Mn), for example, high-manganese fluorapatite and **beusite $CaMn_2[PO_4]_2$**, named after our famous geochemist and mineralogist A. A. Beus, can be considered characteristic of granite pegmatites. With the subsequent hydrothermal change of pegmatites, apatite disappears altogether, and the predominant Fe-Mn-phosphates are replaced by such calcium-free minerals as rare alumophosphates **montebrasite $LiAlPO_4(OH)$** and **childrenite $Fe^{2+}AlPO_4(OH)_2 \cdot H_2O$**.

32. Metamorphite apatite has characteristic differences from igneous apatite. Among the characteristic minerals of metamorphites can be called **goyazite $SrAl_3(PO_4)(PO_3OH)(OH)_6$** – aluminum and strontium phosphate from the crandallite group, as well as the appearance of a low-temperature florencite association **$(Ce,La,Nd)Al_3(PO_4)_2(OH)_6$** and **crandallite $CaAl_3(PO_4)_2(OH)_5 \cdot H_2O$** – the extreme aluminum members of the group of aluminum-sulfate-phosphates from the supergroup of alunite.

33. An increase in the temperature of metamorphism up to anatexis reduces the REE content in primary magmatic apatites and lowers Sr/Y - due to a simul-

taneous increase in Y concentrations and a decrease in Sr concentrations. On the logarithmic graph LREE – Sr/Y, the compositions of apatites form two disjoint fields. The **LM field** (a wide, non-diagnostic range of values for the Sr/Y ordinate and the minimum LREE contents for the abscissa) are low- and medium-graded metamorphites, which are characterized by dissolution and redeposition of apatite – with a corresponding loss of REE. **The HM field** (low Sr/Y values and moderate LREE contents) are apatites from high-grade metamorphites and metasomatites; apatite compositions from anatectic metamorphite leukosomes also fall here.

34. *Hydrothermal apatites* (including apatites from various ores) are characterized by high variability of composition. In particular, fluorapatites from Ural *quartz-vein Au ores associated* with granitoids are distinguished by the presence of a noticeable SO3 content – up to 1% by weight. %. *In Norilsk sulfide ores with PGE mineralization*, Moscow geochemists isolated up to 3 generations of apatite, the composition of which indicates the discrete evolution of fluids accompanying ore formation: from water-chloride to chloride, then from water-chloride-fluoride to significantly fluoride. Lanthanides released during the replacement of chlorapatite-I with fluorapatite-II were probably part of the pneumatolite zonal orthite-(Ce).

Fluorapatite from iron ore deposits of the "Kiruna type" is low–calcium, with a small admixture of hydroxyl and REE. This apatite is a relict that has undergone a strong change with the removal of Na, Cl and REE. The removed REES were included in the composition of secondary monazite, and partly also in allanite and xenotime, forming either independent crystals or inclusions in apatite. For apatite from *Fe-Cu-Au ores of the giant Olmpik Dam* deposit in South. Australia is characterized by the accumulation of MREE – which is expressed by the bell-shaped shape of the curve in the "spectrum" of REE normalized by chondrite.

35. *Bioapatites* are represented by both modern teeth and bones (including human ones) and ancient ones - buried in sediments and sedimentary rocks. These groups vary greatly in composition. *Modern bioapatites* are represented by poorly crystallized hydroxyapatites, which become noticeably carbonate in diseases (caries, coxoarthrosis). They are, as a rule, very poor in impurity elements (Mn, Sr, REE, U). **Ancient bioapatites** (vertebrate bones, ichthyolites, and especially conodonts) are much richer in fluorine and impurity cations due to diagenesis than modern ones. For example, the REE content in conodonts can reach or even exceed 1000 ppm.

36. The compositions of *hypergenic apatites* in phosphorites most often correspond to fluorocarbonatapatite – *francolite*. Such commonly used indicators of apatites as Sr/Y, La/Yb, ΣREE, the ratio of LRSE, MRSE, HRSE, the magnitude of Ce- and Eu anomalies, the ratio of REE with the isotopic composition of carbonates associated with phosphorites and organic matter – vary greatly. Nevertheless, according to the composition of hypergenic apatites, geologists persistently try to recognize the conditions of sedimentation (in particular, topo- and hydropha-

tion) and lithogenesis (especially diagenesis). According to Ural geologist A.V. Maslov, in relation to phosphorites, these attempts are not effective enough due to multifactorial effects on the composition of apatites. Among the factors are:

– the composition of seawater of different epochs, which did not remain constant;

– the speed and redox conditions of sedimentation;

– the content and composition of organic matter and carbonates associated with phosphorites;

– diagenetic changes, among which poorly understood microbial processes played an important or even decisive role; complications of sedimentation by exposure to endogenous hydrotherms.

In general, we can conclude that *the diagnostic application of the composition of hypergenic apatites is still in the process of development* – it is necessary to find such indicators that could be trusted without special reservations.

37. As for the theory and practice of using apatite for thermochronology – *by the track method*, these materials are included in this review only "for completeness", since these materials have nothing to do with the composition of apatites (of course, except for data on the contents in apatites 238U). However, *they complement the characteristic of apatite, which has no analogue – in terms of the variety of use as a unique indicator mineral.*

RUSSIAN REFERENCES

1. Avdonina I.S., S.V. Pribavkin. Magmatic anhydrite and apatite in epidote-bearing porphyries in the Middle Urals // Lithosphere, 2013, No. 4. P. 62–72.

Авдонина И.С., Прибавкин С.В. Магматический ангидрит и апатит в эпидотсодержащих порфирах Среднего Урала // Литосфера, 2013, № 4. С. 62–72.

2. Arzhannikova A.V., Jolivet M., Arzhannikov S. G., Vassallo, R., Chauvet, A. The age of formation and destruction of the Mesozoic-Cenozoic surface alignment in East Sayan // GEOL. and geofiz., 2013, vol. 54, No. 7. Pp. 894–905.

Аржанникова А.В., Жоливе М., Аржанников С.Г., Вассалло Р., Шове А. Возраст формирования и деструкции мезозойско-кайнозойской поверхности выравнивания в Восточном Саяне // Геол. и геофиз., 2013, т. 54, № 7. С. 894–905.

3. Barkov A.Y. Nikiforov A.A. A new criterion of search areas of platinum mineralization of the type "Kivakka reef" // Vestn. Voronezh. State University. Ser. Geology, 2015, No. 4. pp. 75–83. [electronic resource].

Барков А.Ю., Никифоров А.А. Новый критерий поиска зон платинометалльной минерализации типа «Кивакка риф» // Вестн. Воронеж. гос. ун-та. Сер. Геология, 2015, № 4. С. 75–83. [Электронный ресурс].

4. Baturin G.N. Phosphate Accumulation in the Ocean. – M.: Nauka, 2004. 464 pp.

Батурин Г.Н. Фосфатонакопление в океане. – М.: Наука, 2004. 464 с.

5. Baturin G.N. Phosphorites at the Bottom of the Oceans. – M.: Nauka, 1978. 232 pp.

Батурин Г.Н. Фосфориты на дне океанов. – М.: Наука, 1978. 232 с.

6. Baturin. G.N. Phosphorites of the Sea of Japan // Oceanology, 2012, vol. 52, No. 5. p. 721.

Батурин Г.Н. Фосфориты Японского моря // Океанология, 2012, т. 52, № 5. С. 721.

7. Baturin G.N., Dubinchuk V.T. Genesis of uranium minerals and rare earths in the bone detritus of rare metal deposits // Dokl. RAS, 2011, vol. 438, No. 4. pp. 506–509.

Батурин Г.Н., Дубинчук В.Т. Генезис минералов урана и редких земель в костном детрите редкометалльных месторождений // Докл. РАН, 2011, т. 438, № 4. С. 506–509.

8. Baturin, G.N., Dubinchuk V.T., Azarova L.A. Anashkina N.A., Ozhogin D.O. The apatite and associated igneous minerals in ferromanganese crusts from the Magellan Mountains // Oceanology, 2006, vol. 46, No. 6. Pp. 922–928.

Батурин Г.Н., Дубинчук В.Т., Азарнова Л.А., Анашкина Н.А., Ожогин Д.О. Апатит и ассоциирующие с ним минералы в железомарганцевых корках с Магеллановых гор // Океанология, 2006, т. 46, № 6. С. 922–928.

*9. Bliskovsky V.Z. Material Composition and Dressing of Phosphorite Ores. –
M.: Nedra, 1983. 200 pp.*

*Блисковский В.З. Вещественный состав и обогатимость фосфоритовых
руд. – М.: Недра, 1983. 200 с.*

*10. Bocharnikova T.D., Kholodnov V.V., Shagalov V.E. Halogens in apatite
– as a reflection of the fluid regime in petro- and ore genesis of the Magnitogorsk
ore-magmatic complex (Southern Urals) // Vestn. Ural. branch Ros. mineral. Soc.,
2012, № 9. Pp. 28–33.*

*Бочарникова Т.Д., Холоднов В.В., Шагалов В.Е. Галогены в апатите –
как отражение флюидного режима в петро- и рудогенезе Магнитогорского
рудно-магматического комплекса (Южный Урал) // Вестн. Урал. отд-ния
Рос. минерал. о-ва, 2012, № 9. С. 28–33.*

*11. Gorbachev N.C., Shapovalov Yu.B., Kostyuk V.A. Experimental study of
the system apatite–carbonate–H2O at P = 0.5 GPA, T= 1200 oC: efficiency of
fluid transport in carbonatites // Dokl. Rus. Acad. Sci., 2017, vol. 473, No. 3. Pp.
331–335.*

*Горбачев Н.С., Шаповалов Ю.Б., Костюк А.В. Экспериментальные
исследования системы апатит–карбонат–H2O при P = 0.5 ГПА, T= 1200
oC: эффективность флюидного транспорта в карбонатитах // Докл. РАН,
2017, т. 473, № 3. С. 331–335.*

*12. Gordienko V.V. Typomorphism of the chemical composition of garnet
and apatite granitic pegmatites // Vopr. geokhim. and typomorphism of minerals,
2008, No. 6. Pp. 114–128.*

*Гордиенко В.В. Типоморфизм химического состава граната и апатита
гранитных пегматитов // Вопр. геохим. и типоморфизм минералов, 2008,
№6. С. 114–128.*

*13. Grabezhev A.I., Voronina L.K. Sulfur in apatites from copper-porphyry
systems of the Urals // Yearbook-2011: Collection. – Ekaterinburg: IGG URO
RAN, 2012. Pp. 68–70 (Tr. IGG URO RAN, vol. 159).*

*Грабежев А.И., Воронина Л.К. Сера в апатитах из медно-порфировых
систем Урала // Ежегодник-2011: Сборник. – Екатеринбург: ИГГ УрО РАН,
2012. С. 68–70 (Тр. ИГГ УрО РАН, вып. 159).*

*14. Gusev A.I., Gusev N.I. Magnetite-apatite mineralization in the Western
part of the Central Asian fold belt // Modern high technologies, 2013, no 2. Pp.
74–78.*

*Гусев А.И., Гусев Н.И. Апатит-магнетитовое оруденение западной части
Центрально-Азиатского складчатого пояса // Современные наукоемкие
технологии, 2013, №2. С. 74–78.*

*15. Gusev A. I., Gusev N.I. Geochemistry of ores and minerals pegmatite
manifestations of Danilovskoe (Gorny Altai) // Intern. Journ. of applied and
fundamental research, 2016, №10. Pp. 102–106.*

Гусев А.И., Гусев Н.И. Геохимия руд и минералов пегматитового проявления Даниловское (Горный Алтай) // Международный журнал прикладных и фундаментальных исследований, 2016, №10. С. 102–106.

16. Denisova Yu. V. Thermometry apatite from the Nikolaishor granite massif (polar Urals) // 7 readings in the memory of corresponding member. RAS S.N. Ivanov: All-Russian scientific conference dedicated to the 70th anniversary of the founding of the Ural branch of the Russian mineralogical society, Yekaterinburg, 2018, IGG URO RAN. – Yekaterinburg: IGG URO RAN, 2018. Pp. 61–63.

Денисова Ю.В. Термометрия апатита из гранитов Николайшорского массива (Приполярный Урал) // 7 Чтения памяти член-корр. РАН С.Н. Иванова: Всероссийская научная конференция, посвященная 70-летию основания Уральского отделения Российского минералогического общества, Екатеринбург, 2018, ИГГ УрО РАН. – Екатеринбург: ИГГ УрО РАН, 2018. С. 61–63.

17. Di Matteo A., Kuznetsova T.V., Nikolaev V.I., Spasskaya N.N., Yakumin P. Isotopic studies of bone remains of Yakut Pleistocene horses // Ice and snow, 2013, № 2. Pp. 93–101.

Ди Маттео А., Кузнецова Т.В., Николаев В.И., Спасская Н.Н., Якумин П. Изотопные исследования костных остатков якутских плейстоценовых лошадей // Лед и снег, 2013, № 2. С. 93–101.

18. Dubyna O.V., Krivak S.G., Samchuk A.I., Krasyuk O.P., Amashukeli Y. A. regularities of REE, Y, and Sr in apatite endogenous deposits of the Ukrainian shield (according to the ICP-MS) // Mineral. W., 2012, vol. 34, No. 2. Pp. 80–99.

Дубина О.В., Кривдік С.Г., Самчук А.І., Красюк О.П., Амашукелі Ю.А. Закономерности распределения REE, Y и Sr в апатитах эндогенных месторождений Украинского щита (по данным ICP-MS) // Мінерал. ж., 2012, т. 34, № 2. С. 80–99.

19. Dubyna O.V., Krivak S. G., Sobolev V.B. Isomorphism in TR-apatite of the Chernigov carbonatite massif. Izomorphism in TR-apatites of the Chernigivsky carbonatite massif // Mineral. Zh., 2012. vol. 34, No. 3. Pp. 22–33.

Дубина О.В., Кривдік С.Г., Соболев В.Б. Ізоморфізм в TR-апатитах Чернігівського карбонатитового масиву // Мінерал. ж., 2012. т. 34, №3. С. 22–33.

20. Dudkin O.V. Apatite as a possible indicator of the sequence of formation of rocks of the Khibiny deposits // Petrology and mineralogy of the Kola region: 5 All-Russian. Fersman scientific session, dedicated to the 90th anniversary of the birth of E.K. Kozlov, Apatity 14–15 Apr., 2008. – Apatity: Geol. Inst. KSC RAS, 2008. Pp. 94–97.

Дудкин О.Б. Апатит как возможный индикатор последовательности формирования пород хибинских месторождений // Петрология и минерагения Кольского региона: 5 Всеросс. Ферсмановская научная сессия, посвящ. 90-летию со дня рождения д. г.-м. н. Е. К. Козлова, Апатиты 14-15 апр., 2008. – Апатиты: Геол. ин-т КНЦ РАН, 2008. С. 94–97.

21. Dudkin O.B. REE of the Khibiny massif // Geology and Strategic Minerals of the Kola region: Proceedings of 10 Vseros. (with intern. participation) Fersman scientific session dedicated to 150th anniversary of the birth of Academician V.I. Vernadsky, Apatity, 7–10 Apr., 2013. – Apatity: Geol. Inst. KSC RAN, 2013. Pp. 124–127.

Дудкин О.Б. Редкие земли Хибинского массива // Геология и стратегические полезные ископаемые Кольского региона: Труды 10 Всерос. (с междун. участием) Ферсмановской научной сессии, посвящ. 150-летию со дня рождения акад. В. И. Вернадского, Апатиты, 7–10 апр., 2013. – Апатиты: Геол. ин-т КНЦ РАН, 2013. С. 124–127.

22. Dudchenko N.O. The peculiarity of the formation of a nitrogen-based radical in biogenic hydroxylapatite on the EPR data // Mineral. Zh., 2011, vol. 33, No. 3. Pp. 46–49.

Дудченко Н.О. Особливості формування азотвмісного радикала у зразках біогенного гідроксилапатиту за даними ЕПР // Мінерал. ж., 2011, т. 33, №3 . С. 46–49

23. Erokhin Yu.V., Ivanov K.S., Ponomarev V.S. Goyazite from metamorphic rocks of the Pre-Jurassic basement of the West Siberian megabasin // Vestn. Ural. branch Ros. mineral. Soc., 2016, No. 13. Pp. 52–61.

Ерохин Ю.В., Иванов К.С., Пономарев В.С. Гояцит из метаморфических пород доюрского фундамента Западно-Сибирского мегабассейна // Вестн. Урал. отд-ния Рос. минерал. о-ва, 2016, № 13. С. 52–61.

24. Erokhin Yu.V., Hiller V.V., Ivanov K.S., Burlakov E.V., Kleimenov D.A., Berzin S.V. Phosphates from meteorites "Ural", "Ozernoye" and "Chelyabinsk" // Vestn. Ural. branch Ros. mineral. Soc., 2014, No. 11. Pp. 39–47.

Ерохин Ю.В., Хиллер В.В., Иванов К.С., Бурлаков Е.В., Клейменов Д.А., Берзин С.В. Фосфаты из метеоритов "Урал", "Озерное" и "Челябинск" // Вестн. Урал. отд-ния Рос. минерал. о-ва, 2014, № 11. С. 39–47.

25. Zanin Yu.N., Zamiralov A.G., Fomin A.N., Pisarev G.M. Strontium in the structure of sedimentary apatite in the process of catagenesis // Dokl. Russian Academy of Sciences, 1997, vol. 352, No. 2. Pp. 235–237.

Занин Ю.Н., Замирайлова А.Г., Фомин А.Н., Писарева Г.М. Стронций в структуре осадочного апатита в процессах катагенеза // Докл. РАН, 1997, т. 352, № 2. С. 235–237.

26. Ivanovskaya A.V., Zanin Yu. N. Phosphorites of the stalinogorsk formation of the Middle Riphean Turukhansk uplift, Eastern Siberia // Lithosphere, 2008, №1. Pp. 90–99.

Ивановская А.В., Занин Ю.Н. Фосфориты стрельногорской свиты среднего рифея Туруханского поднятия, Восточная Сибирь // Литосфера, 2008, №1. С. 90–99.

27. Ilyin V.A. Ancient (Ediacaran) Phosphorites. – M.: GEOS, 2008. 160 Pp. (Tr. GIN RAS, vol. 587).

Ильин А.В. Древние (эдиакарские) фосфориты. – М.: ГЕОС, 2008. 160 с. (Тр. ГИН РАН, вып. 587).

28. *Kalinichenko E.A., Brik A.V., Kalinichenko A. M., Gatsenko V.A., Frank-Kamenetskaya O.V., Bagmut N.N. The particular properties of apatites from different species of the Chemerpole (Middle Near-Bug) according radiospectroscopy // Mineral. Z., 2014, vol. 36, No. 4. Pp. 50–65.*

Калиниченко Е.А., Брик А.Б., Калиниченко А.М., Гаценко В.А., Франк-Каменецкая О.В., Багмут Н.Н. Особенности свойств апатитов из разных пород Чемерполя (Среднее Побужье) по данным радиоспектроскопии // Мінерал. ж., 2014, т. 36, № 4. С. 50–65.

29. *Katkova V.I. Pseudomorphs of bioapatite on octocalciumphosphate // Vestn. In-ta geol. Komi Scientific Center of the Ural Branch of the Russian Academy of Sciences, 2012, No. 6. Pp. 11–14.*

Каткова В.И. Псевдоморфозы биоапатита по октакальцийфосфату // Вестн. Ин-та геол. Коми НЦ УрО РАН, 2012, № 6. С. 11–14.

30. *Kiseleva D.V., Zaitseva M.V. Determination of the trace element composition of REE in biogenic apatite of Upper Devonian conodonts (Southern Urals) by the ISP-MS method with laser ablation // Ural Mineralogical School, 2017, No. 23. Pp. 98–101.*

Киселева Д.В., Зайцева М.В. Определение микроэлементного состава РЗЭ в биогенном апатите верхнедевонских конодонтов (Южный Урал) методом ИСП-МС с лазерной абляцией // Уральская минералогическая школа, 2017, № 23. С. 98–101.

31. *Kogarko L.N. Rare-earth potential of apatite in deposits and waste products of apatite-nepheline ores of the Khibiny massif // Tr. Fersman sci. sessions of the GI KSC RAN, 2019, No. 16. Pp. 271–275.*

Когарко Л.Н. Редкоземельный потенциал апатита в месторождениях и отходах производства апатито-нефелиновых руд Хибинского массива // Тр. Ферсмановской науч. сессии ГИ КНЦ РАН, 2019, № 16. С. 271–275.

32. *Kolonin R.G., Shironosova G.P., Palessky S.V., Fedorin M.A., Kandinv M.N., Pohova V.I., Repina S.A., Shvetsova I.V. Rare-earth elements of Ural monazites and models of physico-chemical conditions of mineral formation // Mineralogy of the Urals-2007: Mater. 5 Vseros. Meeting, Miass, August 20-25, 2007: Collection of scientific articles. – Miass, Yekaterinburg: Ural Branch of the Russian Academy of Sciences, 2007. Pp. 246–250.*

Колонин Р.Г., Широносова Г.П., Палесский С.В. , Федорин М.А., Кандинов М.Н., Попова В.И., Репина С.А., Швецова И.В. Редкоземельные элементы монацитов Урала и модели физико-химических условий минералообразования // Минералогия Урала-2007: Матер. 5 Всерос. совещ., Миасс, 20–25 августа 2007 г.: Сборник научных статей. – Миасс, Екатеринбург: УрО РАН, 2007. С. 246–250.

33. *Konovalova E.V., Pribilkin S.V., Zamyatin D.A., Kholodnov V.V. Sulfur in apatites of granites of the Shartash massif and the Berezovsky gold deposit // Yearbook-2011: Collection. – Ekaterinburg: IGG URO RAN, 2012. Pp. 134–138 (Tr. IGG URO RAN, vol. 159).*

Коновалова Е.В., Прибавкин С.В., Замятин Д.А., Холоднов В.В. Сера в апатитах гранитов Шарташского массива и Березовского золоторудного месторождения // Ежегодник-2011: Сборник. – Екатеринбург: ИГГ УрО РАН, 2012. С. 134–138 (Тр. ИГГ УрО РАН, вып. 159).

34. *Konovalova E. V., Kholodnov V. V., Pribavkin S. V., Zamyatin D. A. Elements-mineralizer (sulfur and Halogens) in Apatity Shartash granite massif and Berezovsky gold deposits // Lithosphere, 2013, No. 6. Pp. 65–72.*

Коновалова Е.В., Холоднов В.В., Прибавкин С.В., Замятин Д.А. Элементы-минерализаторы (сера и галогены) в апатитах Шарташского гранитного массива и Березовского золоторудного месторождения // Литосфера, 2013, № 6. С. 65–72.

35. *Konopleva N.G., Ivanyuk G.Yu., Pakhomovsky Ya.A., Yakovenchuk V.N., Mikhailova Yu.A. Typomorphism of fluorapatite in the Khibiny alkaline massif (Kola Peninsula) // Zap. Rus. Mineral. Soc. 2013, vol. 142, No. 3. Pp. 65–83.*

Коноплева Н.Г., Иванюк Г.Ю., Пахомовский Я.А., Яковенчук В.Н., Михайлова Ю.А. Типоморфизм фторапатита в Хибинском щелочном массиве (Кольский полуостров) // Зап. Рос. минерал. о-ва, 2013, т. 142, № 3. С. 65–83.

36. *Korinevsky V.G., Filippova K.A., Kotlyarov V.A., korinevsky E.V., Artemyev D.A. Trace elements in minerals of some rare species of the Southern Urals // Lithosphere, 2019, vol. 19, No. 2. Pp. 269–292.*

Кориневский В.Г., Филиппова К.А., Котляров В.А., Кориневский Е.В., Артемьев Д.А. Элементы-примеси в минералах некоторых редко встречающихся пород Южного Урала // Литосфера, 2019, т. 19, №2. С. 269–292.

37. *Korovko A.V., Kholodnov V.V., Pribavkin S.V., Konovalova E.V., Mikheeva A.V. Halogens and sulfur in hydroxyl-bearing minerals in East Verkhoturye diorite-granodiorite array of mineralizatsii in the form of native copper (Middle Urals) // Yearbook-2017: the Collection. – Ekaterinburg: IGG URO RAN, 2018. Pp. 189–193 (Tr. IGG URO RAN, vol. 165).*

Коровко А.В., Холоднов В.В., Прибавкин С.В., Коновалова Е.В., Михеева А.В. Галогены и сера в гидроксилсодержащих минералах Восточно-Верхотурского диорит-гранодиоритового массива с минерализаций в виде самородной меди (Средний Урал) // Ежегодник-2017: Сборник. – Екатеринбург: ИГГ УрО РАН, 2018. С. 189–193 (Тр. ИГГ УрО РАН вып. 165).

38. Krestianinov E.A. Apatite as an indicator of the genesis of carbonatite Mayksk manifestations (South Ural) // Metallogeny of ancient and modern oceans, 2011, №1. Pp. 252–255.

Крестьянинов Е.А. Апатит как индикатор генезиса Маукского карбонатитового проявления (Южный Урал) // Металлогения древних и современных океанов, 2011, №1. С. 252–255.

39. Lemesheva S.A., Golovanova O.A., Turenkov S. V. Study of the characteristics of the composition of bone tissues // Chemistry for sustainable development, 2009, vol. 17, No. 3. Pp. 327–332.

Лемешева С.А., Голованова О.А., Туренков С.В. Исследование особенностей состава костных тканей человека // Химия в интересах устойчивого развития, 2009, т. 17, № 3. С. 327–332.

40. Liferovich, R.P., Bayanova T. B., Gogol O.V., Sherstennikov O.G., Delenitsin O.A.. Genesis intersects phosphate mineralization within the Kovdor will phoscorite-carbonatite complex // Vestn. MSTU. Tr. Murmansk. State Technical University. 1998, vol. 1, No. 3. Pp. 61–68.

Лиферович Р.П., Баянова Т.Б., Гоголь О.В., Шерстеникова О.Г., Деленицин О.А. Генезис посткарбонатитовой фосфатной минерализации в пределах Ковдорского фоскорит-карбонатитового комплекса // Вестн. МГТУ. Тр. Мурманск. гос. техн. ун-та, 1998, т. 1, №3. С. 61–68.

41. Lobova E.V. Evolution of amphibole and apatite from rocks of the Reftinsky complex (Eastern zone of the Middle Urals) // Vestn. Ural. branch Ros. mineral. Soc., 2012, No. 9. Pp. 84–87, 152.

Лобова Е.В. Эволюция амфибола и апатита из пород Рефтинского комплекса (Восточная зона Среднего Урала) // Вестн. Урал. отд-ния Рос. минерал. о-ва, 2012, № 9. С. 84–87, 152.

42. Malkov B.A., Lysyuk A.Yu., Ivanova T.I. Mineral composition and trace elements of fossilized bones of sea lizards located in Kargort (Komi Republic) // Vestn. Inst geol. Komi SC URO RAN, 2004, No. 1. Pp. 12–16.

Мальков Б.А., Лысюк А.Ю., Иванова Т.И. Минеральный состав и микроэлементы окаменелых костей морских ящеров местонахождения Каргорт (Республика Коми) // Вестн. Ин-та геол. Коми НЦ УрО РАН, 2004, № 1. С. 12–16.

43. Maslov A.V. Pre-Ordovician phosphorites and paleoceanography: a brief geochemical excursion into the systematics of rare earth elements // Lithosphere, 2017, No. 1. Pp. 5–30. [electronic resource].

Маслов А.В. Доордовикские фосфориты и палеоокеанография: краткий геохимический экскурс в систематику редкоземельных элементов // Литосфера, 2017, № 1. С. 5–30. [Электронный ресурс].

44. Maslov A.V. Phosphorites of the Neoproterozoic–Cambrian and paleoceanography: data on the distribution of rare earth elements // Yearbook-2015: Collection. - Yekaterinburg: IGG URO RAN, 2016. pp. 102-107. (Tr. IGG URO RAN, issue 163).

Маслов А.В. Фосфориты неопротерозоя–кембрия и палеоокеанография: данные по распределению редкоземельных элементов // Ежегодник-2015: Сборник. – Екатеринбург: ИГ и Г УрО РАН, 2016. С. 102–107. (Тр. ИГГ УрО РАН, вып. 163).

45. Mineev D.A. Lanthanides in Minerals. – M.: Nedra, 1969. 182 pp.

Минеев Д.А. Лантаноиды в минералах. — М.: Недра, 1969. 182 с.

46. Mineev D.A. Lanthanides in Ores of Rare-Earth and Complex Deposits – M.:Nauka, 1974. 237 pp.

Минеев Д.А. Лантаноиды в рудах редкоземельных и комплексных месторождений – М.:Наука, 1974. 237 с.

47. Oparin N.A., Oleinikov O.V., Baranov L.N. Apatite from kimberlite pipe Manchary (Central Yakutia) // Natural resources of the Arctic and Subarctic, 2020, vol. 25, No. 3. Pp. 15–24.

Опарин Н.А., Олейников О.Б., Баранов Л.Н. Апатит из кимберлитовой трубки Манчары (Центральная Якутия) // Природные ресурсы Арктики и Субарктики, 2020, т. 25, № 3. С. 15–24.

48. Pavlenko Y.V. Phosphates Streltsovsky ore field in South-Eastern Transbaikalia (part II) // Vestn. Zabaikalsky State University, 2021, vol. 27. No.3. pp. 42-52.

Павленко Ю.В. Фосфаты Стрельцовского рудного поля Юго-Восточного Забайкалья (часть II) // Вестн. Забайкальского гос. ун-та, 2021, т. 27. №3. С. 42–52.

49. Potapov S.S. Repina S.A., Potapov D.S. Mineralogical and chemical features of the tooth of a mammoth // Mineralogy of technogenesis, 2007, vol. 8. Pp. 139–145.

Потапов С.С., Репина С.А., Потапов Д.С. Минералого-химические особенности зуба мамонта // Минералогия техногенеза, 2007, т. 8. С. 139–145.

50. Rakhimov I.R., Kholodnov V.V., Salikhov D.N. Accessory apatite from gabbroids late Devonian–early Carboniferous West of the Magnitogorsk zone: morphology and chemical composition, indicator metallogenic role // Geological Bulletin, 2018, no. 3. Pp. 109–123.

Рахимов И.Р., Холоднов В.В., Салихов Д.Н. Акцессорные апатиты из габброидов позднего девона–раннего карбона Западно-Магнитогорской зоны: особенности морфологии и химического состава, индикаторная металлогеническая роль // Геологический вестник, 2018, № 3. С. 109–123.

51. Ripp G.S., Khodyreva E.V., Isbroken I.A., Ramelow M.O., Lastochkin E.I., Posokhov V.F. Genetic nature of the apatite-magnetite ores of the North-Gurvunur deposit (Western Transbaikalia) // Geol. rudn. deposits, 2017, vol. 59, No. 5. Pp. 419–33.

Рипп Г.С., Ходырева Е.В., Избродин И.А., Рампилов М.О., Ласточкин Е.И., Посохов В.Ф. Генетическая природа апатит-магнетитовых руд Северо-Гурвунурского меторождения (Западное Забайкалье) // Геол. рудн. м-ний, 2017, т. 59, № 5. С. 419–433.

52. Rosen O.M., Abbyasov A.A., Baturin G.N., Litvinova T.V. Calculation of the mineral composition of phosphate to facial reconstructions of the chemical analyses (program MINILITH) // Type of sedimentogenesis and lithogenesis and their evolution in the history of the Earth: materials of the 5th all-Russian lithological conference, Ekaterinburg, 14–16 Oct. 2008. Vol. 2. – Ekaterinburg: URO RAN, 2008. Pp. 200–203.

Розен О.М., Аббясов А.А., Батурин Г.Н., Литвинова Т.В. Расчет минерального состава фосфоритов для фациальных реконструкций по химическим анализам (программа MINILITH) // Типы седиментогенеза и литогенеза и их эволюция в истории Земли: Материалы 5 Всероссийского литологического совещания, Екатеринбург, 14–16 окт. 2008. Т. 2. – Екатеринбург: УрО РАН, 2008. С. 200–203.

53. Rosen, O. M., Solov'ev A. V. Fission-track dating of apatite from the core of the deep wells of the Siberian platform – an indicator of the intense heating of the sedimentary cover during the intrusion of platobasalts // Geology, Geophysics and mineral resources of Siberia: materials of the 1st Scientific and practical conference, Novosibirsk, 29-31 Jan., 2014. Vol. 2. – Novosibirsk: SNIIGGIMS, 2014. Pp. 162–163.

Розен О.М., Соловьев А.В. Трековое датирование апатитов из керна глубоких скважин Сибирской платформы — показатель интенсивного прогрева осадочного чехла во время внедрения платобазальтов // Геология, геофизика и минеральное сырье Сибири: Материалы 1 Научно-практической конференции, Новосибирск, 29-31 янв., 2014. Т. 2. – Новосибирск: СНИИГГМС, 2014. С. 162–163.

54. Ryabov V.V., Simonov O.N., Snisar S.G. Fluorine and chlorine in apatites, micas and amphiboles of the trap layered intrusions of the Siberian platform // Geol. and geofiz., 2018, vol. 59, No. 4. Pp. 453–466. [Electronic resource].

Рябов В.В., Симонов О.Н., Снисар С.Г. Фтор и хлор в апатитах, слюдах и амфиболах расслоенных трапповых интрузий Сибирской платформы // Геол. и геофиз., 2018, т. 59, № 4. С. 453–466. [Электронный ресурс].

55. Savelyeva V.B., Bazarova E.P., Sharygin V.V., Karmanov N.S., Kanakin S.V. Metasomatites of the Onguren carbonatite complex (Western Baikal region): geochemistry and composition of accessory minerals // Geol. rudn. deposits, 2017, vol. 59. No. 4. Pp. 319–346.

Савельева В.Б., Базарова Е.П., Шарыгин В.В., Карманов Н.С., Канакин С.В. Метасоматиты Онгуренского карбонатитового комплекса (Западное Прибайкалье): геохимия и состав акцессорных минералов // Геол. рудн. м-ний, 2017, т. 59. № 4. С. 319–346.

56. *Savenko A.V. On the physico-chemical mechanism of diagenetic formation of modern ocean phosphorites // Geochemistry, 2010, No. 2. Pp. 208–215.*

Савенко А.В. О физико-химическом механизме диагенетического формирования современных океанских фосфоритов // Геохимия, 2010, №2. С. 208–215.

57. *Savenko V.S., Savenko A.V. Geochemistry of Phosphorus in the Global Hydrological Cycle. – M.: GEOS, 2007. 248 Pp.*

Савенко В.С., Савенко А.В. Геохимия фосфора в глобальном гидрологическом цикле. – М.: ГЕОС, 2007. 248 с.

58. *Savko K.A., Pilyugin S.M., Novikova M.A. Composition of apatite from rocks of different ages of ferruginous-siliceous formations of the Voronezh crystalline massif – as an indicator of the fluid regime of metamorphism / Vestn. Voronezh. state University. Ser. Geology. 2007, No. 2. Pp. 78–93.*

Савко К.А., Пилюгин С.М., Новикова М.А. Состав апатита из пород разновозрастных железисто-кремнистых формаций Воронежского кристаллического массива – как показатель флюидного режима метаморфизма / Вестн. Воронеж. гос. ун-та. Сер. Геология. 2007, № 2. С. 78–93.

59. *Safin T. H., Dubinin A.V., Kuznetsov, A. B., Rimskaya-Korsakova, M. N. A study of the age of biogenic apatite from nodules of the Cape basin by the strontium isotope chemostratigraphy and establishing growth rates oxyhydroxide phases // Marine studies: 8th conference of young scientists, Vladivostok, June 6–9, 2018: conference proceedings. – Vladivostok: Dalnauka, 2018. Pp. 102–106.*

Сафин Т.Х., Дубинин А.В., Кузнецов А.Б., Римская-Корсакова М.Н. Исследование возраста биогенного апатита из конкреций Капской котловины методом стронциевой изотопной хемостратиграфии и установление скоростей роста оксигидроксидных фаз // Океанологические исследования: 8 конференция молодых ученых, Владивосток, 6-9 июня, 2018: Материалы конференции. – Владивосток: Дальнаука, 2018. С. 102–106.

60. *Serova A.A., Spiridonov E.M. Three types of apatite in Norilsk sulfide ores // Geochemistry, 2018, No. 5. Pp. 474–484 [Electronic resource].*

Серова А.А., Спиридонов Э.М. Три типа апатита в норильских сульфидных рудах // Геохимия, 2018, № 5. С. 474–484 [Электронный ресурс].

61. *Soloviev A.V. Study of Tectonic Processes in the Areas of Convergence of Lithospheric Plates by Methods of Isotope Dating and Structural Analysis: Abstract. dis. for the application of a scientist. degree of Doctor of Geological Sciences – M.: GIN RAS, 2005. 49 pp.*

Соловьев А.В. Изучение тектонических процессов в областях конвергенции литосферных плит методами изотопного датирования и структруного анализа: Автореф. дис. на соискание учен. степени доктора геол.-мин. наук. – М.: ГИН РАН, 2005. 49 с.

62. Soloviev V.A., Garver J.I. Post-collisional exhumation of the complexes in Northern Kamchatka (Lesnovsk lifting) // Dokl. Russian Academy of Sciences, 2012, vol. 443, No. 1. Рp. 92–96.

Соловьев А.В., Гарвер Дж.И. Постколлизионная эксгумация комплексов Северной Камчатки (Лесновское поднятие) // Докл. РАН, 2012, т. 443, № 1. С. 92–96.

63. Soroka E.I., Leonova L.V. Anfimov A.L., Apatite shell of the Devonian foraminifera (Safianovsk copper-pyrite deposit, the Middle Urals) // Izv. Uralsk. state. Gorny University, 2018, No. 3(51). Рp. 34–39.

Сорока Е.И., Леонова Л.В., Анфимов А.Л. Апатитовые раковины девонских фораминифер (Сафьяновское медноколчеданное месторождение, Средний Урал) // Изв. Уральск. гос. Горного ун-та, 2018, № 3(51). С. 34–39.

64. Taylor S.R., McLennan S.M. Continental Crust: its Composition and Evolution: Russian translation). - М.: Mir, 1988. 384 p.

Тейлор С.Р., Мак-Леннан С.М. Континентальная кора: ее состав и эволюция. – М.: Мир, 1988. 384 с.

65. Felitsyn S.B., Bogomolov E.S. Isotope-geochemical systematics of gold-bearing biogenic apatites from the Lower Paleozoic deposits of Baltoscandia // Dokl. RAS, 2013, vol. 451, No. 6. pp. 680–683.

Фелицын С.Б., Богомолов Е.С. Изотопно-геохимические систематики золотосодержащих биогенных апатитов из нижнепалеозойских отложений Балтоскандии // Докл. РАН, 2013, т. 451, № 6. С. 680–683.

66. Faore G. Fundamentals of Isotope Geology: Russian translation. – М.: Mir, 1989. 590 pp.

Фор Г. Основы изотопной геологии. – М.: Мир, 1989. 590 с.

67. Frank-Kamenetskaya O.V., Rozhdestvenskaya I.V., Rosseeva E.V., Zhuravlev A.V. Refinement of the atomic structure of apatite of the albinoi tissue of Upper Devonian conodonts // Crystallography, 2014, vol. 59, No. 1. Рp. 46–52.

Франк-Каменецкая О.В., Рождественская И.В., Россеева Е.В., Журавлев А.В. Уточнение атомной структуры апатита альбидной ткани позднедевонских конодонтов // Кристаллография, 2014, т. 59, № 1. С. 46–52.

68. Khattak N.U., Asif Khan Mohammad, Ali Nawab, Abbas S. M., Tahirkheli T.K. Evaluation of time and level of implementation of the carbonatite complex Silly Patti, district Malakand, North-Western Pakistan: the limitations of the data dating signs of the fission tracks // Geol. and geofiz., 2012, vol. 53, No. 8. Рp. 964–974.

Хаттак Н.У., Азиф Хан Мухаммад, Али Наваб, Аббас С.М., Тахиркели Т. К. Оценка времени и уровня внедрения карбонатитового комплекса Силлай Патти, район Малаканд, Северо-Западный Пакистан: ограничения, накладываемые данными датирования по следам распада // Геол. и геофиз., 2012, т. 53, № 8. С. 964–974.

69. *Kholodnov V.V., Konovalova E.V. Morphology and other typomorphic properties of apatite in granitoids of the Urals with quartz-vein gold mineralization // Ural mineralogical school of 2012. – Ekaterinburg: IGG URO RAN, 2012. Pp. 186–191.*

Холоднов В.В., Коновалова Е.В. Морфология и другие типоморфные свойства апатита в гранитоидах Урала с кварц-жильным золотым оруденением // Уральская минералогическая школа-2012. – Екатеринбург: ИГ и Г УрО РАН, 2012. С. 186–191.

70. *Kholodnov V.V., Salikhov D.N., Rakhimov I.R. Halogens and sulfur in apatite – as an indicator of potential ore-bearing late Paleozoic magmatic complexes of the West Magnitogorsk zone on Cr-Ni, Fe-Ti and Au mineralization // Geology, minerals and problems of geoecology of Bashkortostan, the Urals and adjacent territories, 2016, No. 11. Pp. 168–170.*

Холоднов В.В., Салихов Д.Н., Рахимов И.Р. Галогены и сера в апатитах – как индикатор потенциальной рудоносности позднепалеозойских магматических комплексов Западно-Магнитогорской зоны на Сг-Ni, Fe-Ti и Au оруденение // Геология, полезные ископаемые и проблемы геоэкологии Башкортостана, Урала и сопредельных территорий, 2016, № 11. С. 168–170.

71. *Kholodnov V.V., Salikhov D.N., Rakhimov I.R., Shagalov E.S., Konovalova E.V. Halogens and sulfur in apatites as a sign of specialization and Late Paleozoic accretion-collisional gabbro-dolerites of the West Magnitogorsk zone on Cu-Ni and Au mineralization // Yearbook-2014: Collection. – Ekaterinburg: IGG URO RAN, 2015. Pp. 214–221 (Tr. IGG URO RAN, vol. 162).*

Холоднов В.В., Салихов Д.Н., Рахимов И.Р., Шагалов Е.С., Коновалова Е.В. Галогены и сера в апатитах как признак специализации и позднепалеозойских аккреционно-коллизионных габбро-долеритов Западно-Магнитогорской зоны на Cu-Ni и Au оруденение // Ежегодник-2014: Сборник. – Екатеринбург: ИГ и Г УрО РАН, 2015. С. 214–221 (Тр. ИГГ УрО РАН, вып. 162).

72. *Kholodnov V.V., Salikhov D.N., Shagalov E.S., Konovalova E.V., Rakhimov I.R. The Role of halogens and sulfur in apatites in the assessment of potential ore-bearing gabbros of the Late Paleozoic of West Magnitogorsk zone (S. Ural) on Cu-Ni, Fe-Ti and Au mineralization // Mineralogy, 2015, No. 3. Pp. 45–61.*

Холоднов В.В., Салихов Д.Н., Шагалов Е.С., Коновалова Е.В., Рахимов И.Р. Роль галогенов и серы в апатитах при оценке потенциальной рудоносности позднепалеозойских габброидов Западно-Магнитогорской зоны (Ю. Урал) Cu-Ni, Fe-Ti и Au оруденение // Минералогия, 2015, № 3. С. 45–61.

73. Kholodnov V.V., Shagalov E.S., Konovalova E.V. Geochemistry of apatite in intrusive rocks of the Urals characterized by various ore specialization // Yearbook-2009: Collection. – Yekaterinburg: IGG UrO RAN, 2010. Pp. 190–195 (Tr. IGG UrO RAN, issue 157).

Холоднов В.В., Шагалов Е.С., Коновалова Е.В. Геохимия апатита в интрузивных породах Урала, характеризующихся различной рудной специализацией // Ежегодник-2009: Сборник. – Екатеринбург: ИГГ УрО РАН, 2010. С. 190–195 (Тр. ИГГ УрО РАН, вып. 157).

74. Chaika I.F., Izokh A.E. Phosphate-fluoride-carbonate mineralization in rocks of lamproite series of Rybinov massif (Central Aldan): mineralogical and geochemical characteristics and genesis problem // Mineralogy, 2017, vol. 3, No. 1. Pp. 38–51.

Чайка И.Ф., Изох А.Э. Фосфатно-фторидно-карбонатная минерализация в породах лампроитовой серии массива Рябиновый (Центральный Алдан): минералого-геохимическая характеристика и проблема генезиса // Минералогия, 2017, т. 3, №1. С. 38–51.

75. Chaikina M. V. Bulina N. V., Prosanov I.Yu., Ishchenko A.V., Medvedko O.V., Aronov A.M. Mechanochemical synthesis of hydroxyapatite with SIO_4^{4-} substitutions // Chemistry for sustainable development, 2012, vol. 20, No. 4. P. 477-489.

Чайкина М.В., Булина Н.В., Просанов И.Ю., Ищенко А.В., Медведко О.В., Аронов А.М. Механохимический синтез гидроксилапатита с SIO_4^{4-} замещениями // Химия в интересах устойчивого развития, 2012, т. 20, №4. С. 477–489.

76. Chuprov A.A., Badmatsyrenova R.A., Batueva A.A. Apatite mineralization of the Oshurekov gabbro-pegmatite massiv, Transbaikalia: data from LA-ICP-MS analysis // Metallogeny of ancient and modern oceans, 2021, vol. 27. Pp. 144–146.

Чупрова А.А., Бадмацыренова Р.А., Батуева А.А. Апатитовая минерализация Ошурековского габбро-пегматитового массива, Забайкалье: данные ЛА-ИСП-МС анализа // Металлогения древних и современных океанов, 2021, т. 27. С. 144–146.

77. Shatrov V.A., Voitsekhovsky G.V. Reconstruction of phosphate formation environments // Geol. and geophys., 2009, vol. 50, No. 10. Pp.1104–1118.

Шатров В.А., Войцеховский Г.В. Реконструкция обстановок фосфатообразования // Геол. и геофиз., 2009, т. 50, №10. С.1104–1118.

78. Shironosova G.P., Kolonin G.R. Thermodynamic modeling of REE distribution between monazite, fluorite and apatite // Dokl. RAN, 2013, vol. 450, No. 4. Pp. 455–459.

Широносова Г.П., Колонин Г.Р. Термодинамическое моделирование распределения РЗЭ между монацитом, флюоритом и апатитом // Докл. РАН, 2013, т. 450, № 4. С. 455–459.

79. Shnug E., Haneklaus N. Extraction of uranium from phosphate ores:

ecological aspects // Atomic engineering abroad, 2013, No. 9. Pp. 20–24.

Шнуг Э., Ханеклаус Н. Извлечение урана из фосфатных руд: экологические аспекты // Атомная техника за рубежом, 2013, №9. С. 20–24.

80. Yudovich Ya.E., Ketris M.P. Geochemical Indicators of Lithogenesis (Lithological Geochemistry). – Syktyvkar: Geoprint, 2011. 740 pp.

Юдович Я.Э., Кетрис М.П. Геохимические индикаторы литогенеза (литологическая геохимия). – Сыктывкар: Геопринт, 2011. 740 с.

81. Yudovich Ya.E., Ketris M.P., Rybina N.V. Geochemistry of Phosphorus. – Syktyvkar: IG Komi SC UrO RAN, 2020. 512 pp.

82. Юдович Я.Э., Кетрис М.П., Рыбина Н.В. Геохимия фосфора. – Сыктывкар: ИГ Коми НЦ УрО РАН, 2020. 512 с.

OTHER REFERENCES

82. Adcock C.T., Hausrath E.M., Forster P.M., Tschauner O., Sefein K.J. Synthesis and characterization of the Mars-relevant phosphate minerals Fe- and Mg-whitlockite and merrillite and a possible mechanism that maintains charge balance during whitlockite to merrillite transformation // Amer. Mineral., 2014, vol. 99, № 7. P. 1221–1232.

83. Barham M., Murray J., Joachimski M.M., Williams D.M. The onset of the Permo-Carboniferous glaciation: reconciling global stratigraphic evidence with biogenic apatite $\delta^{18}O$ records in the late Visean // J. Geol. Soc., 2012, vol.169, № 2. P. 119–122.

84. Belousova E.A., Griffin W.L., O'Reilly S.Y., Fisher N.I. Apatite as an indicator mineral for mineral exploration: Trace-element compositions and their relationship to host rock type // J. Geochem. Explor., 2002, vol. 76, № (1). P. 45–69.

85. Belousova E.A., Walters S., Griffin W.L., O'Reilly S.Y. Trace-element signatures of apatites in granitoids from the Mt Isa Inlier, Northwestern Queensland // Aust. J. Earth Sci., 2001, vol. 48. P. 603–619.

86. Bromiley G.D. Do concentrations of Mn, Eu and Ce in apatite reliably record oxygen fugacity in magmas? // Lithos, 2021, vol. 384–385. 105900.

87. Broom-Fendley S., Heaton T., Wall F., Gunn G. Tracing the fluid source of heavy REE mineralisation in carbonatites using a novel method of oxygen-isotope analysis in apatite: The example of Songwe Hill, Malawi // Chem. Geol., 2016. 440. P. 275–287. [Electronic resource].

88. Brown W.F., Lehr J.R., Smith J.R., William A.F. Crystallography of octocalciumphosphate // J. Amer. Chem. Soc., 1957, vol. 79, № 19. P. 5378–5379.

89. Buggisch W., Joachimsry M.M., Sevastopulo G., Morrow J.R. Mississippian $\delta13C_{karb}$ and conodont apatite $\delta^{18}O$ records – Their relation to the Late Palaeozoic Glaciation // Palaeogeogr., Palaeoclim., Palaeoecol., 2008, vol. 69, № 3–4. P. 273–292.

90. Cavazza W., Federici I., Okay A.I., Zattin M. Apatite fission-track thermochronology of the Western Pontides (NW Turkey) // Geol. Mag., 2012., vol. 149, № 1. P. 133–140.

91. Chakhmouradian A.R., Reguir E.P., Zaitsev A.N., Couëslan C., Xu C., Kynický J., Mumin A.H., Yang P. Apatite in carbonatitic rocks: Compositional variation, zoning, element partitioning and petrogenetic significance // Lithos : An International Journal of Mineralogy, Petrology and Geochemistry, 2017, vol. 274-275. P. 188–213. [Electronic resource].

92. Charlier B., Namurn O., Bolle O., Latypov R., Duchesne J.-C. Fe–Ti–V–P ore deposits associated with Proterozoic massif-type anorthosites and related rocks // Earth-Science Reviews, 2015, vol. 141. P. 56–81.

93. Chen J., Algeo T.J., Zhao L., Chen Z.-Q., Cao L., Zhang L., Li Y. Diagenetic uptake of rare earth elements by bioapatite, with an example from Lower Triassic conodonts of South China // Earth-Science Reviews, 2015, vol. 149. P. 181–202.

94. Corcoran D.V., Dore A. G. A review of techniques for the estimation of magnitude and timing of exhumation in offshore basins // Earth-Science Reviews, 2005, vol. 72, № 3–4. P. 129–168.

95. Dempster T.J., Jolivet M., Tubrett M.N., Braithwaite C.J.R. Magmatic zoning in apatite: a monitor of porosity and permeability change in granites // Contrib. Mineral. Petrology, 2003, vol. 145. P. 568–577.

96. Dutta A., Fermani S., Tekalur S.A., Vanderberg A., Falini G. Calcium phosphate scaffold from biogenic calcium carbonate by fast ambient condition reactions // J. Cryst. Growth., 2011, vol. 336, № 1. P. 50–55.

97. Economou-Eliopoulos M. Apatite and Mn, Zn, Co-enriched chromite in Ni-laterites of northern Greece and their genetic significance // J. Geochem. Explor., 2003, vol. 80, № 1. P. 41–54.

98. Elrick M., Reardon D., Labor W., Martin J., Desrochers A., Pope M. Orbital-scale climate change and glacioeustasy during the earlyate Ordovician (pre-Hirnantian) determined from $\sigma^{18}O$ values in marine apatite // Geology, 2013, vol. 41, № 7. P. 775–778.

99. Emerson N.R., Simo J.A. (Toni), Byers C.W., Fournelle J. Correlation of (Ordovician, Mohawkian) K-bentonites in the upper Mississippi valley using apatite chemistry: implications for stratigraphic interpretation of the mixed carbonate-siliciclastic Decorah Formation // Palaeogeogr., Palaeoclim., Palaeoecol., 2004, vol. 210. P. 215–233.

100. Enkelmann E., Ehlers T.A., Buck G., Schatz A.-K. Advantages and challenges of automated apatite fission track counting // Chem. Geol., 2012, vol. 322-323. P. 278–289.

101. Fang W., Zhang H., Yin J., Yang B., Zhang Y., Li J., Yao F. Hydroxyapatite crystal formation in the presence o polysaccharide // Cryst. Growth and Des., 2016, vol. 16, № 3. P. 1247–1255.

102. Finger F., Krenn E., Schulz B., Harlov D., Schiller D. "Satellite monazites" in polymetamorphic basement rocks of the Alps: Their origin and petrological significance // Amer. Mineral., 2016, vol. 101, № 5-6. P. 1094–1103.

103. Galliski M.Á., Černý P., Márquez-Zavala M.F., Chapman R. An association of secondary Al—Li—Be—Ca—Sr phosphates in the San Elas pegmatite, San Luis, Argentina // Can. Miner., 2012, vol. 50, № 4. P. 9339–9342.

104. Garcia A.K. Development of an apatite oxygen paleobarometer: Experimental characterization of Sm^{3+}-substituted apatite fluorescence as a function of oxygen availability // Precambrian. Res., 2020, vol. 349. 105389.

105. Georgieva S., Velinova N. Florencite-(Ce, La, Nd) and crandallite from the advanced argillic alteration in the Chelopech high-sulphidation epithermal Cu-Au deposit, Bulgaria // Докл. Бълг. АН, 2014, vol. 67, № 12. P. 1669–1678.

106. Héran M.-A., Lécuyer C., Legendre S. Cenozoic long-term terrestrial climatic evolution in Germany tracked by $\delta^{18}O$ of rodent tooth phosphate // Palaeogeogr., Palaeoclim., Palaeoecol., 2010, vol. 285, № 3-4. P. 331–342.

107. Horie K., Hidaka H., Gauthier-Lafaye F. Elemental distribution in apatite, titanite and zircon during hydrothermal alteration: Durability of immobilization mineral // Phys. Chem. Earth, 2008, vol. 33. P. 962–968.

108. Joachimski M.M., von Bitter P.H., Buggisch W. Constraints on Pennsylvanian glacioeustatic sea-level changes using oxygen isotopes of conodont apatite // Geology, 2006, vol. 34, № 4. P. 277–280.

109. Kocsis L., Dulai A., Bitner M.A., Vennemann T. Cooper Matthew Geochemical compositions of Neogene phosphatic brachiopods: Implications for ancient environmental and marine conditions // Palaeogeogr., Palaeoclim., Palaeoecol., 2012, vol. 326-328. P. 66–77.

110. Krneta S., Ciobanu C.L., Cook N.J., Ehrig K., Kontonikas-Charos A. A petrogenetic tool // Lithos: An International Journal of Mineralogy, Petrology and Geochemistry, 2016, vol. 262. P. 470–485. [Electronic resource].

111. Lieberovich R.F., Mitchell R.H. Apatite-group minerals from nepheline syenite, Pilansberg alkaline complex, South Africa // Mineral. Mag., 2006, vol. 70, № 5. P. 463–484.

112. Liu Wen-hao, Zhang J., Li Wan-ting, Sun T., Jiang Man-rong, Wang J., Wu Jian-yang, Chen Cao-jun // Diqiu kexue = Earth Sci. : Zhongguo dizhi daxue xuebao Zhongguo dizhi daxue xuebao, 2012, vol. 37, № 5. P. 966–980.

113. Llorens T., Moro M.C. Fe-Mn phosphate associations as indicators of the magmatic-hydrothermal and supergene evolution of the Jálama batholith in the Navasfras Sn-W District, Salamanca, Spain // Mineral. Mag., 2012, vol. 76, № 1. P. 1–24.

114. Lu J., Chen W., Ying Y., Jiang S., Zhao K. Apatite texture and trace element chemistry of carbonatite-related REE deposits in China: Implications for petrogenesis // Lithos, 2020, vol. 398. 106276.

115. Matton O., Cloutier R., Stevenson R. Apatite for destruction: Isotopic and geochemical analyses of bioapatites and sediments from the Upper Devonian Escuminac Formation (Miguasha, Québec) // Palaeogeogr., Palaeoclim.., Palaeoecol., 2012, vol. 361-362. P. 73–83.

116. Onac B.P., Effenberger H.S., Breban R.C. High-temperature and "exotic" minerals from the Cioclovina Cave, Romania: A review // Stud. Univer. Babes

Ya. E. Yudovich, M. P. Ketris, N. V. Rybina

THE APATITE-DECEIVER AS AN UNIQUE INDICATOR PARENT ROCKS AND ORES, AS WELL AS PETRO-, LITHO- AND ORE GENESIS

Monograph

Information about the authors

YUDOVICH Yakov Elievich,
Chief Researcher of the Komi Scientific Center's
Institute of Geology, the Ural Branch of the Russian
Academy of Sciences;
Doctor of Geological and Mineralogical Sciences,
Academician of the Russian Academy of Natural
Sciences and the New York Academy of Sciences,
laureate of the A. P. Vinogradov Prize of the Russian
Academy of Sciences (2011).

KETRIS Marina Petrovna,
Senior Researcher at the Institute of Geology of the
Komi Scientific Center of the Ural Branch of the Russian
Academy of Sciences;
winner of the A. P. Vinogradov Prize of the Russian
Academy of Sciences (2011).

RYBINA Natalia Valerievna,
Senior Laboratory Assistant at the Institute of Geology
of the Komi Scientific Center of the Ural Branch
of the Russian Academy of Sciences